FEDERAL UNIVERSITY OF SANTA CATARINA
DEPARTMENT OF AUTOMATION AND SYSTEMS ENGINEERING

Carla de Souza

Control of classes of linear discrete-time parameter-varying systems under input constraints

Florianópolis
2021

Carla de Souza

Control of classes of linear discrete-time parameter-varying systems under input constraints

Thesis submitted to Department of Automation and Systems Engineering of Federal University of Santa Catarina for the obtaining of the title of Ph.D. in Automation and Systems Engineering.
Supervisor:: Prof. Dr. Eugênio de Bona Castelan Neto
Co-supervisor:: Prof. Dr. Valter Júnior de Souza Leite

Florianópolis
2021

Ficha de identificação da obra elaborada pelo autor,
através do Programa de Geração Automática da Biblioteca Universitária da UFSC.

de Souza, Carla
Control of classes of linear discrete-time parameter varying systems underinput constraints / Carla de Souza ; orientador, Eugênio de Bona Castelan Neto, coorientador, Valter Júnior de Souza Leite, 2021.
122 p.

Tese (doutorado) - Universidade Federal de Santa Catarina, Centro Tecnológico, Programa de Pós-Graduação em Engenharia de Automação e Sistemas, Florianópolis, 2021.

Inclui referências.

1. Engenharia de Automação e Sistemas. 2. Linear parameter- varying systems. 3. Time-delay systems. 4. Saturating actuators. 5. Event-triggered control. I. de Bona Castelan Neto, Eugênio. II. Júnior de Souza Leite, Valter. III. Universidade Federal de Santa Catarina. Programa de Pós-Graduação em Engenharia de Automação e Sistemas. IV. Título.

Carla de Souza

Control of classes of linear discrete-time parameter-varying systems under input constraints

O presente trabalho em nível de doutorado foi avaliado e aprovado por banca examinadora composta pelos seguintes membros:

Prof. Dr. Daniel Coutinho,
Universidade Federal de Santa Catarina

Prof. Dr. Jeferson Vieira Flores,
Universidade Federal do Rio Grande do Sul

Prof. Dr. Pedro Luis Dias Peres,
Universidade Estadual de Campinas

Prof. Dr. Alexandre Seuret,
Laboratoire d'analyse et d'architecture des systèmes

Certificamos que esta é a **versão original e final** do trabalho de conclusão que foi julgado adequado para obtenção do título de Ph.D. in Automation and Systems Engineering.

Documento assinado digitalmente
Werner Kraus Junior
Data: 08/10/2021 08:31:14-0300
CPF: 531.085.239-53
Verifique as assinaturas em https://v.ufsc.br

Coordenação do Programa de
Pós-Graduação

Documento assinado digitalmente
Eugenio de Bona Castelan Neto
Data: 07/10/2021 17:15:25-0300
CPF: 429.477.669-20
Verifique as assinaturas em https://v.ufsc.br

Prof. Dr. Eugênio de Bona Castelan Neto
Supervisor

Florianópolis, 2021.

This work is dedicated to my parents and siblings.

ACKNOWLEDGEMENTS

To God.

To my parents, Sebastião and Miraci, and siblings, Cláudia, Mônica, and Luis Fernando, for all the encouragement, support, and love.

To my advisers Eugênio and Valter, for all their teaching, dedication, patience, encouragement, and friendship. I couldn't have better professionals and human beings working by my side during this doctorate. I extend these thanks to Sophie Tarbouriech, who guided me during the doctoral sandwich at LAAS in Toulouse, France.

To all my friends from Florianópolis and Toulouse for the countless moments of amusement during this doctorate. In particular, I would like to thank Thamiris, Ivan, Thiago, Matteo, Lorenzo, Maria, and Vinícius. Without you, this journey would not have been so pleasant and memorable.

To Neusa for having welcomed me into her home in Florianópolis with open hugs and for treating me like a daughter during the 2 years, I lived there.

To CAPES for the financial support provided by a Ph.D. Scholarship and the Sandwich Doctoral Program.

“Some men see things as they are, and say ‘Why?’
I dream of things that never were and say ‘Why not?’.”
George Bernard Shaw

ABSTRACT

This work proposes control laws for the regional stabilization of two classes of discrete-time linear parameter-varying (LPV) systems under input constraints. The first one consists of systems subject to time-varying delay in the states, saturating actuators, and energy bounded disturbances. For such a class, we establish convex conditions to design static state-feedback controllers as well as dynamic output-feedback controllers ensuring the regional input-to-state stability (ISS) of the control loop. The proposed conditions take into account the variation of the delay between two consecutive instants, which leads to better estimates of the region of attraction supporting higher levels of disturbances. The approach is based on rewriting the time-delay system with input saturation as an augmented delay-free switched system with a dead-zone nonlinearity. The second class comprises the systems with saturating actuators inserted in communication networks with limited bandwidth. In this case, we formulate convex conditions to synthesize event-triggering state-feedback controllers as well as event-triggering dynamic output feedback controllers ensuring the regional asymptotic stability of the closed-loop system while indirectly reducing the number of data transmissions over the communication channels. The proposed event-triggering policies indicate, for instance, whether the states or the output should be transmitted over the network or not. The use of the Lyapunov theory in all cases leads to conditions in the form of linear matrix inequalities (LMIs), which can be efficiently solved by computational packages. Some numerical examples are provided to testify the validity and the effectiveness of our approach and to make comparisons with similar ones in the literature.

Keywords: Linear parameter-varying systems. Saturating actuators. Time-varying delays. Event-triggering control. Lyapunov based approach.

RESUMO EXPANDIDO

Controle de classes de sistemas lineares a parâmetros variantes (LPV) discretos no tempo sob restrições na entrada

Palavras-chave: Sistemas lineares a parâmetros variantes. Atuadores saturantes. Atrasos variantes no tempo. Controle a eventos. Abordagem baseada em Lyapunov.

Introdução

Com os avanços tecnológicos que ocorreram principalmente nas últimas décadas, o uso das redes de comunicação tornou-se comum nas malhas de controle industriais. Isso porque elas trazem uma série de benefícios quando comparadas as conexões ponto-a-ponto, como, por exemplo, redução dos custos, facilidade de reconfiguração, implementação e manutenção. No entanto, como a capacidade de transmissão das redes (largura de banda) é geralmente limitada, alguns problemas surgem com a utilização delas, como, por exemplo, congestionamento e elevado consumo de energia em sistemas de rede sem fio. Neste contexto, com o objetivo de melhorar o uso dos recursos das redes, estratégias de controle aperiódicas tem sido estudas, no qual a tarefa de controle é executada somente quando certa condição é verificada. Entre essas estratégias, o paradigma de controle acionado por eventos se destaca. Em tal técnica, um gerador de eventos monitora determinada variável do sistema, estado ou saída, e gera um evento (transmite a informação) apenas quando algum critério baseado nessa variável monitorada é verificado. Desse modo, o controle acionado por eventos é capaz de reduzir a taxa de transmissão de informações enquanto garante a estabilidade e certo índice de desempenho da malha-fechada. Portanto, a introdução de um mecanismo de disparo de eventos que reduz o desperdício de recursos e computação de forma eficiente, torna-se significativo em tal cenário.

Além disso, é notório que os sistemas de controle práticos podem ter seus comportamentos dinâmicos afetados por atrasos, incertezas, distúrbios externos, não linearidades como a saturação, entre outras características que podem gerar transtornos à malha de controle. O atraso, por exemplo, pode causar oscilação, baixo desempenho e até mesmo instabilidade. Para contornar tais problemas, diversas técnicas têm sido propostas na literatura (FRIDMAN, 2014). Ainda assim, a análise e o projeto de controladores de sistemas com atraso podem se tornar teoricamente mais complicados na presença de atuadores saturantes, pois mesmo que o sistema seja estável na ausência de restrições de controle, ele pode desestabilizar, caso contrário, para algumas condições iniciais. Assim, uma tarefa fundamental, neste caso, é determinar o con-

junto de todas as condições iniciais cujas trajetórias convergem garantidamente para a origem, o que é reconhecidamente desafiador (TARBOURIECH et al., 2011). No caso de sinais de distúrbio afetando o sistema, também é importante caracterizar o conjunto de sinais de distúrbio admissíveis para os quais as trajetórias são garantidamente limitadas. Portanto, o desenvolvimento de melhores técnicas de controle que lidem com todas essas dificuldades tornou-se um dos grandes desafios dos últimos tempos.

Este trabalho se enquadra em ambos contextos, no qual novas metodologias são propostas para a análise e o controle de duas classes de sistemas LPV discretos no tempo sob restrições na entrada. A primeira consiste em sistemas sujeitos a atraso variante no tempo nos estados, saturação de atuadores e distúrbios limitados em energia. A segunda compreende os sistemas com saturação de atuadores inseridos em redes de comunicação com largura de banda limitada.

Objetivos

O principal objetivo desta tese é desenvolver condições convexas para análise e síntese de controladores, que garantam a estabilidade e certo desempenho de duas classes de sistemas: *i)* sistemas LPV discretos no tempo com atraso variante no tempo nos estados sujeitos a saturação de atuadores e distúrbios limitados em energia e *ii)* sistemas LPV discretos no tempo sujeitos a saturação de atuadores inseridos em uma rede de comunicação com largura de banda limitada.

Como objetivos específicos, pode-se enumerar:

1. Desenvolver um método para o projeto de controladores dependente de parâmetros do tipo realimentação de estados para a classe de sistemas *i)*, explorando a modelagem aumentada e chaveada pelo valor do atraso (HETEL et al., 2008);

2. Desenvolver um método para o projeto de controladores dependente de parâmetros do tipo realimentação dinâmica da saída para a classe de sistemas *i)*, explorando a modelagem aumentada e chaveada pelo valor do atraso (HETEL et al., 2008);

3. Desenvolver um método para o projeto simultâneo de um controlador dependente de parâmetros do tipo realimentação dinâmica da saída e dois mecanismos de disparo de eventos, os quais transmitem as saídas da planta e do controlador, para a classe de sistemas *ii)*;

4. Desenvolver um método para o projeto simultâneo de um controlador dependente de parâmetros do tipo realimentação dos estados e dois mecanismos de disparo

de eventos, os quais transmitem o estado e o parâmetro variante, para a classe de sistemas *ii*;

5. Implementar computacionalmente os métodos propostos e compará-los com outras abordagens simulares na literatura;

Contribuições da tese

Dentre as contribuições da pesquisa realizada, nos capítulos 2 e 3 é investigado o problema de estabilização regional de sistems LPV discretos no tempo com atraso variante no tempo nos estados sujeitos a saturação de atuadores e distúrbios limitados em energia. No Capítulo 2, são propostas condições convexas para a síntese de controladores dependente de parâmetros do tipo realimentação dos estados, cuja estrutura pode incluir estados atrasados, sem requerer o conhecimento do atraso. Em contrapartida, no Capítulo 3 são propostas condições convexas para a síntese de controladores dependente de parâmetros do tipo realimentação da saída. O controlador proposto, neste último caso, possue as seguintes características: sua ordem pode ser escolhida como um múltiplo inteiro da ordem do sistema original; sua estrutura permite que o usuário realimente não apenas a saída atual mas também as saídas atrasadas; e um ganho de anti-windup é incluido como uma tentativa de atenuar os efeitos da saturação. Ambas abordagens são baseadas na reescrita do sistema com atraso sob saturação de atuadores em um sistema aumentado e chaveado pelo valor do atraso com uma não-linearidade do tipo zona-morta. Para lidar com os distúrbios limitados em energia, é empregado o conceito de estabilidade entrada-estado. Com o auxílio de uma função de Lyapunov mais geral e da condição de setor generalizada, as condições propostas são estabelecidas na forma de desigualdades matriciais lineares. Quando factíveis, elas garantem a estabilidade entrado-estado regional das malhas de controle, e estimam as regiões de atração da origem. Além disso, é importante mencionar que as condições levam em conta a variação do atraso entre dois instantes consecutivos, o que permite alcançar resultados menos conservadores.

Em adição, nos capítulos 3 e 4 é investigado o problema de controle acionado por eventos de sistemas LPV discretos no tempo sujeito a saturação de atuadores. No Capítulo 3, são propostas condições convexas para a síntese simultânea de um controlador dependente de parâmetros do tipo realimentação dinâmica da saída com ação *anti-windup* e dois mecanismos de disparo de eventos. Tais mecanismos são responsáveis por transmitir as saídas da planta e do controlador através dos canais de comunicação. Em contrapartida, no Capítulo 4 são propostas condições convexas para a síntese simultânea de um controlador dependente de parâmetros do tipo realimen-

tação dos estados e dois mecanismos de disparo de eventos. Neste caso, os mecanismos gerenciam de forma independente a transmissão dos estados e do parâmetro variante através do canal de comunicação entre o sensor e o controlador. Tal fato permite que os parâmetros variantes do controlador e da planta possam diferir um do outro, o que confere certo grau de robustez quanto aos desvios dos parâmetros. Ambas as abordagens são formuladas com o auxílio de uma função de Lyapunov dependente de parâmetros e da condição generalizada do setor, o que leva a um conjunto de desigualdades matriciais lineares que, se factíveis, garantem a estabilidade assintótica regional do sistema em malha-fechada e fornece uma estimativa da região de atração da origem.

Conclusão

Esta tese propõe leis de controle para a estabilização regional de duas classes de sistemas LPV discretos no tempo sob restrições na entrada. A primeira consiste em sistemas sujeitos a atraso variante no tempo nos estados, atuadores saturantes e sinais de distúrbio com energia limitada. Para tal classe, são projetados controladores do tipo realimentação de estado bem como controladores do tipo realimentação dinâmica da saída, que garantem a estabilidade entrada-estado regional da malha de controle. A abordagem é baseada na reescrita do sistema com atraso sob saturação de atuadores em termos de um sistema aumentado e chaveado pelo valor do atraso com uma não linearidade do tipo zona morta, o que confere características particulares aos controladores. A segunda classe compreende os sistemas LPV discretos no tempo sujeitos a atuadores saturantes inseridos em uma rede de comunicação com largura de banda limitada. Neste caso, são sintetizados controladores do tipo realimentação de estados bem como controladores do tipo realimentação dinâmica da saída, ambos com mecanismos de acionamento de eventos, que garantem a estabilidade regional assintótica da malha fechada enquanto reduzem indiretamente o número de dados transmitidos nos canais de comunicação. As políticas de acionamento de eventos propostas indicam, por exemplo, se os estados ou a saída devem ser transmitidos através da rede ou não. O uso da teoria de Lyapunov em todos os casos conduz a condições na forma de desigualdades matriciais lineares, que podem ser eficientemente resolvidas por meio de pacotes computacionais. Além disso, alguns procedimentos de otimização são formulados para atingir diferentes obejtivos de controle, como, por exemplo, maximizar a estimativa de região de atração, melhorar a tolerância ao distúrbio, e minimizar a taxa de transmissão das informações. Alguns exemplos numéricos são fornecidos para atestar a validade e eficiência dessas abordagens e também para fazer comparações com trabalhos similares encontrados na literatura.

LIST OF FIGURES

Figure 1 – Regions $\mathcal{R}_{\mathcal{A}}$, $\mathcal{R}_{\mathcal{E}}$ and $\mathcal{R}_{\mathcal{E}0}$. 32
Figure 2 – Saturation and dead-zone functions. 33
Figure 3 – Projections of the estimated attraction region and the trajectories of the current states for the system (46) with perturbation. 41
Figure 4 – $R_{\%} \times \Delta\tau_{\max}$ for $\bar{\tau}$ varying from 2 up to 7. 42
Figure 5 – Cuts of the estimated attraction region for different control gain structures. 43
Figure 6 – Cuts of the estimated attraction region and the current states' trajectories for the system (46) without perturbation. 43
Figure 7 – $\delta^{-1} \times \sigma$ for $\bar{\tau}$ varying from 1 up to 7. 58
Figure 8 – Projection of the estimated attraction region and the trajectories of the current states for the system with perturbation. 60
Figure 9 – The closed-loop temporal response for six different disturbance signals. 61
Figure 10 – $\delta^{-1} \times \sigma$ for different control gain structures. 62
Figure 11 – Projections area $\times\sigma$ for $\bar{\tau}$ varying from 1 up to 6. 62
Figure 12 – Comparison between the estimated attraction regions obtained through our approach and (SONG, G.; WANG, Z., 2013). 63
Figure 13 – Event-triggering closed-loop system. 68
Figure 14 – An inverted pendulum (WU, W. et al., 2014) 79
Figure 15 – $\mathcal{R}_{\mathcal{E}}$ and $\mathcal{X}_0 = \mathcal{E}(R, 1)$ with $R_{11} = \texttt{diag}\{76, 2\}$. 80
Figure 16 – The closed-loop response of system (128) - $\mathcal{X}_0 = \mathcal{E}(R, 1)$ with $R_{11} = \texttt{diag}\{76, 2\}$. 81
Figure 17 – $\mathcal{R}_{\mathcal{E}}$ and $\mathcal{X}_0 = \mathcal{E}(R, 1)$ with $R_{11} = \texttt{diag}\{26.60, 0.70\}$. 82
Figure 18 – The closed-loop response of system (128) - $\mathcal{X}_0 = \mathcal{E}(R, 1)$ with $R_{11} = \texttt{diag}\{26.60, 0.70\}$. 83
Figure 19 – Event-triggering closed-loop system. 89
Figure 20 – Average update rate of the scheduling parameter and the state. . . . 100
Figure 21 – The estimate of the region of attraction $\mathcal{R}_{\mathcal{E}}$ for $g = 0.8$. 100
Figure 22 – The closed-loop temporal response for the system (169) 101
Figure 23 – Inter-event interval of the event generators. 102

LIST OF TABLES

Table 1 – Some types of ETMs employed in the literature. 25
Table 2 – Measures of the axes of the ellipses (cuts) and the radius of the circles (μ_{max}) of the estimates of the regions of attraction. 64
Table 3 – Comparison of the number of samplings - Example (128). 83
Table 4 – Comparison of the average sampling time - Example (129). 84
Table 5 – Comparison of the updates rates - Example (130). 86
Table 6 – Percentage of transmission rate achieved by the proposed method and those from 1-(GOLABI et al., 2017) and 2-(GOLABI et al., 2016). 103
Table 7 – Relative robustness (δ/δ_0) achieved by the proposed method and that from (SHANBIN; BUGONG, 2013) and the percentage of transmission rate. 104

LIST OF ABBREVIATIONS AND ACRONYMS

ETC	Event-triggered control
ETM	Event-triggering mechanism
ISS	Input-to-state stability
LMI	Linear matrix inequality
LPV	Linear parameter-varying
LTI	Linear time-invariant
NCS	Networked control systems
TTC	Time-triggered control

LIST OF SYMBOLS

$\subset$ ($\subseteq$)	Subset (subset or equal)
$\in$	Included
$\forall$	For all
$\mathbb{R}$	Set of real numbers
$\mathbb{R}^+$	Set of non-negative real numbers
$\mathbb{R}^n$	n-dimensional real vector space
$\mathbb{R}^{n\times m}$	$n \times m$-dimensional real matrix space
$\mathbb{Z}^+$	Set of non-negative integer numbers
$\mathbf{0}_{n\times m}$ ($\mathbf{0}_n$)	Null matrix of dimension $n \times m$ ($n \times n$)
$\mathbf{I}_n$	Identity matrix of dimension n
$a_{(i)}$	i^{th} element of a vector a
$A_{(i)}$	i^{th} element of a matrix A
$A^\top$ ($a^\top$)	Transpose of matrix (vector) A (a)
A^{-1}	Inverse of a matrix A
$\|A\|$	Euclidean norm of a matrix A
$\mathtt{tr}(A)$	Trace of A.
$\mathtt{det}(A)$	Determinant of A.
$\mathtt{diag}(A, B)$	Block-diagonal matrix with main diagonal blocks A and B
$\mathcal{I}[a, b]$	Integer numbers belonging to the interval from $a \in \mathbb{Z}^+$ up to $b \in \mathbb{Z}^+$
$A > B$	$A - B$ is positive definite
$A \geq B$	$A - B$ is positive semi-definite
$\star$	Symmetric block with respect to the main diagonal of a matrix
$\bullet$	Represents an element that has no influence on development
ℓ_2	Energy-bounded signal space

CONTENTS

1 INTRODUCTION 18
1.1 CONTEXTUALIZATION 18
1.1.1 LPV systems 19
1.1.2 Delayed systems 20
1.1.3 Saturating systems 22
1.1.4 Networked Control Systems 24
1.1.4.1 Event-triggered control 24
1.2 OBJECTIVES 27
1.3 STRUCTURE OF THE THESIS 27
2 SYNTHESIS OF PARAMETER-DEPENDENT STATE-FEEDBACK CONTROLLERS 29
2.1 PROBLEM STATEMENT 29
2.2 PRELIMINARY RESULTS 32
2.2.1 Augmented model description 32
2.2.2 Auxiliary Results 33
2.3 MAIN RESULTS 35
2.3.1 Optimization design procedures 39
2.3.1.1 Maximization of the disturbance tolerance (δ^{-1}) 39
2.3.1.2 Maximization of the estimate of the region of attraction ($\mathcal{R}_{\mathcal{E}}$) 39
2.4 NUMERICAL EXAMPLES 40
2.5 CONCLUDING REMARKS 43
3 SYNTHESIS OF PARAMETER-DEPENDENT DYNAMIC OUTPUT CONTROLLERS 45
3.1 PROBLEM STATEMENT 45
3.2 PRELIMINARY RESULTS 47
3.2.1 Augmented model description 47
3.2.2 Regional stability analysis 49
3.3 MAIN RESULTS 52
3.3.1 Optimization design procedures 56
3.3.1.1 Maximization of disturbance tolerance (δ^{-1}) 56
3.3.1.2 Maximization of the estimate of the region of attraction $\mathcal{R}_{\mathcal{E}}$ 57
3.4 NUMERICAL EXAMPLES 57
3.4.1 Example 1 57
3.4.2 Example 2 60
3.5 CONCLUDING REMARKS 65
4 EVENT-TRIGGERED DYNAMIC OUTPUT-FEEDBACK CONTROL CO-DESIGN 66

4.1 PROBLEM STATEMENT 66
4.2 PRELIMINARY RESULTS 69
4.3 EMULATION-BASED APPROACH 71
4.4 CO-DESIGN APPROACH 74
4.4.1 Optimization design procedures 76
4.4.1.1 Minimization of the update rate 76
4.4.1.2 Minimization of the update rate for a given region of admissible initial conditions $\mathcal{X}_0$: 77
4.5 NUMERICAL EXAMPLES 78
4.5.1 Example 1 78
4.5.2 Example 2 84
4.5.3 Example 3 85
4.6 CONCLUDING REMARKS 86
5 EVENT-TRIGGERED CO-DESIGN UNDER PARAMETER-ERROR . 88
5.1 PROBLEM STATEMENT 88
5.2 PRELIMINARY RESULTS 91
5.3 MAIN RESULTS 92
5.3.1 Optimization design procedure 98
5.4 NUMERICAL EXAMPLES 99
5.4.1 Example 1 99
5.4.2 Example 2 101
5.4.3 Example 3 103
5.5 CONCLUDING REMARKS 104
6 CONCLUSION 105
6.1 PERSPECTIVES 106
6.2 PUBLICATIONS 107
REFERÊNCIAS 109

1 INTRODUCTION

1.1 CONTEXTUALIZATION

With the technological advances that occurred mainly in the last few decades, the use of communication networks has become common in industrial control loops (ZHANG, W. et al., 2001; TIPSUWAN; CHOW, 2003). This can be explained by the several advantages that this configuration offers compared to dedicated point-to-point connections, such as lower cost, ease of maintenance, and flexibility. However, as the network is often limited, some problems arise with its introduction, such as network congestion and elevated energy consumption on wireless systems. In this context, aiming at better use of network resources, aperiodic control strategies have been studied, where a control task is executed only when some condition is met. Among these strategies, the event-triggered control (ETC) (TABUADA, 2007) paradigm stands out. In such a technique, an event generator monitors some system variable (state or output) and generates an event only when a criterion based on this monitored variable is verified. Consequently, the ETC is capable of reducing the transmission activity while guaranteeing stability and some performance index of the control system. Therefore, the introduction of an efficient event-triggering mechanism to reduce unnecessary waste of resources and computation becomes meaningful in such a scenario.

Moreover, it is well-known that the practical control systems can have their dynamic behaviors affected by time delay, uncertainties, external disturbances, nonlinearities such as saturation, among other characteristics that can generate inconveniences to the control loop. The time delay, for instance, can cause oscillation, poor performance, and even instability. To overcome such issues, several techniques have been proposed in the literature (FRIDMAN, 2014). Still, the analysis and control design of time-delay systems can become theoretically more involved in the presence of saturating actuators because even if the system is stable in the absence of control constraints, it can destabilize otherwise for some initial conditions. So, a fundamental task, in such a case, is to determine a set of all initial conditions such that the trajectories are guaranteed to converge to the origin, which is admittedly challenging (TARBOURIECH et al., 2011). In the case of exogenous signals affecting the system, it is also important to characterize a set of admissible signals for which the trajectories are guaranteed to be bounded. Therefore, the development of better control techniques that deal with all these difficulties has become one of the significant challenges in recent times.

This work fits in both scenarios, in which new methodologies are proposed for the control of two classes of discrete-time linear parameter varying systems under input constraints. The first one considers that the system is also affected by time-varying delays in the states and external energy-bounded disturbances, and the second assumes that the system is inserted into a communication network with limited bandwidth. In

sequence, the main topics related to this work are described and their main objectives are enumerated.

1.1.1 LPV systems

Linear parameter-varying (LPV) systems concern a class of linear dynamical systems whose state-space matrices depend linearly on parameters that change over time (BRIAT, 2015). These parameters are usually unknown but supposed to be measured or estimated in real-time. Such a feature allows us to model a wide variety of time-varying and nonlinear plants. As a consequence, the analysis and control design of LPV systems has been extensively studied and employed in various engineering applications in the last decades as nonholonomic mobile robotic (HUANG, J. et al., 2014), missile autopilots (WHITE, B. A. et al., 2007), semi-active vehicle suspension design (POUSSOT-VASSAL et al., 2008), turbofan engines (GILBERT et al., 2007), among others (see (WHITE, A. P. et al., 2013) and the references therein).

The paradigm of LPV systems was first introduced by Shamma (1988) in his Ph.D. thesis for systematic analysis and synthesis of “gain-scheduled” controllers. In broad terms, the design of a gain-scheduled controller for a nonlinear plant can be described as a four-step procedure. First, determine a family of Linear time-invariant (LTI) models by selecting several operating conditions that cover the range of the plant’s dynamics. Then, design a linear controller for each linearized model. Next, based on the current value of the parameter-varying (measured or estimated online), schedule the local controller using some interpolation or switching method. The final step consists of verifying the closed-loop stability and performance using extensive simulation. Although the system performance can be improved by increasing the number of local models (at the price of increasing the computational burden), this approach may be unreliable, since the closed-loop stability and performance are only verified through simulation. In contrast, the modern control approaches start from an LPV representation and derive conditions for the synthesis of parameter-dependent controllers with a guarantee of stability, performance, and robustness for the closed-loop system. The computational tools of the convex optimization are usually employed in this case (MOHAMMADPOUR; SCHERER, C. W., 2012).

The scheduling parameters that govern the variation of the system dynamics can be classified into two types: *i)* exogenous, if they are a function of internal plant variables and exogenous signals, or *ii)* endogenous, if they are a function of the state variables. This latter case comes from the approximation of nonlinear systems as LPV systems, in which the nonlinear terms are used as scheduling variables. The resulting model is better known as *quasi*–LPV systems (RUGH; SHAMMA, 2000). A similar framework is based on Takagi-Sugeno systems where nonlinear systems can be represented in terms of a state-dependent convex combination of LTI systems (TAKAGI; SUGENO,

1985).

In the last decades, many approaches addressing stability analysis and control design of LPV systems have been proposed. The Lyapunov theory has been fundamental in both cases, mainly because it leads to convex optimization conditions involving Linear matrix inequality (LMI), which can be solved efficiently using specialized packages as the Matlab toolbox YALMIP (LOFBERG, 2004). The first works used the notion of quadratic stability, where the Lyapunov matrix is assumed constant and independent of the scheduling parameters. However, it is well known that the use of these functions, although appealing from a computation point of view, can lead to conservative results. This occurs because of the absence of restrictions on how fast the parameters may vary. To improve accuracy and precision, the parameter-dependent Lyapunov functions have been introduced with linear (polytopic) and affine structures by, amongst others, (DAAFOUZ; BERNUSSOU, 2001; MONTAGNER et al., 2005; OLIVEIRA; PERES, 2008; DE CAIGNY et al., 2010), and homogeneous polynomial parameter-dependent matrices in, for instance, (OLIVEIRA; PERES, 2009; DE CAIGNY et al., 2009; WANG, L.; LIU, X., 2011; DE CAIGNY et al., 2012; RODRIGUES et al., 2018).

Despite the theoretical advances in the LPV control field, the implementation of LPV controllers in physical hardware often meets significant difficulties, as the continuous-time control design approaches are commonly preferred in the literature over the discrete-time ones. In these cases, an efficient discretization of such a system representation is required, which is not an easy task (TÓTH et al., 2008). On the other hand, LPV identification methods are almost exclusively developed for discrete-time (VERDULT, 2002; TÓTH, 2010), as in this setting it is much easier to handle the estimation of parameter-varying dynamics (LAURAIN et al., 2011). Such facts have motivated the research on discrete-time LPV control design methods (HEEMELS et al., 2010; DE CAIGNY et al., 2012; EMEDI; KARIMI, 2016; PANDEY; DE OLIVEIRA, 2017; PEIXOTO et al., 2020).

1.1.2 Delayed systems

A characteristic that can be found in a variety of dynamic systems, among them, chemical, mechanical, biological, and economic, is the time-delay (GU et al., 2003; NICULESCU, 2001). Its presence in control loops usually induces complex behaviors such as oscillations, instability, and poor performance. Due to its unavoidable existence and adverse effects, the time-delay systems have been a frequent topic of studies in control systems (see (RICHARD, 2003) for an interesting overview). Usually, stability conditions for time-delay systems can be classified into two types: delay-independent or delay-dependent. In the former, the stability is guaranteed regardless of the size of the delay, while in the latter, the size of the delay is directly taken into account. In general, delay-dependent stability conditions are less conservative than delay-independent ones

especially when the time-delay is small. As a consequence, great attention has been paid to the study of delay-dependent stability conditions to obtain increasingly less conservative results (ZHANG, X. M. et al., 2019). Most of the existing approaches are formulated, by using Lyapunov-Krasovskii functionals, in terms of LMIs, which can be efficiently solved by numerical algorithms.

Although the continuous-time systems with time-delay have been further investigated in the literature, the discrete-time ones have received considerable attention in the last decades. In the mid-1980s, (ASTRÖM; WITTENMARK, 1984) proposed the rewriting of discrete-time systems with time-delay, characterized via delay difference equations, in higher-order delay-free systems. This system augmentation approach has been extensively used in practice, however, to characterize delay-independent stability and deal with time-varying delays, it is not applicable (KAPILA; HADDAD, 1998). Such cases were later treated, for instance, by (SONG, S. H. et al., 1999; CHEN, W. H. et al., 2003; HETEL et al., 2008; MIRANDA; LEITE, V., 2011). In particular, Hetel et al. (2008) proposed to rewrite discrete-time systems with time-varying delay as augmented delay-free switched systems, where the switched law is given by the delay value itself. That is, by considering the augmented state vector $\bar{x}_k = \begin{bmatrix} x_k^\top & x_{k-1}^\top & \dots & x_{k-\bar{\tau}}^\top \end{bmatrix}^\top$, the dynamics of the following discrete-time system

$$x_{k+1} = Ax_k + A_d x_{k-\tau_k}, \tag{1}$$

with time-varying delay $\tau_k \in \mathcal{I}[0, \bar{\tau}]$, can be represented by the augmented delay-free switched system given by

$$\bar{x}_{k+1} = \mathbb{A}(\tau_k)\bar{x}_k \tag{2}$$

where

$$\mathbb{A}(\tau_k) = \left[\begin{array}{ccccc|c} A(\tau_k) & \Gamma_1(\tau_k) & \Gamma_2(\tau_k) & \dots & \Gamma_{\bar{\tau}-1}(\tau_k) & \Gamma_{\bar{\tau}}(\tau_k) \\ \hline \multicolumn{5}{c|}{\mathbf{I}_{n\bar{\tau}}} & \mathbf{0}_{n\bar{\tau}\times n} \end{array}\right]$$

with

$$\Gamma_i(\tau_k) = \begin{cases} A_d, & \text{if } i = \tau_k, \\ \mathbf{0}_{n\times n}, & \text{otherwise,} \end{cases} \quad \forall i \in \mathcal{I}[1, \bar{\tau}].$$

Note that the block A_d changes its position according to i. The asymptotic stability, in this case, can be checked by using the most general form of the Lyapunov-Krasovskii functional, obtained through the sum of all the possible combinations of quadratic forms,

$$V(k, \bar{x}_k, \tau_k) = \bar{x}_k^\top P_{\tau_k} \bar{x}_k = \sum_{i=0}^{\bar{\tau}} \sum_{j=0}^{\bar{\tau}} x_{k-i}^\top P_{\tau_k}^{i,j} x_{k-j}, \quad i, j \in \mathcal{I}[0, \bar{\tau}]. \tag{3}$$

Thus, the approach proposed by Hetel et al. (2008) may lead to less conservative results than the works based on a Lyapunov-Krasovskii theory. On the other hand, the size of the delay imposes a limitation on applying such an approach, due to the dimensional explosion when dealing with large delays. In view of the above, for NCS

applications, the delays induced by the network are relatively small and fits well to the proposed methodology.

Although Hetel et al. (2008) have presented an innovative method of representing the systems with time-varying delay, this method has still been little explored in the literature (see, for instance, the discussion in (DE SOUZA, 2017)).

The LPV systems with time-delay have also been the subject of studies in the past years with a greater focus on continuous-time setup (see (WU, F.; GRIGORIADIS, 2001; BRIAT et al., 2011; ZOPE et al., 2012; JING et al., 2015; NEJEM et al., 2017)) than discrete-time one. In (JUNLING et al., 2008), a new delay-dependent and parameter-dependent $\mathcal{H}_\infty$ performance criterion to design gain-scheduled controllers and state observers is proposed. The problem of $\mathcal{H}_\infty$ static output-feedback control is addressed in (ROSA et al., 2018), in which new synthesis conditions capable of synthesizing either robust or gain-scheduled controllers are provided in terms of sufficient parameter-dependent LMIs with a scalar parameter. In (LEITE, V. J. S. et al., 2010), a partially parameter-dependent dynamic output-feedback controller, which output is based on the current and delayed outputs of the system, is derived through convex conditions. In all the above cases, the systems are affected by time-varying delays and the parameter-dependent Lyapunov approach is used in their formulations. In (MAHMOUD, 2000), conditions for stability analysis (employing the notions of quadratic stability and affine quadratic stability) and synthesis of state-feedback controllers which guarantee quadratic stability and an induced ℓ_2-norm bounded are developed for systems with unknown but bounded delay. For the same system, Zhou and Zheng (2008) applied a parameter-dependent Lyapunov function to establish a new delay-dependent $\mathcal{H}_\infty$ performance condition to design gain-scheduled controllers.

1.1.3 Saturating systems

The saturation is a nonlinearity widely encountered in practical systems. It is related, in general, to the physical/technical and/or safety limits imposed by actuators. Several undesirable problems can arise in a control loop due to its presence such as performance degradation, the occurrence of limit cycles or multiple equilibrium points, and even instability. From the stability point of view, the consequence of saturating actuators is that even if a linear control law stabilizes a system, the origin of the closed-loop system can become unstable for certain initial conditions. Therefore, a fundamental task to be considered in this case refers to the determination of a region of admissible initial conditions, better known as the region of attraction of the origin for the system. As the exact numerical characterization of this region is, generally, a hard task, estimates with a well-fitted analytical representation are then investigated (see, for instance, (HU; LIN, 2001; TARBOURIECH et al., 2011) for more details). However, it is important to point out that the presence of delays and/or parameters-varying in a system makes the

estimation of this region even more challenging.

The saturation effects are perceptible when the controller has slow, critically stable, or unstable modes (DOYLE et al., 1987; TARBOURIECH et al., 2011). This is always the case for a controller with integral action. It is observed that, due to input saturation, the integrator state “winds up” to excessively large values, leading to a large overshoot and a high settling time. To overcome this, an additional control loop, called “anti-windup” compensation can be added to the closed-loop system. The basic principle of anti-windup strategies consists of determining the difference between the signal computed by the controller and the signal effectively applied to the plant and then feed back this amount to the controller using a static or a dynamic structure. From this, acceptable performance is achieved when the actuators saturate, and when they do not, the closed-loop performance remains unchanged. Besides being related to performance improvement, anti-windup compensation can also be used to increase the region of attraction of the origin (or its estimate) for the system (TARBOURIECH et al., 2011).

The presence of disturbance signals is also a challenge when dealing with systems subject to saturating actuators since it makes it impossible to ensure the confinement of the state trajectories within the region of attraction. In this case, it is necessary to determine sets of admissible disturbance signals, besides those of initial conditions, for which the state trajectories are bounded. Furthermore, if the disturbance vanishes, the convergence of the state trajectories to the origin (equilibrium point) must be guaranteed. These admissible sets are in general characterized with bounds on the amplitude (ℓ_∞–norm) or on the energy (ℓ_2–norm) of the disturbance signal. This problem is referred to as Input-to-state stability (ISS) analysis (TARBOURIECH et al., 2011).

During the past years, the class of LPV systems subject to saturating actuators has been investigated with a greater focus on continuous-time systems, (see, for instance, (CAO et al., 2002; MONTAGNER et al., 2007; DO et al., 2011; NGUYEN et al., 2018; RUIZ et al., 2019)) than on the discrete-time ones. An algorithm to design a gain-scheduled state feedback controller that minimizes the worst-case performance of LPV systems with input saturation represented in the polytopic form is proposed in (WANG, L.; LIU, X., 2011) with the aid of homogeneous polynomially parameter-dependent Lyapunov functions. A synthesis approach of dynamic output feedback robust model predictive control for LPV systems with unknown scheduling parameters subject to input saturation and bounded disturbances is investigated in (PING et al., 2017). A nonlinear time-varying parameter-dependent system under input saturation is studied in (JUNGERS; CASTELAN, 2011; CORSO et al., 2009; CASTELAN et al., 2010), where conditions to design a dynamic output feedback (CASTELAN et al., 2010) and a gain-scheduled feedback (of the measured output and the nonlinearity) (CORSO et al., 2009; JUNGERS; CASTELAN, 2011) controllers are formulated based on parameter-

dependent Lyapunov functions.

With respect to the LPV systems with time-delay subject to saturating actuators, some robust approaches have been proposed for both continuous-time (EL HAOUSSI; TISSIR, 2006; LIU, P. L., 2011; DOU et al., 2014; WEI et al., 2015) and discrete-time frameworks (XU et al., 2012; ZHANG, L. et al., 2014; SONG, G. et al., 2015; PAL; NEGI, 2018). However, considering the design of parameter-varying controllers, this number is much smaller. A scheduled controller design method, developed to avoid saturation and to guarantee the locally ISS of the continuous-time closed-loop system is proposed in (LI, P. et al., 2018). A delay partitioning approach was used in (SONG, G.; WANG, Z., 2013) to solve the problem of designing a dynamic output feedback controller that ensures that all trajectories of the discrete-time closed-loop system converge to a smaller ellipsoid for every initial condition from an admissible domain.

1.1.4 Networked Control Systems

Networked control systems (NCS), as its name suggests, are systems in which the control loop is closed through a communication network. This structure allows the information (reference input, plant output, control input, etc.) of the system to be exchanged among all their components (sensors, controllers, actuators, etc.), which are usually geographically distributed. Thus, the NCS connect cyberspace to physical space so that the execution of several tasks is remotely allowed (ZHANG, W. et al., 2001).

In contrast to point-to-point connections, NCS have several advantages as low cost, reduced weight and power requirements, simple installation and maintenance, and high-reliability (ZHANG, W. et al., 2001). As a consequence, NCS have been employed in a variety of fields such as industrial control, aerospace systems, intelligent systems, teleoperation, among others. However, the insertion of a network in a control loop may also cause undesired effects on the account of limited network bandwidth and computing capacity, such as time-varying delays, unequal sampling intervals, and packet dropouts, which usually leads to performance degradation or ever unstable behavior of NCS (MAHMOUD; HAMDAN, 2018; BEMPORAD et al., 2010). Therefore, how to effectively allocate restricted transmission resources while ensuring the desired system performance becomes an essential task.

1.1.4.1 Event-triggered control

In traditional networked control setups, the transmission instants are determined purely based on time. Such a Time-triggered control (TTC) approach is predictable and easy to implement. However, it often results in redundant transmissions, as many of them occur at times when they are not necessary to achieve the desired stability and performance properties. As an alternative, the Event-triggered control (ETC) approach

adapts the transmission instants based on the current state, input and/or output measurement of the plant (HEEMELS et al., 2012). The main idea of ETC is to use the network only when is needed by generated transmissions whenever a state-, input-, and/or output-dependent condition is satisfied. In this way, ETC can significantly reduce the number of data transmissions while maintaining satisfactory control performance. In the context of ETC, two objectives can be pursued: *i)* Emulation: the event-triggering rules have to be designed for a given controller (EQTAMI et al., 2010; HEEMELS et al., 2012) and *ii)* Co-design: the joint design of the control law and the event-triggering rules has to be performed (PENG; YANG, T. C., 2013; ABDELRAHIM et al., 2014; LI, S. et al., 2015).

One of the fundamental challenges of ETC paradigm lies in choosing appropriate functions so that system stability and satisfactory performance are guaranteed and, at the same time, the communication resources are saved. In the last years, different kinds of event-triggering schemes have been proposed in the literature. Among them, the most classical form, the so-called static Event-triggering mechanism (ETM), is proposed on absolute error in (LUNZE; LEHMANN, 2010; ZHANG, J.; FENG, 2014) or relative error in (TABUADA, 2007; MENG; CHEN, T., 2014; MOREIRA et al., 2019) of the sampled value. By adding an internal dynamic variable into the static ETM, (GIRARD, 2014; BORGERS et al., 2017) investigate a dynamic ETM. Lyapunov functions have also been used for the trigger, as presented in (VELASCO et al., 2009; WANG, X.; LEMMON, 2008). Some of these event-triggering rules are shown in Table 1. It is important to point out that, there are several variations of these rules in the literature, which take into account, for instance, the output or the control input instead of the states.

Table 1 – Some types of ETMs employed in the literature.

Static ETM	Absolute error	$\|x(t)-x(t_k)\| \geq \sigma$ (LUNZE; LEHMANN, 2010)
		$\|x(t)-x(t_k)\| \geq \sigma(t)$ (ZHANG, J.; FENG, 2014)
	Relative error	$\|x(t)-x(t_k)\| > \sigma\|x(t)\|$ (TABUADA, 2007)
		$\|x(t)-x(t_k)\|_{Q_\Delta} > \|x(t)\|_{Q_x}$ (MOREIRA et al., 2019)
Dynamic ETM	$\eta(t) + \theta(\sigma\|x(t)\| - \|x(t)-x(t_k)\|) > 0$ (GIRARD, 2014)	
Lyapunov ETM	$V(t_{k+1}) > \sigma V(t_k)$ (VELASCO et al., 2009)	

Speaking of the ETC research for LPV systems, only a few results are available in the literature. (LI, S. et al., 2019) study the event-triggered fault detection problem for a class of continuous-time LPV systems with signal transmission delays. (LI, S. et al.,

2015) proposes the event-triggered $\mathcal{H}_\infty$ control for discrete polytopic LPV systems by jointly designing a mixed event-triggering mechanism and a state-feedback controller. For the same class of systems, (SAADABADI; WERNER, 2020) present a co-design condition for an event generator and a dynamic output feedback controller with bounds on the ℓ_2-performance. Considering the influence of network-induced delays and external disturbances, (HUANG, J. J. et al., 2020) addresses the event-triggered and self-triggered $\mathcal{H}_\infty$ output tracking control for the same class of systems. However, in these works, the information about the scheduling parameters is assumed available for the controller all the time, which does not occur in practice. In contrast, (SHANBIN; BUGONG, 2013) proposes the co-design of an event generator and a state-feedback controller for discrete polytopic LPV systems, where the parameters are not exactly known, but their estimated values satisfy a known uncertainty level. With the same assumption about the scheduling parameters, (XIE et al., 2018) establish a co-design condition in a sense of input-to-state practically stable (ISpS) of a general mixed ETM and a static output-feedback controller. The problem of discretization and event-based digital static output feedback control design for continuous polytopic LPV systems with networked-induced delay is addressed in (BRAGA et al., 2015), where the event mechanism is based on a significant change of the scheduling parameter. (GOLABI et al., 2017) investigate an event-based reference tracking control for discrete polytopic LPV systems by simultaneously designing a state feedback controller and ETMs for the output, the control input, and the scheduling variables.

The ETC research has also been extended to consider saturating actuators, both in the continuous-time (see, for example, (ZHANG, L. et al., 2014; KIENER et al., 2014; NI et al., 2015; SEURET et al., 2016; LIU, D.; YANG, G. H., 2017; LI, L. et al., 2017)) and in the discrete-time setting. (WU, W. et al., 2014) propose a procedure to design a state-feedback controller that maximizes the domain of attraction of a discrete-time system under input saturation for a given event-triggering condition. Another approach to maximize the domain of attraction concerns discrete-time piecewise affine saturated systems under event-based state-feedback controllers. However, the co-design is not addressed in these cases, which may lead to conservative results. The main difficulty in obtaining co-design approaches lies in the nonlinear relations among the optimization variables involved. To overcome such an issue, authors in (ZUO et al., 2016) suggest a cone complementary linearization algorithm for solving a non-convex optimization problem yielding a method to co-design an event-triggering strategy and a state-feedback controller for a discrete-time system under input saturation. (GROFF et al., 2016; DING et al., 2020) address the simultaneous design of a static state-feedback controller and an event-triggered mechanism, using similarity transformations, ensuring the regional stability of saturating discrete-time systems. Also, (DING et al., 2020) considers the co-design based on a dynamic state stabilizing controller.

However, up to now, no ETC research has been reported to discrete-time LPV systems subject to saturating actuators. This also aroused us to investigate this interesting and challenging problem because of its great potential in practical applications.

1.2 OBJECTIVES

Based on the above discussions, the main objective of this thesis is to develop convex conditions for analysis and synthesis of controllers ensuring stability and some performance index for two classes of systems: *i)* discrete-time LPV systems with time-varying delayed states subject to saturating actuators and energy bounded disturbances and *ii)* discrete-time LPV systems subject to saturating actuators inserted into a communication network with limited bandwidth. As specific objectives, we can enumerate:

1. To develop a parameter-dependent state-feedback controller design method for the class of systems *i)*, by exploring the augmented delay-free switched modeling given in (2);
2. To develop a parameter-dependent dynamic output-feedback controller design method for the class of systems *i)*, by exploring the augmented delay-free switched modeling given in (2);
3. To develop a co-design method of a parameter-dependent dynamic output-feedback controller and two independent event-triggering mechanisms, that transmit the output and the control input, for the class of systems *ii)*.
4. To develop a co-design method of a parameter-dependent state-feedback controller and two independent event-triggering mechanisms that transmit the states and the scheduling parameter for the class of systems *ii)*.
5. To implement computationally the developed conditions and compare them with other approaches found in the literature.

1.3 STRUCTURE OF THE THESIS

This thesis is organized into five chapters, as follows:

This chapter presents a brief introduction and a review of the state of the art of the main themes related to the subject of study of this thesis, namely: LPV systems, time-delay, input saturation, and event-triggered control. In addition, the main and specific objectives of the work are delimited in it.

Chapters 2 and 3 address the problem of regional stabilization of discrete-time LPV systems with time-varying delayed states subject to saturating actuators and ℓ_2–energy disturbances. Chapter 2 provides convex conditions for the synthesis of

parameter-dependent state-feedback controllers, while Chapter 3 presents convex conditions for the synthesis of parameter-dependent dynamic output-feedback controllers with anti-windup action. The proposed controllers have characteristics that differentiate them from those normally investigated in the literature, as will be evidenced in the chapters. Both approaches are based on rewriting the delayed system under saturating actuators in an augmented delay-free switched system with a dead-zone nonlinearity. Also, they employ the input-to-state stability concept to handle the energy bounded disturbances. Finally, with the aid of a more generalized Lyapunov function jointly with the generalized sector condition, they provide linear matrix inequalities (LMIs) based formulations. Such a fact also implies a characterization of estimates for the domain of attraction in an augmented space. It is important to highlight that such a methodology presented relevant results in the student's previous works (DE SOUZA, 2017; DE SOUZA et al., 2019b).

Chapters 3 and 4 concern the event-triggered control of discrete-time LPV systems subject to saturating actuators. Chapter 3 provides convex conditions for the co-design of two event generators and a parameter-dependent dynamic output-feedback controller with anti-windup action. The event-triggering mechanisms are responsible for independently transmitting the sensor measurements and the controller output through communication channels. On the other hand, Chapter 4 presents convex conditions for the co-design of two event-generators and a parameter-dependent state-feedback controller. In this case, the event-triggering mechanisms independently manage the transmission of the states and the scheduling parameter from the sensor to the controller. Such a fact allows the controller scheduling parameter to be different from that of the plant, which yields a certain degree of robustness concerning parameter deviations. Both approaches are formulated with the aid of a parameter-dependent Lyapunov function along with the generalized sector condition, which leads to a set of linear matrix inequalities (LMIs) that, if feasible, ensure the regional asymptotic stability of the closed-loop system and provides an estimate of the domain of attraction.

Chapter 5 presents some conclusions and recommendations for future research. The appendices complement the thesis by introducing some additional information useful in understating it.

2 SYNTHESIS OF PARAMETER-DEPENDENT STATE-FEEDBACK CONTROLLERS

This chapter addresses the regional stabilization problem of discrete-time LPV systems with time-varying delayed states subject to saturating actuators and exogenous signals. The proposed controller consists of a parameter-dependent state-feedback one, whose structure may include delayed states, without requiring the online knowledge of the delay. In this sense, convex conditions are established to regionally ensure the input-to-state stability of the closed-loop system for a set of initial conditions and admissible ℓ_2-energy bounded exogenous signals. They take into account the maximum variation of delay between two consecutive instants.

To derive the convex formulation, the Lyapunov theory is used yielding a set of LMI conditions. Additionally, the delayed system with input saturation is rewritten in terms of an augmented delay-free switched system with a dead-zone nonlinearity, which enables the application of the generalized sector condition. Some convex optimization procedures are also proposed allowing to enlarge the set of initial conditions or the maximum allowable disturbance energy. Finally, a numerical example is used to illustrate the effectiveness of the methodology developed. The results presented are based on the work (DE SOUZA et al., 2018). Moreover, they can be seen as an extension of the works (DE SOUZA, 2017; DE SOUZA et al., 2018), in which robust state-feedback controllers are designed. Also, a similar approach can be found in (DE SOUZA et al., 2019c).

2.1 PROBLEM STATEMENT

Consider the class of discrete-time LPV systems with time-varying delay in the states subject to saturating actuators and energy bounded disturbances represented by:

$$x_{k+1} = A(\alpha_k)x_k + A_d(\alpha_k)x_{k-\tau_k} + B(\alpha_k)\text{sat}(u_k) + B_\omega(\alpha_k)\omega_k, \tag{4}$$

with a sequence of initial condition $\varphi_{\bar{\tau},0} = \{x_{-\bar{\tau}}, x_{-\bar{\tau}+1}, \ldots, x_0\}$, where $x_k \in \mathbb{R}^n$ is the state vector, $u_k \in \mathbb{R}^{n_u}$ is the control signal and $\omega_k \in \mathbb{R}^{n_\omega}$ is the disturbance input vector belonging to

$$\mathcal{W}(\delta) = \left\{ \omega_k \in \mathbb{R}^{n_\omega} : \sum_{k=0}^{\infty} \omega_k^\top \omega_k \leq \delta^{-1} \right\}, \tag{5}$$

with $\delta^{-1} \in \mathbb{R}^+$ representing the energy bound of the disturbance. The symmetric decentralized vectorial saturation function, $\texttt{sat}(u_k)$, is defined as

$$\texttt{sat}(u_{k(\ell)}) = \texttt{sign}(u_{k(\ell)}) \min(|u_{k(\ell)}|, \bar{u}_{(\ell)}), \tag{6}$$

with $\bar{u}_{(\ell)} > 0$, $\ell \in \mathcal{I}[1, n_u]$, denoting the symmetric amplitude bound relative to the ℓ^{th} control input. The vector of time-varying parameters, $\alpha_k \in \mathbb{R}^N$, which is assumed

measured and available on-line (BRIAT, 2015), lies in the unitary simplex given by

$$\Lambda \triangleq \left\{ \alpha_k \in \mathbb{R}^N : \sum_{i=1}^{N} \alpha_{k(i)} = 1,\ \alpha_{k(i)} \geq 0, i \in \mathcal{I}[1, N] \right\}. \tag{7}$$

Thus, the parameter-dependent matrices $A(\alpha_k) \in \mathbb{R}^{n\times n}$, $A_d(\alpha_k) \in \mathbb{R}^{n\times n}$, $B(\alpha_k) \in \mathbb{R}^{n\times n_u}$ and $B_\omega(\alpha_k) \in \mathbb{R}^{n\times n_\omega}$ can be written in the polytopic form, that is, as a convex combination of N known vertices according to

$$\begin{bmatrix} A(\alpha_k) & A_d(\alpha_k) & B(\alpha_k) & B_\omega(\alpha_k) \end{bmatrix} = \sum_{i=1}^{N} \alpha_{k(i)} \begin{bmatrix} A_i & A_{di} & B_i & B_{\omega i} \end{bmatrix}. \tag{8}$$

The time-varying delay, $\tau_k \in \mathbb{Z}^+$, satisfies

$$\tau_k \in \mathcal{I}[\underline{\tau}, \bar{\tau}],\ \text{subject to } |\tau_{k+1} - \tau_k| \leq \Delta\tau_{\max} \leq (\bar{\tau} - \underline{\tau}), \tag{9}$$

where $\underline{\tau}, \bar{\tau} \in \mathbb{Z}$ are the minimum and the maximum known delay limits, respectively, and $\Delta\tau_{\max} \in \mathbb{Z}$ is the maximum delay variation between two consecutive instants. According to (DE SOUZA et al., 2018), we can define a set $\mathcal{C}(\tau_k)$ that contains all possible values that the delay can assume at the next instant given its value at the current instant:

$$\mathcal{C}(\tau_k) = \left\{ \tau^+ \in \mathcal{I}[\max(\underline{\tau}, \tau_k - \Delta\tau_{\max}), \min(\bar{\tau}, \tau_k + \Delta\tau_{\max})] \right\},$$

where τ^+ is a shorthand for τ_{k+1}. To exemplify, consider $\underline{\tau} = 0$, $\bar{\tau} = 5$, $\Delta\tau_{\max} = 1$ and $\tau_k = 2$, then we have $\tau^+ \in \{1, 2, 3\} = \mathcal{C}(2)$. In particular, the delay is time-invariant if $\Delta\tau_{\max} = 0$.

To regionally stabilize system (4), we propose the following parameter-dependent state-feedback control law

$$u_k = \mathbb{K}(\alpha_k)\bar{x}_k, \tag{10}$$

where the augmented state $\bar{x}_k \in \mathbb{R}^{(\bar{\tau}+1)n}$ is defined by

$$\bar{x}_k = \begin{bmatrix} x_k^\top & x_{k-1}^\top & \cdots & x_{k-\bar{\tau}}^\top \end{bmatrix}^\top \tag{11}$$

and the control gain matrix $\mathbb{K}(\alpha_k)$ is described as

$$\mathbb{K}(\alpha_k) = \sum_{i=1}^{N} \alpha_{k(i)} K_i, \tag{12}$$

with $\alpha_k \in \Lambda$ and $K_i \in \mathbb{R}^{n_u\times(\bar{\tau}+1)n}$ assuming the full structure $K_i = \begin{bmatrix} K_{i,0} & K_{i,1} & \cdots & K_{i,\bar{\tau}} \end{bmatrix}$ for all $i \in \mathcal{I}[1, N]$. As a consequence of the definition of the augmented vector $\bar{x}_k$, we have that the sequence of initial conditions ensuring the uniqueness of the solution of (4) can be represented by $\varphi_{\bar{\tau},0} = \bar{x}_0 = \begin{bmatrix} x_0^\top & x_{-1}^\top & \cdots & x_{-\bar{\tau}}^\top \end{bmatrix}^\top$.

Remark 2.1 *We can refer to (10), as a complete state-feedback control law, since the whole state-feedback trajectory from $k-\bar{\tau}$ to k are fed back. In this case, the controller depends only on the maximum value of the delay $\bar{\tau}$, and not on its current value τ_k, which makes it independent of the delay. Note that control laws that dispense knowledge of the current value of the delay are easier to implement than those that need this information as, for instance, $u_k = K_0(\alpha_k)x_k + K_{\tau_k}(\alpha_k)x_{k-\tau_k}$* (SILVA et al., 2014)*. Besides, it is interesting to highlight that more specialized forms can be generated from the structure of (10) as, for instance, $u_k = K_0(\alpha_k)x_k$ and $u_k = K_0(\alpha_k)x_k + K_{\bar{\tau}}(\alpha_k)x_{k-\bar{\tau}}$, in which the following structures are imposed on matrix $\mathbb{K}(\alpha_k)$: $\mathbb{K}_{c1}(\alpha_k) = \begin{bmatrix} K_0(\alpha_k) & 0 & \cdots & 0 \end{bmatrix}$ and $\mathbb{K}_{c2}(\alpha_k) = \begin{bmatrix} K_0(\alpha_k) & 0 & \cdots & K_{\bar{\tau}}(\alpha_k) \end{bmatrix}$, respectively.*

Because of saturating actuators, the closed-loop stability must be studied in the context of regional stability (TARBOURIECH et al., 2011). Thus, it is necessary to consider the existence of a region of attraction of the origin for the LPV system (4), $\mathcal{R}_{\mathcal{A}} \subseteq \mathbb{R}^{(\bar{\tau}+1)n}$, which characterization is not an easy task in general. Furthermore, we need to take into account the energy of ω_k such that all the trajectories remain inside $\mathcal{R}_{\mathcal{A}}$. Let us denote $\mathcal{R}_0$ the set of all initial states such that for a given $\delta > 0$ and $\omega_k \in \mathcal{W}(\delta)$ the respective trajectories of the closed-loop system remain in $\mathcal{R}_{\mathcal{A}}$, by noting that $\mathcal{R}_0 \subseteq \mathcal{R}_{\mathcal{A}}$. Therefore, we are interested in computing the estimates of $\mathcal{R}_{\mathcal{A}}$ and $\mathcal{R}_0$, called here $\mathcal{R}_{\mathcal{E}} \subseteq \mathcal{R}_{\mathcal{A}}$ and $\mathcal{R}_{\mathcal{E}0} \subseteq \mathcal{R}_0$, respectively. For this purpose, consider the following definition.

Definition 2.1 *The LPV system (4) in closed-loop with the parameter-dependent state-feedback controller (10) is referred to input-to-state stable (ISS), if for all $\omega_k \in \mathcal{W}(\delta)$, for all $\bar{x}_0 \in \mathcal{R}_{\mathcal{E}0} \subseteq \mathcal{R}_0$, and for all $\alpha_k \in \Lambda$, its trajectories are bounded in $\mathcal{R}_{\mathcal{E}} \subseteq \mathcal{R}_{\mathcal{A}}$ and if the disturbance vanishes, then $\lim_{k\to\infty} \bar{x}_k = 0$.*

This definition is depicted in Figure 1. It is supposed that at the instant k_0 the disturbance signal ω_k starts to act on the system, whose initial condition belongs to $\mathcal{R}_{\mathcal{E}0}$. In this case, the trajectories of the states evolve within the estimated attraction region $\mathcal{R}_{\mathcal{E}}$, which is contained in the attraction region $\mathcal{R}_{\mathcal{A}}$. From the instant $k > k_1$, when the disturbance signal ω_k vanishes, the states asymptotically converge to the origin.

Thus, the problem we intend to solve in this chapter can be stated as follows.

Problem 2.1 *For the saturating LPV system (4), determine the parameter-dependent state-feedback controller (10) and the sets $\mathcal{R}_{\mathcal{E}0} \subseteq \mathcal{R}_0$ and $\mathcal{R}_{\mathcal{E}} \subseteq \mathcal{R}_{\mathcal{A}}$, such that for all $\omega_k \in \mathcal{W}(\delta)$, for all $\bar{x}_0 \in \mathcal{R}_{\mathcal{E}0}$, and for all $\alpha_k \in \Lambda$, the resulting closed-loop system is regionally input-to-state stable (ISS).*

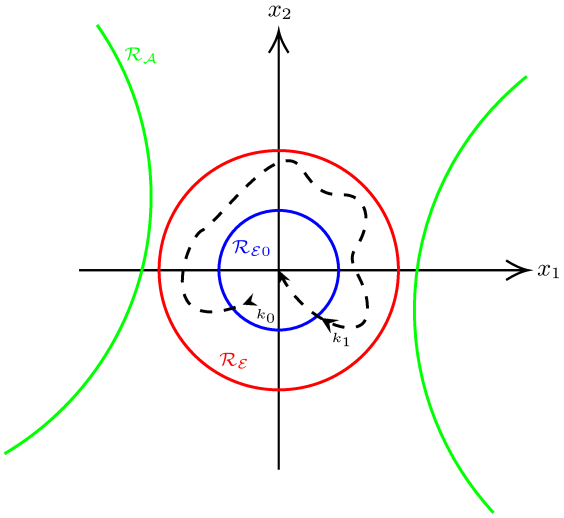

Figure 1 – Regions $\mathcal{R}_{\mathcal{A}}$, $\mathcal{R}_{\mathcal{E}}$ and $\mathcal{R}_{\mathcal{E}0}$.

2.2 PRELIMINARY RESULTS

In this section, we present an augmented model representation of the closed-loop system and some auxiliary results used to establish the main conditions.

2.2.1 Augmented model description

Following the approach proposed by Hetel et al. (2008), the LPV system (4) in closed-loop with the parameter-dependent state-feedback controller (10), can be rewritten, by using (11), as the following augmented delay-free switched discrete-time LPV system, where the switching law is the delay τ_k:

$$\bar{x}_{k+1} = \mathbb{A}(\alpha_k, \tau_k)\bar{x}_k + \mathbb{B}(\alpha_k)\mathtt{sat}(\mathbb{K}(\alpha_k)\bar{x}_k) + \mathbb{B}_\omega(\alpha_k)\omega_k, \tag{13}$$

where

$$\mathbb{A}(\alpha_k, \tau_k) = \left[\begin{array}{cccc|c} A(\alpha_k) + \Gamma_0(\alpha_k, \tau_k) & \Gamma_1(\alpha_k, \tau_k) & \cdots & \Gamma_{\bar{\tau}-1}(\alpha_k, \tau_k) & \Gamma_{\bar{\tau}}(\alpha_k, \tau_k) \\ \hline \multicolumn{4}{c|}{\mathbf{I}_{n\bar{\tau}}} & \mathbf{0}_{n\bar{\tau}\times n} \end{array}\right],$$

with

$$\Gamma_i(\alpha_k, \tau_k) = \left\{\begin{array}{ll} A_d(\alpha_k), & \text{if } i = \tau_k, \\ \mathbf{0}_{n\times n}, & \text{otherwise,} \end{array}\right. \quad \forall i \in \mathcal{I}[\underline{\tau}, \bar{\tau}],$$

$\mathbb{B}(\alpha_k) = \left[B^\top(\alpha_k) \quad \mathbf{0}_{n_u\times\bar{\tau}n}\right]^\top$, and $\mathbb{B}_\omega(\alpha_k) = \left[B_\omega^\top(\alpha_k) \quad \mathbf{0}_{n_\omega\times\bar{\tau}n}\right]^\top$.

By summing and subtracting $\mathbb{B}(\alpha_k)\mathbb{K}(\alpha_k)\bar{x}_k$ in the right side of (13) and using the (symmetric) dead-zone nonlinearity $\Psi(u_k) : \mathbb{R}^{n_u} \to \mathbb{R}^{n_y}$ defined by

$$\Psi(u_k) = \Psi(\mathbb{K}(\alpha_k)\bar{x}_k) = \mathbb{K}(\alpha_k)\bar{x}_k - \mathtt{sat}(\mathbb{K}(\alpha_k)\bar{x}_k), \tag{14}$$

we get

$$\bar{x}_{k+1} = \bar{\mathbb{A}}(\alpha_k, \tau_k)\bar{x}_k - \mathbb{B}(\alpha_k)\Psi(\mathbb{K}\bar{x}_k) + \mathbb{B}_\omega(\alpha_k)\omega_k, \tag{15}$$

where $\bar{\mathbb{A}}(\alpha_k, \tau_k) = \mathbb{A}(\alpha_k, \tau_k) + \mathbb{B}(\alpha_k)\mathbb{K}(\alpha_k)$.

2.2.2 Auxiliary Results

To handle the saturation phenomenon, we consider the (symmetric) dead-zone nonlinearity

$$\Psi(u_k) = u_k - \mathtt{sat}(u_k), \tag{16}$$

which verifies

$$\Psi(u_k)^\top \mathbb{T}(\alpha_k)(\Psi(u_k) - \upsilon_k) \leq 0, \tag{17}$$

for any positive definite diagonal matrix $\mathbb{T}(\alpha_k) \in \mathbb{R}^{n_u \times n_u}$ and for all $u_k, \upsilon_k \in \mathbb{R}^{n_u}$ belonging to the polyhedral set

$$\mathcal{S}(\bar{u}) = \left\{ u_k \in \mathbb{R}^{n_u}, \upsilon_k \in \mathbb{R}^{n_u} : |u_{k(\ell)} - \upsilon_{k(\ell)}| \leq \bar{u}_{(\ell)}, \forall \ell \in \mathcal{I}[1, n_u] \right\}. \tag{18}$$

As we can see, the set $\mathcal{S}(\bar{u})$ does not directly consider the bounds $\bar{u}$ over u_k, but instead over the difference between u_k and υ_k. In this sense, the auxiliary signal υ_k becomes an extra degree of freedom for the control signal u_k, allowing u_k to enlarge beyond its bounds (see (TARBOURIECH et al., 2011) for more details). Figure 2 shows the graphic description of saturation and dead-zone functions.

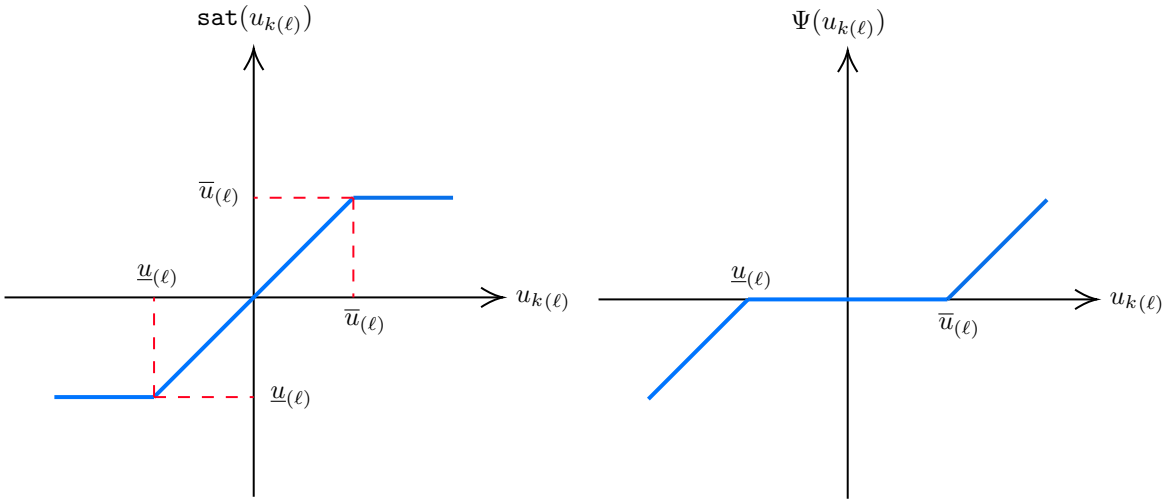

Figure 2 – Saturation and dead-zone functions.

Such a result can be specialized to handle Problem 2.1. Thus, by considering u_k given by (10) and $\upsilon_k = \mathbb{G}(\alpha_k)\bar{x}_k$, we have the following lemma directly derived from (TARBOURIECH et al., 2011, Lemma 1.6).

Lema 2.1 *Consider u_k given by (10), $\bar{u} \in \mathbb{R}^{n_u}$, $\bar{u} > 0$, and a matrix $\mathbb{G}(\alpha_k) = \sum_{i=1}^{N} \alpha_{k(i)} \mathbb{G}_i$, $\mathbb{G}_i \in \mathbb{R}^{n_u \times (\bar{\tau}+1)n}$, $i \in \mathcal{I}[1, N]$, $\alpha_k \in \Lambda$, such that*

$$\mathcal{S}(\bar{u}) \triangleq \left\{ \bar{x}_k \in \mathbb{R}^{(\bar{\tau}+1)n} : |(\mathbb{K}_{(\ell)}(\alpha_k) - \mathbb{G}_{(\ell)}(\alpha_k))\bar{x}_k| \leq \bar{u}_{(\ell)},\ \ell \in \mathcal{I}[1, n_u] \right\}. \tag{19}$$

If $\bar{x}_k \in \mathcal{S}(\bar{u})$, then for any positive definite diagonal matrix $\mathbb{T}(\alpha_k) = \sum_{i=1}^{N} \alpha_{k(i)} \mathbb{T}_i$, $\mathbb{T}_i \in \mathbb{R}^{n_u \times n_u}$, $i \in \mathcal{I}[1, N]$, $\alpha_k \in \Lambda$, the following inequality holds

$$\Psi(\mathbb{K}(\alpha_k)\bar{x}_k)^\top \mathbb{T}(\alpha_k)(\Psi(\mathbb{K}(\alpha_k)\bar{x}_k) - \mathbb{G}(\alpha_k)\bar{x}_k) \leq 0. \tag{20}$$

The regional input-to-state stability of the closed-loop LPV system (13) is investigated with the aid of the Lyapunov theory. Thus, we adopt the candidate Lyapunov function $V(\bar{x}_k, \alpha_k, \tau_k) : \mathbb{R}^{(\bar{\tau}+1)n} \times \Lambda \times \mathcal{I}[\underline{\tau}, \bar{\tau}] \longrightarrow \mathbb{R}^+$ with $V(\bar{x}_0, \alpha_0, \tau_0) = 0$ given by

$$V(\bar{x}_k, \alpha_k, \tau_k) = \bar{x}_k^\top W^{-1}(\alpha_k, \tau_k)\bar{x}_k, \tag{21}$$

where

$$W(\alpha_k, \tau_k) = \sum_{i=1}^{N} \alpha_{k(i)} W_{i,\tau_k}, \ \alpha_k \in \Lambda, \ \tau_k \in [\underline{\tau}, \bar{\tau}]. \tag{22}$$

with $0 < W_{i,\tau_k} = W_{i,\tau_k}^\top \in \mathbb{R}^{(\bar{\tau}+1)n \times (\bar{\tau}+1)n}$. Associated to $V(\bar{x}_k, \alpha_k, \tau_k)$, there exist a level set defined as

$$\mathcal{L}_\mathcal{V}(\mu) = \left\{ \bar{x}_k \in \mathbb{R}^{(\bar{\tau}+1)n} : V(\bar{x}_k, \alpha_k, \tau_k) \leq \mu^{-1}, \ \forall \alpha_k \in \Lambda, \ \forall \tau_k \in \mathcal{I}[\underline{\tau}, \bar{\tau}] \right\}, \tag{23}$$

for some real scalar $0 < \mu < \infty$. In the theorem and corollaries that will be presented later, sufficient conditions are provided to ensure that the level set $\mathcal{L}_\mathcal{V}(\mu)$ is an invariant and contractive set with respect to the trajectories of the closed-loop system (13). Therefore, $\mathcal{L}_\mathcal{V}(\mu)$ constitutes an estimate of the region of attraction of the origin for the system, i.e. $\mathcal{L}_\mathcal{V}(\mu) = \mathcal{R}_\mathcal{E} \subseteq \mathcal{R}_\mathcal{A}$ (TARBOURIECH et al., 2011). By taking inspiration from (JUNGERS; CASTELAN, 2011), we can state the following lemma demonstrating how to compute $\mathcal{L}_\mathcal{V}(\mu)$ from matrices $W(\alpha_k, \tau_k)^{-1}$.

Lema 2.2 *The level set $\mathcal{L}_\mathcal{V}(\mu)$ associated with $V(\bar{x}_k, \alpha_k, \tau_k)$ defined in (21) is computed as*

$$\mathcal{L}_\mathcal{V}(\mu) = \bigcap_{\substack{\forall \tau_k \in \mathcal{I}[\underline{\tau}, \bar{\tau}] \\ \forall \alpha_k \in \Lambda}} \mathcal{E}(W(\alpha_k, \tau_k)^{-1}, \mu) = \bigcap_{\substack{\forall \tau_k \in \mathcal{I}[\underline{\tau}, \bar{\tau}] \\ \forall i \in \mathcal{I}[1, N]}} \mathcal{E}(W_{i,\tau_k}^{-1}, \mu), \tag{24}$$

where $\mathcal{E}(W_{i,\tau_k}^{-1}, \mu)$ denotes the ellipsoidal sets represented by

$$\mathcal{E}(W_{i,\tau_k}^{-1}, \mu) = \left\{ \bar{x}_k \in \mathbb{R}^{(\bar{\tau}+1)n}; \ \bar{x}_k^\top W_{i,\tau_k}^{-1} \bar{x}_k \leq \mu^{-1}, \ \forall i \in \mathcal{I}[1, N], \ \forall \tau_k \in \mathcal{I}[\underline{\tau}, \bar{\tau}] \right\}. \tag{25}$$

The next lemma allows us to show the confinement of trajectories of the closed-loop system (13) in the level set $\mathcal{L}_\mathcal{V}(\mu)$.

Lema 2.3 *Assume that $V(\bar{x}_k, \alpha_k, \tau_k)$ in (21) is a Lyapunov function, $\alpha_k \in \Lambda$, $\tau_k \in \mathcal{I}[\underline{\tau}, \bar{\tau}]$, $\omega_k \in \mathcal{W}(\delta)$ for a given δ, and some $\beta > 0$ such that $\mathcal{L}_\mathcal{V}(\beta) \subseteq \mathcal{R}_0 \subseteq \mathcal{R}_\mathcal{A}$. If*

$$\Delta V(\bar{x}_k, \alpha_k, \tau_k) - \omega_k^\top \omega_k < 0 \tag{26}$$

is verified along the trajectories of system (15) emerging from $\mathcal{L}_\mathcal{V}(\beta)$, then for all $k > 0$,

$$V(\bar{x}_k, \alpha_k, \tau_k) - V(\bar{x}_0, \alpha_0, \tau_0) - \sum_{i=0}^{k} \omega_i^\top \omega_i < 0. \tag{27}$$

Hence, $\forall \bar{x}_0 \in \mathcal{L}_{\mathcal{V}}(\beta)$ *and* $\forall \omega_k \in \mathcal{W}(\delta)$*, it follows that*
1. $V(\bar{x}_k, \alpha_k, \tau_k) < V(\bar{x}_0, \alpha_0, \tau_0) + \|\omega_k\|_2^2 \leq \beta^{-1} + \delta^{-1} = \mu^{-1}$*, for all* $k \geq 0$ *and thus the trajectories of the system remain bounded in* $\mathcal{L}_{\mathcal{V}}(\mu) \subseteq \mathcal{R}_{\mathcal{A}}$*;*
2. *If* $\omega_k = \mathbf{0}$ *for all* $k \geq \bar{k} \geq 0$ *as* $k \to \infty$*, then* $\bar{x}_k \to \mathbf{0}$ *without leaving* $\mathcal{L}_{\mathcal{V}}(\mu) \subseteq \mathcal{R}_{\mathcal{A}}$*.*

Proof: Firstly, from (5) we have that $\sum_{k=0}^{\infty} \omega_k^\top \omega_k \leq \delta^{-1}$, consequently, $V(\bar{x}_k, \alpha_k, \tau_k) \leq V(\bar{x}_0, \alpha_0, \tau_0) + \delta^{-1}$ for all $k > 0$. Moreover, by considering that $\bar{x}_0 \in \mathcal{L}_{\mathcal{V}}(\beta)$, it follows that $V(\bar{x}_0, \alpha_0, \tau_0) \leq \beta^{-1}$. Therefore, $V(\bar{x}_k, \alpha_k, \tau_k) \leq \beta^{-1} + \delta^{-1} = \mu^{-1}$ for some $\mu > 0$, which ensures that the trajectories starting in $\mathcal{L}_{\mathcal{V}}(\beta)$ remains in the set $\mathcal{L}_{\mathcal{V}}(\mu) \subseteq \mathcal{R}_{\mathcal{A}}$, according to statement *1*. On the other hand, if the disturbance vanishes in an instant $k = \bar{k}$, i.e. $\omega_k = \mathbf{0}$ for all $k > \bar{k}$, statement *1* implies that $V(\bar{x}_{\bar{k}}, \alpha_{\bar{k}}, \tau_{\bar{k}}) < \mu^{-1}$, as a result $\bar{x}_{\bar{k}} \in \mathcal{L}_{\mathcal{V}}(\mu)$. Finally, from (26), we have that $\Delta V(\bar{x}_k, \alpha_k, \tau_k) < 0$, which in conformity with Lyapunov theory arguments, means that $\bar{x}_k$ asymptotically goes to the origin without leaving $\mathcal{L}_{\mathcal{V}}(\mu)$ ensuring statement *2*. ∎

2.3 MAIN RESULTS

The following theorem solves Problem 2.1 by providing convex conditions to synthesize control gains ensuring the regional asymptotic stability for the closed-loop system (13).

Theorem 2.1 *Suppose that there exist symmetric positive definite matrices* $W_{i,\tau_k} \in \mathbb{R}^{(\bar{\tau}+1)n \times (\bar{\tau}+1)n}$*, positive definite diagonal matrices* $S_i \in \mathbb{R}^{n_u \times n_u}$*, matrices* $Y_i \in \mathbb{R}^{n_u \times (\bar{\tau}+1)n}$*,* $Z_i \in \mathbb{R}^{n_u \times (\bar{\tau}+1)n}$ *and* $U \in \mathbb{R}^{(\bar{\tau}+1)n \times (\bar{\tau}+1)n}$*, for all* $i \in \mathcal{I}[1, N]$ *and* $\tau_k \in \mathcal{I}[\underline{\tau}, \bar{\tau}]$*, and positive scalars* μ *and* δ*, such that the following LMIs are feasible.*

$$\begin{bmatrix} -W_{r,\tau^+} & 0.5((\mathbb{A}_{i,\tau_k} + \mathbb{A}_{j,\tau_k})U + \mathbb{B}_i Y_j + \mathbb{B}_j Y_i) & -0.5(\mathbb{B}_i S_j + \mathbb{B}_j S_i) & 0.5(\mathbb{B}_{\omega i} + \mathbb{B}_{\omega j}) \\ \star & 0.5(W_{i,\tau_k} + W_{j,\tau_k}) - U - U^\top & 0.5(Z_i + Z_j)^\top & \mathbf{0} \\ \star & \star & -(S_i + S_j) & \mathbf{0} \\ \star & \star & \star & -\mathbf{I}_{n_\omega} \end{bmatrix} < \mathbf{0},$$
$$r, i \in \mathcal{I}[1, N];\ j \in \mathcal{I}[i, N];\ \tau^+ \in \mathcal{C}(\tau_k);\ \tau_k \in \mathcal{I}[\underline{\tau}, \bar{\tau}], \tag{28}$$

$$\begin{bmatrix} W_{i,\tau_k} - U - U^\top & Y_{i(\ell)}^\top - Z_{i(\ell)}^\top \\ \star & -\mu \bar{u}_{(\ell)}^2 \end{bmatrix} < \mathbf{0}, \tag{29}$$
$$\ell \in \mathcal{I}[1, m];\ i \in \mathcal{I}[1, N];\ \tau_k \in \mathcal{I}[\underline{\tau}, \bar{\tau}],$$

and

$$\mu - \delta < 0. \tag{30}$$

Then, the parameter-dependent control gain

$$\mathbb{K}(\alpha_k) = \sum_{i=1}^{N} \alpha_{k(i)} Y_i U^{-1}, \tag{31}$$

employed in the control law (10), ensures that:

1. *for all $\omega_k \neq \mathbf{0}$, with $\omega_k \in \mathcal{W}(\delta)$, and for all $\bar{x}_0$ belonging to the set $\mathcal{R}_{\mathcal{E}0} = \mathcal{L}_{\mathcal{V}}(\beta) \subseteq \mathcal{R}_0$, with $\beta = (\mu^{-1} - \delta^{-1})^{-1}$, the trajectories of the closed-loop LPV system (13) do not leave the set $\mathcal{R}_{\mathcal{E}} = \mathcal{L}_{\mathcal{V}}(\mu) \subseteq \mathcal{R}_{\mathcal{A}}$, for all $k > 0$;*

2. *for all $\omega_k = \mathbf{0}$, the set $\mathcal{R}_{\mathcal{E}}$ is a region of asymptotic stability for the closed-loop LPV system (13), for all $k > 0$.*

Proof: First, by supposing the feasibility of (29), multiply it by $\alpha_{k(i)}$ and sum it up to $i \in \mathcal{I}[1, N]$. Then, replace $Y(\alpha_k)$ and $Z(\alpha_k)$ by $\mathbb{K}(\alpha_k)U$ and $\mathbb{G}(\alpha_k)U$, respectively, and use the fact that $[W(\alpha_k, \tau_k) - U]^\top W^{-1}(\alpha_k, \tau_k)[W(\alpha_k, \tau_k) - U] \geq \mathbf{0}$ to replace the block $(1,1)$ by $-U^\top W^{-1}(\alpha_k, \tau_k)U$, thus obtaining

$$\begin{bmatrix} -U^\top W^{-1}(\alpha_k, \tau_k)U & (\mathbb{K}(\alpha_k)_{(\ell)}U - \mathbb{G}(\alpha_k)_{(\ell)}U)^\top \\ \star & -\mu\bar{u}_{(\ell)}{}^2 \end{bmatrix} < \mathbf{0}. \tag{32}$$

The feasibility of (29) implies $W_{i,\tau_k} - U - U^\top < 0$ and, since $W_{i,\tau_k} > 0$, $U + U^\top > W_{i,\tau_k}$ and U is nonsingular. With the regularity of U, we can pre- and post- multiply (32) by $\mathtt{diag}\{U^{-\top}, 1\}$ and its transpose, respectively, to get

$$\begin{bmatrix} -W^{-1}(\alpha_k, \tau_k) & (\mathbb{K}(\alpha_k)_{(\ell)} - \mathbb{G}(\alpha_k)_{(\ell)})^\top \\ \star & -\mu\bar{u}_{(\ell)}{}^2 \end{bmatrix} < \mathbf{0}. \tag{33}$$

Finally, by applying Schur's complement and pre- and post-multiplying the resulting inequality by $\bar{x}_k^\top$ and $\bar{x}_k$, respectively, we have that

$$-\bar{x}_k^\top W^{-1}(\alpha_k, \tau_k)\bar{x}_k + \bar{x}_k^\top(\mathbb{K}(\alpha_k)_{(\ell)} - \mathbb{G}(\alpha_k)_{(\ell)})^\top \times (\mu\bar{u}_{(\ell)}{}^2)^{-1}(\mathbb{K}(\alpha_k)_{(\ell)} - \mathbb{G}(\alpha_k)_{(\ell)})\bar{x}_k \leq 0, \tag{34}$$

which, from (21) and (19), ensures the inclusion $\mathcal{R}_{\mathcal{E}} = \mathcal{L}_{\mathcal{V}}(\mu) \subseteq \mathcal{S}(\bar{u})$ and, consequently, Lemma 2.1 applies. Therefore, any trajectory of the closed-loop system (13) starting in $\mathcal{R}_{\mathcal{E}}$ remains in $\mathcal{S}(\bar{u})$.

Moreover, if (28) is also satisfied, multiply its left-hand side by $\alpha_{k+1(r)}$, $\alpha_{k(i)}$, $\alpha_{k(j)}$ and sum it up to r, $i \in \mathcal{I}[1, N]$ and $j \in \mathcal{I}[i, N]$. Then, replace $Y(\alpha_k)$ and $Z(\alpha_k)$ by $\mathbb{K}(\alpha_k)U$ and $\mathbb{G}(\alpha_k)U$, respectively, and use again the fact that $-U^\top W^{-1}(\alpha_k, \tau_k)U \leq W(\alpha_k, \tau_k) - U^\top - U$ to obtain

$$\begin{bmatrix} -W(\alpha^+, \tau^+) & \mathbb{A}(\alpha_k, \tau_k)U + \mathbb{B}(\alpha_k)\mathbb{K}(\alpha_k)U & -\mathbb{B}(\alpha_k)S & \mathbb{B}_\omega(\alpha_k) \\ \star & -U^\top W^{-1}(\alpha_k, \tau_k)U & U^\top\mathbb{G}(\alpha_k)^\top & \mathbf{0} \\ \star & \star & -2S(\alpha_k) & \mathbf{0} \\ \star & \star & \star & -\mathbf{I}_{n_\omega} \end{bmatrix} < \mathbf{0}, \tag{35}$$

where α^+ represents α_{k+1}. With the regularity of U, we can pre- and post-multiply (35) by $\mathtt{diag}\{\mathbf{I}_{(\bar{\tau}+1)n}, U^{-\top}, S(\alpha_k)^{-\top}, \mathbf{I}_{n_\omega}\}$ and its transpose, respectively, to get

$$\begin{bmatrix} -W(\alpha^+,\tau^+) & \mathbb{A}(\alpha_k,\tau_k)+\mathbb{B}(\alpha_k)\mathbb{K}(\alpha_k) & -\mathbb{B}(\alpha_k) & \mathbb{B}_\omega(\alpha_k) \\ \star & -W^{-1}(\alpha_k,\tau_k) & \mathbb{G}(\alpha_k)^\top S(\alpha_k)^{-1} & \mathbf{0} \\ \star & \star & -2S(\alpha_k)^{-1} & \mathbf{0} \\ \star & \star & \star & -\mathbf{I}_{n_\omega} \end{bmatrix} < \mathbf{0}. \tag{36}$$

Next, replacing $\mathbb{A}(\alpha_k,\tau_k)+\mathbb{B}(\alpha_k)\mathbb{K}(\alpha_k)$ by $\bar{\mathbb{A}}(\alpha_k,\tau_k)$ and applying Schur's complement, we have that

$$\begin{bmatrix} -W^{-1}(\alpha_k,\tau_k) & \mathbb{G}(\alpha_k)^\top S(\alpha_k)^{-1} & \mathbf{0} \\ \star & -2S(\alpha_k)^{-1} & \mathbf{0} \\ \star & \star & -\mathbf{I}_{n_\omega} \end{bmatrix} + \begin{bmatrix} \tilde{\mathbb{A}}(\alpha_k,\tau_k)^\top \\ -\mathbb{B}(\alpha_k)^\top \\ \mathbb{B}_\omega(\alpha_k)^\top \end{bmatrix} W^{-1}(\alpha^+,\tau^+) \times \begin{bmatrix} \tilde{\mathbb{A}}(\alpha_k,\tau_k) & -\mathbb{B}(\alpha_k) & \mathbb{B}_\omega(\alpha_k) \end{bmatrix} < \mathbf{0}. \tag{37}$$

Then, pre- and post-multiplying (37) by the augmented vector $\begin{bmatrix} \bar{x}_k^\top & \Psi(\mathbb{K}\bar{x}_k)^\top & \omega_k^\top \end{bmatrix}$ and its transpose, respectively, and replacing $\bar{\mathbb{A}}(\alpha_k,\tau_k)\bar{x}_k - \mathbb{B}(\alpha_k)\Psi(\mathbb{K}(\alpha_k)\bar{x}_k) + \mathbb{B}_\omega(\alpha_k)\omega_k$ by $\bar{x}_{k+1}$, according to (15), results in

$$\bar{x}_{k+1}^\top W^{-1}(\alpha^+,\tau^+)\bar{x}_{k+1} - \bar{x}_k^\top W^{-1}(\alpha_k,\tau_k)\bar{x}_k - 2\Psi(\mathbb{K}(\alpha_k)\bar{x}_k)^\top S(\alpha_k)^{-1}(\Psi(\mathbb{K}(\alpha_k)\bar{x}_k) - \mathbb{G}(\alpha_k)\bar{x}_k) - \omega_k^\top\omega_k < 0. \tag{38}$$

From (21), we have that $\bar{x}_{k+1}^\top W^{-1}(\alpha^+,\tau^+)\bar{x}_{k+1} - \bar{x}_k^\top W^{-1}(\alpha_k,\tau_k)\bar{x}_k = V(\bar{x}_{k+1},\alpha_{k+1},\tau_{k+1}) - V(\bar{x}_k,\alpha_k,\tau_k) = \Delta V(\bar{x}_k,\alpha_k,\tau_k)$. By taking this into account and denoting $\mathbb{T}(\alpha_k) = S(\alpha_k)^{-1}$, we conclude that

$$\Delta V(\bar{x}_k,\alpha_k,\tau_k) - 2\Psi(\mathbb{K}(\alpha_k)\bar{x}_k)^\top\mathbb{T}(\alpha_k)(\Psi(\mathbb{K}(\alpha_k)\bar{x}_k) - \mathbb{G}(\alpha_k)\bar{x}_k) - \omega_k^\top\omega_k \leq 0. \tag{39}$$

By supposing that $\bar{x}_k \in \mathcal{S}(\bar{u})$, the generalized sector condition presented in Lemma 2.1 ensures the non-positivity of $2\Psi(\mathbb{K}(\alpha_k)\bar{x}_k)^\top\mathbb{T}(\alpha_k)(\Psi(\mathbb{K}(\alpha_k)\bar{x}_k) - \mathbb{G}(\alpha_k)\bar{x}_k)$, which implies $\Delta V(\bar{x}_k,\alpha_k,\tau_k) - \omega_k^\top\omega_k \leq 0$. Because of the positivity of $W(\alpha_k,\tau_k)$, we can assume that there exist a sufficiently small $\epsilon_0 > 0$ such that

$$\epsilon_0\|\bar{x}_k\|^2 \leq V(\bar{x}_k,\alpha_k,\tau_k) \leq \epsilon_1\|\bar{x}_k\|^2, \text{ with } \epsilon_1^{-1} = \min_{i\in\mathcal{I}[1,N]} \lambda_{\min}{}_{\tau_k\in\mathcal{I}[\underline{\tau},\bar{\tau}]} W_{i,\tau_k} > 0. \tag{40}$$

Additionally, from (39) with $\omega_k = \mathbf{0}$, we have that

$$\Delta V(\bar{x}_k,\alpha_k,\tau_k) < 2\Psi(\mathbb{K}(\alpha_k)\bar{x}_k)^\top\mathbb{T}(\alpha_k)(\Psi(\mathbb{K}(\alpha_k)\bar{x}_k) - \mathbb{G}(\alpha_k)\bar{x}_k) \leq -\epsilon_2\|\bar{x}_k\|^2 < 0 \tag{41}$$

for some $\epsilon_2 > 0$. Therefore, $V(\bar{x}_k,\alpha_k,\tau_k)$ given in (21) is a Lyapunov function and $\mathcal{R}_\mathcal{E} = \mathcal{L}_\mathcal{V}(\mu)$ is an estimate of the region of attraction of the origin for the closed-loop system (13). ∎

Now, consider that the LPV system (13) is not subject to any external perturbation, i.e. $\omega_k = \mathbf{0}$ for all $k \geq 0$. In this case, the stabilization can be handled by the following corollary, which is a consequence of statement 2 of Theorem 2.1.

Corollary 2.1 *Suppose that there exist symmetric positive definite matrices* $W_{i,\tau_k} \in \mathbb{R}^{(\bar{\tau}+1)n\times(\bar{\tau}+1)n}$*, positive definite diagonal matrices* $S_i \in \mathbb{R}^{n_u\times n_u}$*, and matrices* $Y_i \in \mathbb{R}^{n_u\times(\bar{\tau}+1)n}$*,* $Z_i \in \mathbb{R}^{n_u\times(\bar{\tau}+1)n}$ *and* $U \in \mathbb{R}^{(\bar{\tau}+1)n\times(\bar{\tau}+1)n}$*, for all* $i \in \mathcal{I}[1, N]$ *and* $\tau_k \in \mathcal{I}[\underline{\tau}, \bar{\tau}]$*, such that the following LMI and (29) with* $\mu = 1$ *are feasible.*

$$\begin{bmatrix} -W_{r,\tau^+} & 0.5((\mathbb{A}_{i,\tau_k} + \mathbb{A}_{j,\tau_k})U + \mathbb{B}_i Y_j + \mathbb{B}_j Y_i) & -0.5(\mathbb{B}_i S_j + \mathbb{B}_j S_i) \\ \star & 0.5(W_{i,\tau_k} + W_{j,\tau_k}) - U - U^\top & 0.5(Z_i + Z_j)^\top \\ \star & \star & -(S_i + S_j) \end{bmatrix} < 0. \qquad (42)$$
$$r, i \in \mathcal{I}[1, N];\ j \in \mathcal{I}[i, N];\ \tau^+ \in \mathcal{C}(\tau_k);\ \tau_k \in \mathcal{I}[\underline{\tau}, \bar{\tau}]$$

Then, the parameter-dependent state-feedback controller with gain computed as in (31) ensures that regional asymptotic stability of the closed-loop LPV system (13) for every initial condition $\bar{x}_0$ *belonging to* $\mathcal{R}_\mathcal{E} = \mathcal{L}_\mathcal{V}(1) \subseteq \mathcal{R}_\mathcal{A}$*. That concludes the proof.*

Proof: The proof follows the same steps as in Theorem 2.1 by disregarding the terms referring to the disturbance. ∎

Remark 2.2 *Theorem 2.1 and Corollary 2.1 can also be adapted to treat both LTI and non-saturating systems. In the first case (LTI systems), it is necessary to set* $r = i = j = 1$*, which leads to fixed matrices. In the second case (non-saturation), one has to impose:* i) *the row and column* 3 *are deleted in the LMIs (28) and (42), and* (ii) *the LMI (29) is discarded.*

Remark 2.3 *The conditions in Theorem 2.1 and Corollary 2.1 yield a full gain matrix* $\mathbb{K}(\alpha_k) = \begin{bmatrix}\mathbb{K}_0(\alpha_k) & \mathbb{K}_1(\alpha_k) & \dots & \mathbb{K}_{\bar{\tau}}(\alpha_k)\end{bmatrix}$*. The special forms assumed by* $\mathbb{K}(\alpha_k)$*, as discussed in Remark 2.1, can be recovered from (31) by imposing certain structures on the matrices* U *and* $Y(\alpha_k)$*. For* $\mathbb{K}_{c1}(\alpha_k) = \begin{bmatrix}K_0(\alpha_k) & 0 & \dots & 0\end{bmatrix}$*, it is required to impose*

$$Y(\alpha_k) = \begin{bmatrix} Y(\alpha_k)_{1,n_u\times n} & 0 \end{bmatrix} \text{ and } U = \begin{bmatrix} U_{1,n\times n} & 0 \\ U_{2,\bar{\tau}n\times n} & U_{3,\bar{\tau}n\times\bar{\tau}n} \end{bmatrix}.$$

Similarly, for $\mathbb{K}_{c2}(\alpha_k) = \begin{bmatrix}K_0(\alpha_k) & 0 & K_{\bar{\tau}}(\alpha_k)\end{bmatrix}$*, it is necessary to consider*

$$Y(\alpha_k) = \begin{bmatrix} Y(\alpha_k)_{1,n_u\times n} & 0 & Y(\alpha_k)_{2,n_u\times n} \end{bmatrix}$$

and

$$U = \begin{bmatrix} U_{1,n\times n} & 0 & U_{2,n\times n} \\ U_{3,(\bar{\tau}-1)n\times n} & U_{4,(\bar{\tau}-1)n\times(\bar{\tau}-1)n} & U_{5,(\bar{\tau}-1)n\times n} \\ U_{6,n\times n} & 0 & U_{7,n\times n} \end{bmatrix}.$$

Remark 2.4 *The numerical complexity of the proposed LMI conditions is related with the number of scalar variables,* $\mathcal{K}$*, and the number of rows,* $\mathcal{R}$*. By denoting* $\hat{\tau} = \bar{\tau} - \underline{\tau} + 1$*, we can compute these quantities as follows: for Theorem 2.1, we have that:* $\mathcal{K}_1 =$

$(0.5((\bar{\tau}+1)n+1)N\hat{\tau}+(\bar{\tau}+1)n)(\bar{\tau}+1)n+(n_u+2(\bar{\tau}+1)n)n_uN+2$ *and* $\mathcal{R}_1 = 0.5(2(\bar{\tau}+1)n+n_u+n_\omega)(\hat{\tau}^2-(\hat{\tau}-1-\Delta\tau_{\max})(\hat{\tau}-\Delta\tau_{\max}))N^2(N+1)+((\bar{\tau}+1)n+1)n_uN\hat{\tau}+1$*. On the other hand, for Corollary 2.1, we have that:* $\mathcal{K}_2 = \mathcal{K}_1 - 2$ *and* $\mathcal{R}_2 = 0.5(2(\bar{\tau}+1)n+n_u)(\hat{\tau}^2-(\hat{\tau}-1-\Delta\tau_{\max})(\hat{\tau}-\Delta\tau_{\max}))N^2(N+1)+((\bar{\tau}+1)n+1)n_uN\hat{\tau}+1$*. Thus, observe that the number of LMI rows reduce with lower values of* $\Delta\tau_{\max}$*, i.e., with slower delay variations. Therefore, the worst case is achieved with* $\Delta\tau_{\max} = \bar{\tau}-\underline{\tau}$*, which is the condition usually handled in the literature.*

2.3.1 Optimization design procedures

The proposed convex conditions can be exploited to optimize some interest characteristics of the closed-loop system as presented in the sequence.

2.3.1.1 Maximization of the disturbance tolerance (δ^{-1})

The maximization of the disturbance tolerance (δ^{-1}) consists of designing a state-feedback control gain $\mathbb{K}(\alpha_k)$ given in (10), such that, for a given set of admissible initial states $\mathcal{R}_0$, the set of admissible disturbances $\mathcal{W}(\delta)$ is maximized, that is, δ^{-1} is as big as possible. In particular, if the system is in equilibrium, i.e., $\bar{x}_0 = \mathbf{0}$, it follows that $\delta^{-1} = \mu^{-1}$ and the problem of maximization of the set $\mathcal{W}(\delta)$ can be addressed as (see also page 73 of (TARBOURIECH et al., 2011)):

$$\mathcal{O}_1 : \begin{cases} \min & \mu, \\ \text{subject to} & \text{LMIs (28) and (29).} \end{cases} \tag{43}$$

2.3.1.2 Maximization of the estimate of the region of attraction ($\mathcal{R}_\mathcal{E}$)

Suppose that the closed-loop LPV system (4) is not subject to disturbance input, i.e. $\omega_k = \mathbf{0}$, for all $k > 0$. In this case, the objective is to design a state-feedback control gain given in (10), that maximizes the estimate of the region of attraction, $\mathcal{R}_\mathcal{E}$. One possibility is to maximize the volume of an ellipsoidal set $\mathcal{E}(R^{-1},1)$, defined similarly as in (24), such that $\mathcal{E}(R^{-1},1) \subseteq \mathcal{L}_\mathcal{V}(\mu)$, which can be ensured by

$$\mu - 1 \leq 0 \text{ and } \begin{bmatrix} R & R \\ \star & W_{i,\tau_k} \end{bmatrix} > \mathbf{0}. \qquad i \in \mathcal{I}[1,N]; \tau_k \in \mathcal{I}[\underline{\tau},\bar{\tau}] \tag{44}$$

Since the volume of $\mathcal{E}(R^{-1},1)$ is proportional to $\sqrt{\det(R)}$ (see (BOYD et al., 1994)), such a maximization of $\mathcal{R}_\mathcal{E}$ can be done through $\max \ln(\det(R))$, or equivalently by:

$$\mathcal{O}_2 : \begin{cases} \min & -\ln(\det(R)), \\ \text{subject to} & \text{LMIs (29), (28), and (44).} \end{cases} \tag{45}$$

Other possibilities are *i)* to maximize the volume of an ellipsoidal set $\mathcal{E}(R,1)$, defined similarly as in (25), such that $\mathcal{E}(R,1) \subseteq \mathcal{L}_\mathcal{V}(\mu)$, and *ii)* to maximize the volume

of the intersection of W_{i,τ_k}^{-1} for all $i \in \mathcal{I}[1, N]$ and $\tau_k \in \mathcal{I}[\underline{\tau}, \bar{\tau}]$. Furthermore, we can be interested in, for example, to maximize the set of admissible initial conditions $\mathcal{R}_{\mathcal{E}0}$ for a given set of admissible exogenous signals $\mathcal{W}(\delta)$. All these cases can be found in (DE SOUZA, 2017).

2.4 NUMERICAL EXAMPLES

Consider LPV system (4) with the following data:

$$A_1 = \begin{bmatrix} -1.1 & 0.4 \\ -0.2 & 1.1 \end{bmatrix}, \; A_2 = \begin{bmatrix} -0.2 & 0.7 \\ 0.6 & 1.3 \end{bmatrix}, \; A_{d1} = \begin{bmatrix} 0.06 & 0.04 \\ 0 & -0.05 \end{bmatrix}, \; A_{d2} = \begin{bmatrix} 0.02 & 0.06 \\ 0 & -0.07 \end{bmatrix},$$

$$B_1 = \begin{bmatrix} 0 \\ 1.2 \end{bmatrix}, \; B_2 = \begin{bmatrix} 0 \\ 1.3 \end{bmatrix}, \; B_{\omega 1} = \begin{bmatrix} 0 \\ 0.12 \end{bmatrix}, \; B_{\omega 2} = \begin{bmatrix} 0 \\ 0.13 \end{bmatrix}, \tag{46}$$

time-varying delay $\tau_k \in \mathcal{I}[0, 2]$ and symmetric saturation limit $\bar{u} = 0.7$.

Maximization of the disturbance tolerance: First of all, we compare the amount of admissible disturbance to system (46) when a parameter-dependent gain, $\mathbb{K}(\alpha_k)$, is used instead of a constant (robust) gain, $\mathbb{K}$. In this last case, to compute the gain matrices $\mathbb{K}$, we impose $i = j = 1$ on matrices Y , S and Z in LMIs (28) and (29).

By solving the optimization procedure $\mathcal{O}_1$ given in (43), we designed control gains that maximize the tolerable energy of the disturbance signals ω_k. For a parameter-dependent control gain, we got $\delta^{-1} = 36.1011$, i.e. $\|\omega_k\|_2 \leq 6.0084$ and, for a fixed control gain, $\delta^{-1} = 30.6748$, i.e. $\|\omega_k\|_2 \leq 5.5384$. Therefore, when a parameter-dependent gain is assumed instead of a fixed one there is an increase of 7.82% in the tolerable energy of the disturbance signals.

In particular, for the time-varying case, we use the gain $\mathbb{K}(\alpha_k)$ in (12) with

$$\mathbb{K}_1 = \begin{bmatrix} -0.5526 & -0.3960 & 0.0110 & 0.0674 & 0.0149 & 0.0008 \end{bmatrix}, \text{ and}$$
$$\mathbb{K}_2 = \begin{bmatrix} -0.2582 & -0.5938 & -0.0021 & 0.0157 & -0.0014 & 0.0226 \end{bmatrix},$$

to close the loop and to simulate the system response to a set of disturbance signals with the form $\omega_k = \begin{bmatrix} \omega_1 & \omega_2 & \mathbf{0}_{1,18} \end{bmatrix}$, with ω_1 swept from –6.0084 up to 6.0084 and $\omega_2 = \pm\sqrt{6.0084^2 - \omega_1^2}$. For each sequence ω_k, ten simulations were performed with α_k and τ_k randomly chosen. The projections of $\mathcal{E}(W_{i,\tau_k}, \mu)$ (cyan lines), for all $i \in \mathcal{I}[1, N]$ and $\tau_k \in \mathcal{I}[\underline{\tau}, \bar{\tau}]$, and $\mathcal{R}_{\mathcal{E}}$ (blue lines) on the plan x_k jointly with the current states' trajectories (colored lines) are shown on the left-hand side of Figure 3 and, on its right-hand side, the projection of $\mathcal{R}_{\mathcal{E}}$ on the planes x_k (blue lines), x_{k-1} (magenta dashed lines) and x_{k-2} (green dash-dotted lines). Note that the trajectories do not go beyond $\mathcal{R}_{\mathcal{E}}$ and do not touch their bounds, which indicates a certain conservatism of the approach.

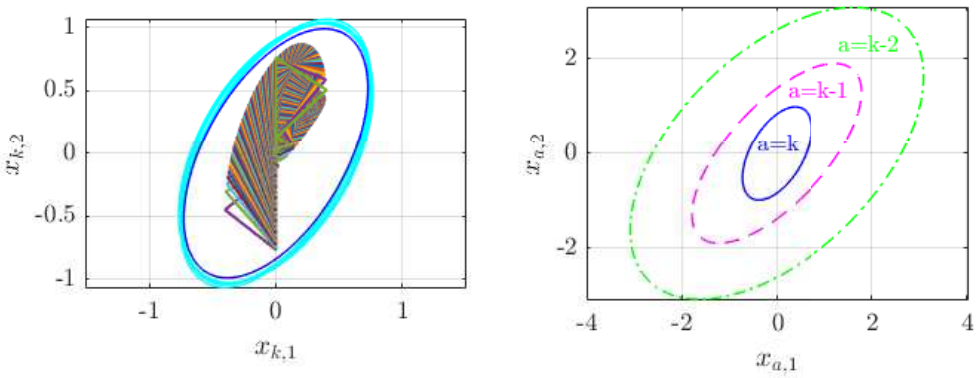

Figure 3 – On the left: projections of $\mathcal{E}(W_{i,\tau_k}, \mu)$ (–), for all $i \in \mathcal{I}[1, N]$ and $\tau_k \in \mathcal{I}[\underline{\tau}, \bar{\tau}]$, and $\mathcal{R}_{\mathcal{E}}$ on the plane x_k jointly with the current states' trajectories (colored lines); On the right: projections of $\mathcal{R}_{\mathcal{E}} = \mathcal{L}_{\mathcal{V}}(\mu)$ on the planes x_k (–), x_{k-1} (– –) and x_{k-2} (–.).

Then, we consider the design of the other possible structures assumed by the parameter-dependent control gain (see Remark 2.3). For $\mathbb{K}_{c2}(\alpha_k)$, we got δ^{-1} = 31.1526, i.e. $\|\omega_k\|_2 \leq 5.5814$, and for $\mathbb{K}_{c1}(\alpha_k)$, δ^{-1} = 31.9489, i.e. $\|\omega_k\|_2 \leq 5.6523$. In these cases, we have a reduction in the system tolerance to disturbance signals of 7.65% and 6.30% when we consider the design of gains $\mathbb{K}_{c2}(\alpha_k)$ and $\mathbb{K}_{c1}(\alpha_k)$, respectively, w.r.t the full gain $\mathbb{K}(\alpha_k)$. Therefore, the feedback of delayed states is clearly justified by higher tolerances obtained in such a case. It is also interesting to note that even considering non-complete parameter-dependent gains, whose structures corresponds to feedback only part of the system's states, a greater tolerance is still achieved than when it is considered a complete robust (invariant) gain, whose structure correspond to feedback all the states.

Still assuming parameter-dependent gains, we evaluate the influence of the limitation on the maximum rate of variation of the delay in the size of the set of admissible disturbances $\mathcal{W}(\delta)$ considering different maximum delay values. Thus, for each $\bar{\tau} \in \mathcal{I}[2, 7]$, we have varied $\Delta\tau_{\max}$ from 0 up to $\bar{\tau}$ and computed the maximum disturbance tolerance δ^{-1} through optimization procedure $\mathcal{O}_1$ given in (43). The results are shown in Figure 4, where $R_{\%}$ is the percentage of augmentation in the values of δ^{-1} in relation to the case of maximum rate of variation of the delay ($\Delta\tau_{\max} = \bar{\tau}$), i.e $R_{\%} = (\delta^{-1}_{\Delta\tau_{\max}}/\delta^{-1}_{\Delta\tau_{\max}=\bar{\tau}} - 1) \times 100\%$. This clearly shows the relevance of considering the bounds on the delay variation to get higher energy tolerances of exogenous signals.

Finally, by assuming that the system (46) is not subject to any restriction on input signals, we compare our approach with that proposed by (SILVA et al., 2016). From (SILVA et al., 2016), we have that δ^{-1} = 0.1368, i.e. $\|\omega_k\|_2 \leq 0.3698$. In this case, the designed fuzzy control law guarantees the input-to-state stability of the closed-loop

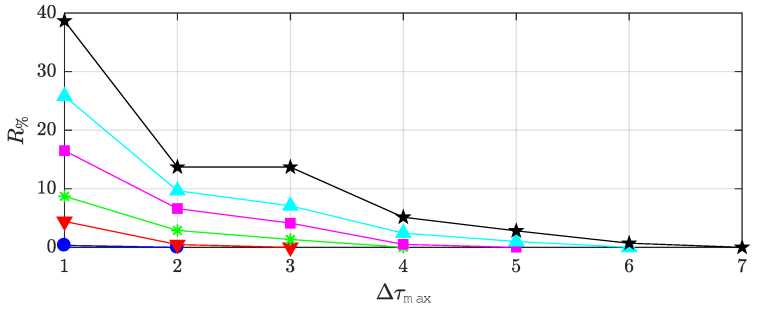

Figure 4 – Augmentation percentage of the disturbance tolerance ($R_{\%}$, see the text) as a function of the maximum rate variation of the delay, for $\bar{\tau} = 2$(•),$\bar{\tau} = 3$(▼), $\bar{\tau} = 4$(∗),$\bar{\tau} = 5$(■), $\bar{\tau} = 6$(▲) and $\bar{\tau} = 7$(★).

system in a region of validity defined by the parameters $L = \begin{bmatrix} 1 & 0 \end{bmatrix}$ and $\eta = 0.05$. Considering the following highlights to the optimization problem (43): *i)* the changes proposed in Remark 2.2 to disregard saturation and *ii)* addition of the constraint referring to the validity region of system (46) proposed by (SILVA et al., 2016), we got $\delta^{-1} = 0.1699$, i.e. $\|\omega_k\|_2 \leq 0.4121$. Therefore, an 11.44% increase in energy tolerance to disturbance signals was obtained considering our proposal.

Maximization of the estimate of the region of attraction $\mathcal{R}_{\mathcal{E}}$: We compare the size of the estimates of the regions of attraction when the parameter-dependent control gains, $\mathbb{K}(\alpha_k)$, $\mathbb{K}_{c1}(\alpha_k)$, and $\mathbb{K}_{c2}(\alpha_k)$, are used instead of a constant gain, $\mathbb{K}$. All gains were obtained through the optimization procedure $\mathcal{O}_2$ given in (45), however, to obtain $\mathbb{K}_{c1}$ and $\mathbb{K}_{c2}$, we use the changes proposed in Remark 2.3, and to obtain $\mathbb{K}$, we impose $i = j = 1$ on the matrices Y, Z and S in the LMIs (42) and (29).

Figure 5 shows the cuts of the estimates of the region of attraction on the plans x_k, x_{k-1} and x_{k-2} for the gains $\mathbb{K}(\alpha_k)$ (blue lines), $\mathbb{K}_{c1}(\alpha_k)$ (green dash-dotted lines), $\mathbb{K}_{c2}(\alpha_k)$ (red dashed lines) and $\mathbb{K}$ (black lines). Note that better estimates are achieved when considering complete parameter-dependent control gains.

Moreover, for the LPV system (4) in closed-loop with the complete parameter-dependent control law, we plotted on the left-hand side of Figure 6 the cuts of $\mathcal{E}(W_{i,\tau_k}, 1)$ (cyan lines), for all $i \in \mathcal{I}[1, N]$ and $\tau_k \in \mathcal{I}[\underline{\tau}, \bar{\tau}]$, and $\mathcal{E}(R^{-1}, 1)$ (blue line) on the plan x_k jointly with some convergent (magenta dashed lines) and some divergent (green dash-dotted lines) trajectories starting from the points marked with (•) and (x), respectively. For the convergent trajectories, we also plotted the current states (magenta lines) and the control input (blue lines) on the right-hand side of Figure 6. In all simulations, we chose α_k and τ_k randomly. Note that the trajectories inside $\mathcal{R}_{\mathcal{E}}$ converge to origin without leaving $\mathcal{R}_{\mathcal{E}}$.

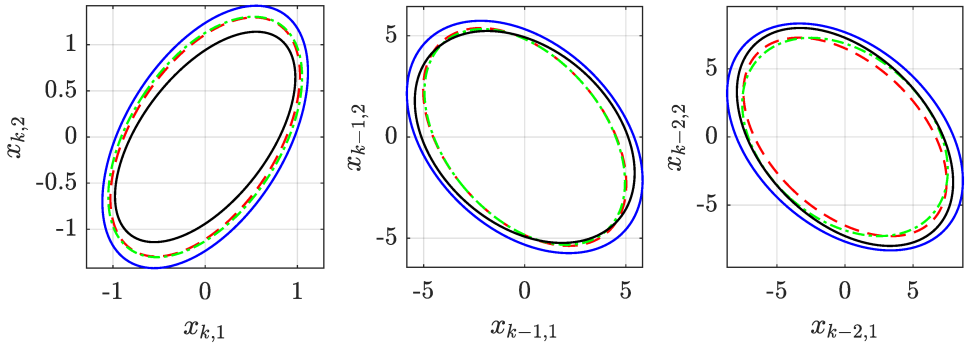

Figure 5 – Cuts of $\mathcal{R}_{\mathcal{E}} = \mathcal{L}_{\mathcal{V}}(1)$ considering the control gain structures: $\mathbb{K}(\alpha_k)$(–),$\mathbb{K}_{c1}(\alpha_k)$(– –), $\mathbb{K}_{c2}(\alpha_k)$(–.) and $\mathbb{K}$(–).

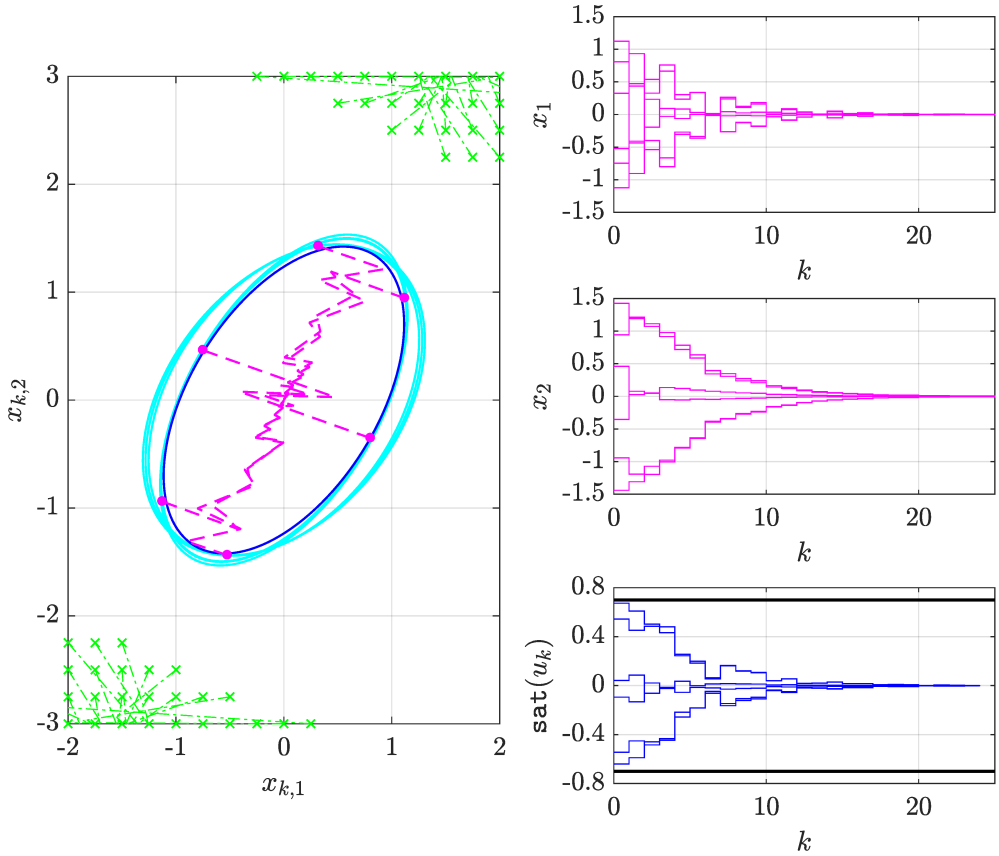

Figure 6 – On the left: Cuts of $\mathcal{E}(W_{i,\tau_k}, 1)$, for all $i \in \mathcal{I}[1, N]$ and $\tau_k \in \mathcal{I}[\underline{\tau}, \bar{\tau}]$, and $\mathcal{R}_{\mathcal{E}}$ on the plan x_k jointly with the current states' trajectories; On the right: the closed-loop temporal response.

2.5 CONCLUDING REMARKS

This chapter has addressed a control design method that regionally stabilizes discrete-time LPV systems with time-varying delays subject to saturating actuators and

exogenous disturbances. The main contributions can be summarized as *i)* a convex delay-dependent condition to design parameter-dependent state feedback controllers *ii)* the proposed controller structure may include delayed states, without requiring the online knowledge of the delay, which facilitates its implementation; *iii)* the proposed procedure allows estimating the region of attraction of the origin on an augmented space *vi)* the control design takes into account the maximum delay variation between two consecutive instants, yielding less conservative results; *v)* the provided methodology allows the design considering optimization problems aiming at maximizing the admissible disturbance energy and enlarging the region of attraction.

To illustrate the effectiveness of the proposal, a numerical example has been explored in several aspects. As it can be seen, the parameter-dependent gains led to better results than the robust ones (those proposed in (DE SOUZA et al., 2019b)). Additionally, the configuration that feeds back all states, current and delayed, proved to be more advantageous than those that consider less delayed states. Furthermore, it was evident that the limitation of the maximum variation of the delay results in higher tolerances to disturbance signals. Although the simulation results may seem conservative in some points, for example i) the state trajectories did not reach the borders of the estimate of the region of attraction, even for disturbance signals with the maximum allowed energy; and ii) in the absence of disturbance signals, the control signal did not saturate for initial conditions in the edges of the estimate of the region of attraction, it is important to point out that the conditions hold for any α_k and τ_k sequences. Finding the worst sequences to be used in such cases is not a simple task. Finally, it is relevant to mention that, this method becomes impracticable for systems where the states are not fully available. In the next chapter, an approach considering dynamic output-feedback controllers is proposed.

3 SYNTHESIS OF PARAMETER-DEPENDENT DYNAMIC OUTPUT CONTROLLERS

This chapter presents a control design technique for discrete-time LPV systems with time-varying delayed states subject to saturating actuators and exogenous signals. The control law considered is a parameter-dependent dynamic output-feedback with some particularities. First, the controller's order can be set as an integer multiple of the original system's order. Second, its structure enables the user feeds back not only the current output but also the delayed ones. Lastly, anti-windup gains are added as an attempt to mitigate the undesired effects of saturation.

Basically, LMI conditions are proposed to regionally ensure the input-to-state stability of the closed-loop system in the ℓ_2-sense. Such conditions take into account the maximum variation of delay between two consecutive instants. As in the previous chapter, the approach is based on the Lyapunov theory and on rewriting the LPV delayed system as an augmented delay-free one switched by the delay. Also, a dead-zone linearity is used to handle the saturation through the generalized sector condition. Furthermore, some (convex) optimization problems are formulated to both maximize the domain of attraction and improve the disturbance tolerance. Finally, numerical examples are considered to demonstrate the effectiveness of the proposal. The results presented here are based on the works (DE SOUZA et al., 2021a, 2019a).

3.1 PROBLEM STATEMENT

Consider the class of system in (4) with the addition of the measured output signal $y_k \in \mathbb{R}^{n_y}$ represented by

$$\begin{aligned} x_{k+1} &= A(\alpha_k)x_k + A_d(\alpha_k)x_{k-\tau_k} + B(\alpha_k)\mathtt{sat}(u_k) + B_\omega(\alpha_k)\omega_k, \\ y_k &= Cx_k, \end{aligned} \tag{47}$$

where $x_k \in \mathbb{R}^n$ is the state vector, $u_k \in \mathbb{R}^{n_u}$ is the control signal, $\omega_k \in \mathbb{R}^{n_\omega}$ is the disturbance input vector, $\tau_k \in \mathcal{I}[\underline{\tau}, \bar{\tau}]$ is the time-varying delay and $\alpha_k \in \mathbb{R}^N$ is the vector of time-varying parameters belonging to the unitary simplex

$$\Lambda \triangleq \left\{ \alpha_k \in \mathbb{R}^N : \sum_{i=1}^{N} \alpha_{k(i)} = 1,\ \alpha_{k(i)} \geq 0, i \in \mathcal{I}[1, N] \right\}. \tag{48}$$

Thus, the parameter-dependent matrices $A(\alpha_k) \in \mathbb{R}^{n\times n}$, $A_d(\alpha_k) \in \mathbb{R}^{n\times n}$, $B(\alpha_k) \in \mathbb{R}^{n\times n_u}$ and $B_\omega(\alpha_k) \in \mathbb{R}^{n\times n_\omega}$ can be written as a convex combination of N known vertices according to

$$\begin{bmatrix} A(\alpha_k) & A_d(\alpha_k) & B(\alpha_k) & B_\omega(\alpha_k) \end{bmatrix} = \sum_{i=1}^{N} \alpha_{k(i)} \begin{bmatrix} A_i & A_{di} & B_i & B_{\omega i} \end{bmatrix}. \tag{49}$$

The saturation function, $\mathtt{sat}(u_k)$, is defined as

$$\mathtt{sat}(u_{k(\ell)}) = \mathtt{sign}(u_{k(\ell)}) \min(|u_{k(\ell)}|, \bar{u}_{(\ell)}), \tag{50}$$

with $\bar{u}_{(\ell)} > 0$, $\ell \in \mathcal{I}[1, n_u]$, denoting the symmetric amplitude bound of the ℓ^{th} control input. As in the previous chapter, the disturbance input is supposed to belong to

$$\mathcal{W}(\delta) = \left\{ \omega_k \in \mathbb{R}^{n_\omega} : \sum_{k=0}^{\infty} \omega_k^\top \omega_k \leq \delta^{-1} \right\}, \tag{51}$$

with $\delta^{-1} \in \mathbb{R}^+$ representing the energy bound of the disturbance. Also, the maximum variation of the delay between two consecutive instants, $\Delta\tau_{\max}$, is assumed bounded, i.e. $|\tau_{k+1} - \tau_k| \leq \Delta\tau_{\max} \leq (\bar{\tau} - \underline{\tau})$, where $\underline{\tau}$ and $\bar{\tau}$ are the minimum and the maximum known delay limits, respectively. To deal with this, we define the following set $\mathcal{C}(\tau_k)$ that contains all possible values assumed by the delay at the next instant given its value at the current one,

$$\mathcal{C}(\tau_k) = \left\{ \tau^+ \in \mathcal{I}[\max(\underline{\tau}, \tau_k - \Delta\tau_{\max}), \min(\bar{\tau}, \tau_k + \Delta\tau_{\max})] \right\}. \tag{52}$$

To regionally stabilize system (47), we propose the following parameter-dependent dynamic output feedback controller with anti-windup action:

$$\begin{aligned} x_{c,k+1} &= A_c(\alpha_k, \tau_k) x_{c,k} + \sum_{j=0}^{\bar{\tau}} B_{cj}(\alpha_k) y_{k-j} - E_c(\alpha_k) \Psi(u_k), \\ u_k &= C_c(\alpha_k) x_{c,k} + \sum_{j=0}^{\bar{\tau}} D_{cj}(\alpha_k) y_{k-j}, \end{aligned} \tag{53}$$

where $x_{c,k} \in \mathbb{R}^{\sigma n}$, with $\sigma \in \mathcal{I}[1, (\bar{\tau} + 1)]$, is the controller state vector, y_{k-j} is the measured output signal delayed by $j \in \mathcal{I}[0, \bar{\tau}]$ samples, and $\Psi(u_k)$ is the dead-zone nonlinearity described in (16). The controller's matrices $A_c(\alpha_k, \tau_k) \in \mathbb{R}^{\sigma n \times \sigma n}$, $B_{cj}(\alpha_k) \in \mathbb{R}^{\sigma n \times n_y}$, $E_c(\alpha_k) \in \mathbb{R}^{\sigma n \times n_u}$, $C_c(\alpha_k) \in \mathbb{R}^{n_u \times \sigma n}$ and $D_{cj}(\alpha_k) \in \mathbb{R}^{n_u \times n_y}$, in the same way as those of the system, are represented in the polytopic form, as will be shown later. Due to the controller structure adopted, we are assuming here that the time-varying delay τ_k is known a priori.

Note that, unlike the works in the literature, the choice of σ determines the controller's order as an integer multiple of the system's order. Thus, the controller's order can be chosen from the system's actual order, n, up to the augmented delay-free system's order, $n(\bar{\tau} + 1)$. Another feature is that the current and the (already available) delayed outputs of the system are fed back into the controller, providing an enlarged set of information about the system's behavior. Also, the anti-windup gain matrix $E_c(\alpha_k)$ is added to the compensator's dynamics to help the mitigation of the saturating effects, and it acts only when saturation occurs, i.e., when $\Psi(u_k) \neq 0$.

Thus, the problem we intend to solve in this chapter can be stated as follows.

Problem 3.1 *For the saturating LPV system (47), determine the parameter-dependent dynamic controller (53) and the sets $\mathcal{R}_{\mathcal{E}0} \subseteq \mathcal{R}_0$ and $\mathcal{R}_{\mathcal{E}} \subseteq \mathcal{R}_{\mathcal{A}}$, such that for all $\omega_k \in \mathcal{W}(\delta)$, for all $\xi_0 = \begin{bmatrix} \bar{x}_0^\top & x_{c,0}^\top \end{bmatrix}^\top \in \mathcal{R}_{\mathcal{E}0}$, and for all $\alpha_k \in \Lambda$, the resulting closed-loop system is regionally ISS (see Definition 2.1).*

3.2 PRELIMINARY RESULTS

In this section, we present the augmented model representation of the closed-loop system and an auxiliary result useful on the formulation of the stabilization condition.

3.2.1 Augmented model description

Let us start introducing some matrix notations

$$\begin{aligned}
\mathfrak{B}_c(\alpha_k) &= \begin{bmatrix} B_{c0}(\alpha_k) & B_{c1}(\alpha_k) & \cdots & B_{c\sigma-1}(\alpha_k) \end{bmatrix}, \\
\bar{\mathfrak{B}}_c(\alpha_k) &= \begin{bmatrix} B_{c\sigma}(\alpha_k) & B_{c\sigma+1}(\alpha_k) & \cdots & B_{c\bar{\tau}}(\alpha_k) \end{bmatrix}, \\
\mathfrak{D}_c(\alpha_k) &= \begin{bmatrix} D_{c0}(\alpha_k) & D_{c1}(\alpha_k) & \cdots & D_{c\sigma-1}(\alpha_k) \end{bmatrix}, \\
\bar{\mathfrak{D}}_c(\alpha_k) &= \begin{bmatrix} D_{c\sigma}(\alpha_k) & D_{c\sigma+1}(\alpha_k) & \cdots & D_{c\bar{\tau}}(\alpha_k) \end{bmatrix}.
\end{aligned}$$

From this, we can establish the following assumption regarding the controller matrices.

Assumption 3.1 *The controller matrices (53) are supposed to have the following structure:*

$$\begin{bmatrix} A_c(\alpha_k, \tau_k) & \mathfrak{B}_c(\alpha_k) & \bar{\mathfrak{B}}_c(\alpha_k) \end{bmatrix} = 0.5 \sum_{i=1}^{N} \sum_{j=i}^{N} (1 + \rho_{ij}) \alpha_{k(i)} \alpha_{k(j)} \begin{bmatrix} A_{cij,\tau_k} & \mathfrak{B}_{cij} & \bar{\mathfrak{B}}_{cij} \end{bmatrix},$$

$$\begin{bmatrix} C_c(\alpha_k) & \mathfrak{D}_c(\alpha_k) & \bar{\mathfrak{D}}_c(\alpha_k) \end{bmatrix} = \sum_{i=1}^{N} \alpha_{k(i)} \begin{bmatrix} C_{ci} & \mathfrak{D}_{ci} & \bar{\mathfrak{D}}_{ci} \end{bmatrix}, \; E_c(\alpha_k) = \sum_{i=1}^{N} \alpha_{k(i)} E_{ci}, \quad (54)$$

with $\alpha_k \in \Lambda$ and ρ_{ij} satisfying

$$\rho_{ij} = \begin{cases} 1, & \text{if } i \neq j, \\ 0, & \text{otherwise.} \end{cases}$$

These matrices are assumed to satisfy this particular form due to the appearance of matrix products with indexes i and j in the formulation of the conditions. However, let us stress that any dynamic controller in the standard polytopic form can be easily described according to Assumption 3.1, by using the following equivalence: $\left(\sum_{i=1}^{N} \alpha_{k(i)}\right) \left(\sum_{i=1}^{N} \alpha_{k(i)} M_i\right) = 0.5 \sum_{i=1}^{N} \sum_{j=i}^{N} (1 + \rho_{ij}) \alpha_{k(i)} \alpha_{k(j)} M_{ij}$, with $\alpha_k \in \Lambda$ and

$\rho_{ij} = 1$ if $i \neq j$ and $\rho_{ij} = 0$ otherwise. To illustrate this, consider a dynamic controller with matrices $A_c(\alpha_k, \tau_k)$, $\mathfrak{B}_c(\alpha_k)$ and $\bar{\mathfrak{B}}_c(\alpha_k)$ in linear form with $N = 2$, i.e. $M(\alpha_k) = \sum_{i=1}^{2} \alpha_{k(i)} M_i = \alpha_{k(1)} M_1 + \alpha_{k(2)} M_2$, where M represents A_c, $\mathfrak{B}_c$ and $\bar{\mathfrak{B}}_c$. In such a case, the matrices M_{11}, M_{12} and M_{22} of Assumption 3.1 are computed from M_1 and M_2 as: $M_{11} = 2M_1$, $M_{12} = (M_1 + M_2)$ and $M_{22} = 2M_2$. Indeed, we have that

$$\begin{aligned}(\alpha_{k(1)} M_1 + \alpha_{k(2)} M_2) &= 0.5\alpha_{k(1)}^2 M_{11} + \alpha_{k(1)}\alpha_{k(2)} M_{12} + 0.5\alpha_{k(2)}^2 M_{22} \\ &= \alpha_{k(1)}^2 M_1 + \alpha_{k(1)}\alpha_{(2)}(M_1 + M_2) + \alpha_{k(2)}^2 M_2 \\ &= \underbrace{(\alpha_{k(1)} + \alpha_{k(2)})}_{=1}(\alpha_{k(1)} M_1 + \alpha_{k(2)} M_2)\end{aligned} \tag{55}$$

However, as the structure proposed in Assumption 3.1 is more general than the polytopic one, the converse is not always possible. Moreover, a similar but simpler development could be performed assuming $A_c(\alpha_k, \tau_k)$, $\mathfrak{B}_c(\alpha_k)$ and $\bar{\mathfrak{B}}_c(\alpha_k)$ with polytopic description while matrices C_c, $\mathfrak{D}_c$ and $\bar{\mathfrak{D}}_c$ do not depend on α_k, i.e., they would be time-invariant (see, for instance, (CASTELAN et al., 2010)).

Now, consider the following augmented state vector

$$\xi_k = \begin{bmatrix} x_k^\top & x_{k-1}^\top & \cdots & x_{k-\bar{\tau}}^\top & x_{c,k}^\top \end{bmatrix}^\top \in \mathbb{R}^{(\bar{\tau}+1+\sigma)n}. \tag{56}$$

Thus, the closed-loop system can be described as:

$$\begin{aligned}\xi_{k+1} &= \mathbb{A}(\alpha_k, \tau_k)\xi_k - \mathbb{B}(\alpha_k)\Psi(\mathbb{K}(\alpha_k)\xi_k) + \mathbb{B}_\omega(\alpha_k)\omega_k, \\ u_k &= \mathbb{K}(\alpha_k)\xi_k,\end{aligned} \tag{57}$$

where

$$\mathbb{A}(\alpha_k, \tau_k) = 0.5 \sum_{i=1}^{N} \sum_{j=i}^{N} (1 + \rho_{ij})\alpha_{k(i)}\alpha_{k(j)}\mathbb{A}_{ij,\tau_k},$$

$$\begin{bmatrix} \mathbb{B}(\alpha_k) & \mathbb{B}_\omega(\alpha_k) & \mathbb{K}(\alpha_k)^\top \end{bmatrix} = \sum_{i=1}^{N} \alpha_{k(i)} \begin{bmatrix} \mathbb{B}_i & \mathbb{B}_{\omega i} & \mathbb{K}_i^\top \end{bmatrix},$$

with

$$\mathbb{A}_{ij,\tau_k} = \left[\begin{array}{c|c|c} \begin{matrix} \mathfrak{A}_{i,\tau_k} + \mathfrak{A}_{j,\tau_k} \\ + \begin{bmatrix} (B_i\mathfrak{D}_{cj} + B_j\mathfrak{D}_{ci})\mathfrak{C} \\ \mathbf{0} \end{bmatrix} \end{matrix} & \begin{matrix} \bar{\mathfrak{A}}_{i,\tau_k} + \bar{\mathfrak{A}}_{j,\tau_k} \\ + \begin{bmatrix} (B_i\bar{\mathfrak{D}}_{cj} + B_j\bar{\mathfrak{D}}_{ci})\bar{\mathfrak{C}} \\ \mathbf{0} \end{bmatrix} \end{matrix} & \begin{bmatrix} B_iC_{cj} + B_jC_{ci} \\ \mathbf{0} \end{bmatrix} \\ \hline \begin{bmatrix} \mathbf{0} & \mathbf{I}_n \\ \mathbf{0} & \mathbf{0} \end{bmatrix} & \begin{bmatrix} \mathbf{0} & \mathbf{0} \\ \mathbf{I}_{(\bar{\tau}-\sigma)n} & \mathbf{0} \end{bmatrix} & \begin{bmatrix} \mathbf{0} \\ \mathbf{0} \end{bmatrix} \\ \hline \mathfrak{B}_{cij}\mathfrak{C} & \bar{\mathfrak{B}}_{cij}\bar{\mathfrak{C}} & A_{cij,\tau_k} \end{array}\right],$$

$$\mathfrak{A}_{i,\tau_k} = \left[\begin{array}{ccc|c} A_i + \Gamma_{0i} & \cdots & \Gamma_{(\sigma-2)i} & \Gamma_{(\sigma-1)i} \\ \hline \multicolumn{3}{c|}{\mathbf{I}_{(\sigma-1)n}} & \mathbf{0} \end{array}\right], \; \bar{\mathfrak{A}}_{i,\tau_k} = \left[\begin{array}{ccc} \Gamma_{\sigma i} & \Gamma_{(\sigma+1)i} & \cdots \; \Gamma_{\bar{\tau}i} \\ \hline \multicolumn{3}{c}{\mathbf{0}} \end{array}\right],$$

$$\mathbb{B}_i = \begin{bmatrix} B_i \\ \mathbf{0} \\ E_{ci} \end{bmatrix}, \; \mathbb{B}_{\omega i} = \begin{bmatrix} B_{\omega i} \\ \mathbf{0} \\ \mathbf{0} \end{bmatrix}, \; \mathbb{K}_i = \begin{bmatrix} \mathfrak{D}_{ci}\mathfrak{C} & \bar{\mathfrak{D}}_{ci}\bar{\mathfrak{C}} & C_c \end{bmatrix}, \; \mathfrak{C} = \mathbf{I}_{\sigma n} \otimes C, \; \bar{\mathfrak{C}} = \mathbf{I}_{(\bar{\tau}+1-\sigma)n} \otimes C,$$

$$\Gamma_{si} = \begin{cases} A_{di}, & \text{if } s = \tau_k, \\ \mathbf{0}, & \text{otherwise,} \end{cases} \qquad \rho_{ij} = \begin{cases} 1, & \text{if } i \neq j, \\ 0, & \text{otherwise.} \end{cases}$$

Note that, in matrices $\mathbb{A}_{ij,\tau_k}$, the blocks $(2,1)$, $(2,2)$, and $(2,3)$, with dimensions $(\bar{\tau}+1-\sigma)n \times \sigma n$, $(\bar{\tau}+1-\sigma)n \times (\bar{\tau}+1-\sigma)n$, and $(\bar{\tau}+1-\sigma)n \times \sigma n$, respectively, disappear with $\sigma = \bar{\tau}+1$, i.e., when the controller has full order, $x_{c,k} \in \mathbb{R}^{(\bar{\tau}+1)n}$. A similar fact occurs with blocks $(2,1)$ of matrices $\mathbb{B}_i$ and $\mathbb{B}_{\omega i}$ and block $(1,2)$ of $\mathbb{K}_i$, thus matching the fact that matrices $\bar{\mathfrak{A}}$, $\bar{\mathfrak{B}}_c$, $\bar{\mathfrak{C}}$, and $\bar{\mathfrak{D}}_c$ also disappear in this case.

3.2.2 Regional stability analysis

The following lemma can be used to analyze the regional stability of the closed-loop system (57). The LMI conditions are based on the Lyapunov theory and, more specifically, on the use of the following candidate Lyapunov function

$$V(\xi_k, \alpha_k, \tau_k) = \xi_k^\top W^{-1}(\alpha_k, \tau_k)\xi_k, \;\; W(\alpha_k, \tau_k) = \sum_{i=1}^{N} \alpha_{k(i)} W_{i,\tau_k}, \tag{58}$$

with $0 < W_{i,\tau_k} = W_{i,\tau_k}^\top \in \mathbb{R}^{(\bar{\tau}+1+\sigma)n \times (\bar{\tau}+1+\sigma)n}$, $\alpha_k \in \Lambda$ and $\tau_k \in \mathcal{I}[\underline{\tau}, \bar{\tau}]$.

We also use Lemma 2.2 to guarantee the confinement of the trajectories of the closed-loop system (57) in the level set $\mathcal{L}_\mathcal{V}(\mu)$ associated to (58) and Lemma 2.1 to deal with the saturation effects.

Lema 3.1 *Consider the closed-loop system (57) with given controller matrices A_{cij,τ_k}, $\mathfrak{B}_{cij}$, $\bar{\mathfrak{B}}_{cij}$ C_{ci}, $\mathfrak{D}_{ci}$, $\bar{\mathfrak{D}}_{ci}$, and E_{ci}. Suppose that there exist symmetric positive definite matrices $W_{i,\tau_k} \in \mathbb{R}^{(\bar{\tau}+1+\sigma)n \times (\bar{\tau}+1+\sigma)n}$, positive definite diagonal matrix $S \in \mathbb{R}^{n_u \times n_u}$, matrices $H_i \in \mathbb{R}^{n_u \times (\bar{\tau}+1+\sigma)n}$ and $U \in \mathbb{R}^{(\bar{\tau}+1+\sigma)n \times (\bar{\tau}+1+\sigma)n}$, with $i \in \mathcal{I}[1,N]$ and $\tau_k \in \mathcal{I}[\underline{\tau}, \bar{\tau}]$, and positive scalars δ and μ, such that the following LMIs are feasible.*

$$\begin{bmatrix} -W_{r,\tau^+} & 0.5\mathbb{A}_{ij,\tau_k}U & -0.5\mathbb{B}_i S & 0.5(\mathbb{B}_{\omega i} + \mathbb{B}_{\omega j}) \\ \star & 0.5(W_{i,\tau_k} + W_{j,\tau_k}) - U - U^\top & 0.5(H_i + H_j)^\top & \mathbf{0} \\ \star & \star & -2S & \mathbf{0} \\ \star & \star & \star & -\mathbf{I}_{n_\omega} \end{bmatrix} < \mathbf{0}, \tag{59}$$

$$r, i \in \mathcal{I}[1,N]; \; j \in \mathcal{I}[i,N]; \; \tau^+ \in \mathcal{C}(\tau_k); \; \tau_k \in \mathcal{I}[\underline{\tau}, \bar{\tau}],$$

$$\begin{bmatrix} W_{i,\tau_k} - U^\top - U & U^\top \mathbb{K}_{i(\ell)}^\top - H_{i(\ell)}^\top \\ \star & -\mu \bar{u}_{(\ell)}^2 \end{bmatrix} < 0, \\ \ell \in \mathcal{I}[1, m];\ i \in \mathcal{I}[1, N];\ \tau_k \in \mathcal{I}[\underline{\tau}, \bar{\tau}], \tag{60}$$

and

$$\mu - \delta < 0. \tag{61}$$

Then,

1. *for all $\omega_k \neq 0$, with $\omega_k \in \mathcal{W}(\delta)$, and for all ξ_0 belonging to the set $\mathcal{R}_{\mathcal{E}0} = \mathcal{L}_\mathcal{V}(\beta) \subseteq \mathcal{R}_0$, with $\beta^{-1} = \mu^{-1} - \delta^{-1}$, the trajectories of the closed-loop system (57) do not leave the set $\mathcal{R}_\mathcal{E} = \mathcal{L}_\mathcal{V}(\mu) \subseteq \mathcal{R}_\mathcal{A}$, for all $k > 0$;*

2. *for all $\omega_k = 0$, the set $\mathcal{R}_\mathcal{E}$ is a region of asymptotic stability for the closed-loop system (57), for all $k > 0$.*

Proof: First, by supposing the feasibility of (60), multiply its left-hand side by $\alpha_{k(i)}$ and sum it up to $i \in \mathcal{I}[1, N]$. Then, replace $H(\alpha_k)$ by $\mathbb{G}(\alpha_k)U$ and use the fact that $[W(\alpha_k, \tau_k) - U]^\top W^{-1}(\alpha_k, \tau_k)[W(\alpha_k, \tau_k) - U] \geq 0$ to replace the block $(1,1)$ by $-U^\top W^{-1}(\alpha_k, \tau_k)U$, thus obtaining

$$\begin{bmatrix} -U^\top W^{-1}(\alpha_k, \tau_k)U & (\mathbb{K}(\alpha_k)_{(\ell)}U - \mathbb{G}(\alpha_k)_{(\ell)}U)^\top \\ \star & -\mu \bar{u}_{(\ell)}{}^2 \end{bmatrix} < 0. \tag{62}$$

With the regularity of U, we can pre- and post-multiply (62) by $\mathtt{diag}\{U^{-\top}, 1\}$ and its transpose, respectively, to get

$$\begin{bmatrix} -W^{-1}(\alpha_k, \tau_k) & (\mathbb{K}(\alpha_k)_{(\ell)} - \mathbb{G}(\alpha_k)_{(\ell)})^\top \\ \star & -\mu \bar{u}_{(\ell)}{}^2 \end{bmatrix} < 0. \tag{63}$$

Finally, applying Schur's complement and pre- and post-multiplying the resulting inequality by $\xi_k^\top$ and ξ_k, we have that

$$-\xi_k^\top W^{-1}(\alpha_k, \tau_k)\xi_k - \xi_k^\top (\mathbb{K}(\alpha_k)_{(\ell)} - \mathbb{G}(\alpha_k)_{(\ell)})^\top \\ \times (\mu \bar{u}_{(\ell)}{}^2)^{-1} (\mathbb{K}(\alpha_k)_{(\ell)} - \mathbb{G}(\alpha_k)_{(\ell)})\xi_k \leq 0, \tag{64}$$

which, from (58) and (19), ensures the inclusion $\mathcal{R}_\mathcal{E} = \mathcal{L}_\mathcal{V}(\mu) \subseteq \mathcal{S}(\bar{u})$ and, consequently, Lemma 2.1 applies. Therefore, any trajectory of the closed-loop system (57) starting in $\mathcal{R}_\mathcal{E}$ remains in $\mathcal{S}(\bar{u})$.

Moreover, if (59) is also satisfied, multiply its left-hand side by $\alpha_{k+1(r)}$, $\alpha_{k(i)}$, $\alpha_{k(j)}$ and ρ_{ij} with $\rho_{ij} = 1$ if $i \neq j$ and $\rho_{ij} = 0$ otherwise, and sum it up to r, $i \in$

$\mathcal{I}[1,N]$ and $j \in \mathcal{I}[i,N]$. Then, replace $H(\alpha_k)$ by $\mathbb{G}(\alpha_k)U$ and use again the fact that $-U^\top W^{-1}(\alpha_k,\tau_k)U \leq W(\alpha_k,\tau_k) - U^\top - U$ to obtain

$$\begin{bmatrix} -W(\alpha^+,\tau^+) & \mathbb{A}(\alpha_k,\tau_k)U & -\mathbb{B}(\alpha_k)S & \mathbb{B}_\omega(\alpha_k) \\ \star & -U^\top W^{-1}(\alpha_k,\tau_k)U & U^\top\mathbb{G}(\alpha_k)^\top & \mathbf{0} \\ \star & \star & -2S & \mathbf{0} \\ \star & \star & \star & -\mathbf{I}_{n_\omega} \end{bmatrix} < \mathbf{0}, \tag{65}$$

where α^+ represents α_{k+1}. With the regularity of U, we can pre- and post-multiply (65) by $\mathtt{diag}\{\mathbf{I}_{(\bar{\tau}+1+\sigma)n}, U^{-\top}, S^{-\top}, \mathbf{I}_{n_\omega}\}$ and its transpose, respectively, to get

$$\begin{bmatrix} -W(\alpha^+,\tau^+) & \mathbb{A}(\alpha_k,\tau_k) & -\mathbb{B}(\alpha_k) & \mathbb{B}_\omega(\alpha_k) \\ \star & -W^{-1}(\alpha_k,\tau_k) & \mathbb{G}(\alpha_k)^\top S^{-1} & \mathbf{0} \\ \star & \star & -2S^{-1} & \mathbf{0} \\ \star & \star & \star & -\mathbf{I}_{n_\omega} \end{bmatrix} < \mathbf{0}. \tag{66}$$

Next, applying Schur's complement, we have that

$$\begin{bmatrix} -W^{-1}(\alpha_k,\tau_k) & \mathbb{G}(\alpha_k)^\top S^{-1} & \mathbf{0} \\ \star & -2S^{-1} & \mathbf{0} \\ \star & \star & -\mathbf{I}_{n_\omega} \end{bmatrix} + \begin{bmatrix} \mathbb{A}(\alpha_k,\tau_k)^\top \\ -\mathbb{B}(\alpha_k)^\top \\ \mathbb{B}_\omega(\alpha_k)^\top \end{bmatrix} W^{-1}(\alpha^+,\tau^+) \times \begin{bmatrix} \mathbb{A}(\alpha_k,\tau_k) & -\mathbb{B}(\alpha_k) & \mathbb{B}_\omega(\alpha_k) \end{bmatrix} < \mathbf{0}. \tag{67}$$

Then, pre- and post-multiplying (67) by the augmented vector $\begin{bmatrix} \xi_k^\top & \Psi(\mathbb{K}(\alpha_k)\xi_k)^\top & \omega_k^\top \end{bmatrix}$ and its transpose, respectively, and replacing $\mathbb{A}(\alpha_k,\tau_k)\xi_k - \mathbb{B}(\alpha_k)\Psi(\mathbb{K}(\alpha_k)\xi_k) + \mathbb{B}_\omega(\alpha_k)\omega_k$ by ξ_{k+1}, according to (57), results in

$$\xi_{k+1}^\top W^{-1}(\alpha^+,\tau^+)\xi_{k+1} - \xi_k^\top W^{-1}(\alpha_k,\tau_k)\xi_k - 2\Psi(\mathbb{K}(\alpha_k)\xi_k)^\top S^{-1}(\Psi(\mathbb{K}(\alpha_k)\xi_k) - \mathbb{G}(\alpha_k)\xi_k) - \omega_k^\top\omega_k < 0. \tag{68}$$

From (21), we have that $\xi_{k+1}^\top W^{-1}(\alpha^+,\tau^+)\xi_{k+1} - \xi_k^\top W^{-1}(\alpha_k,\tau_k)\xi_k = V(\xi_{k+1},\alpha_{k+1},\tau_{k+1}) - V(\xi_k,\alpha_k,\tau_k) = \Delta V(\xi_k,\alpha_k,\tau_k)$. By taking this into account and denoting $\mathbb{T} = S^{-1}$, we conclude that

$$\Delta V(\xi_k,\alpha_k,\tau_k) - 2\Psi(\mathbb{K}(\alpha_k)\xi_k)^\top\mathbb{T}(\Psi(\mathbb{K}(\alpha_k)\xi_k) - \mathbb{G}(\alpha_k)\xi_k) - \omega_k^\top\omega_k \leq 0. \tag{69}$$

By supposing that $\xi_k \in \mathcal{S}(\bar{u})$, the generalized sector condition presented in Lemma 2.1 ensures the non-positivity of $2\Psi(\mathbb{K}(\alpha_k)\xi_k)^\top\mathbb{T}(\Psi(\mathbb{K}(\alpha_k)\xi_k) - \mathbb{G}(\alpha_k)\xi_k)$, which implies $\Delta V(\xi_k,\alpha_k,\tau_k) - \omega_k^\top\omega_k \leq 0$. Because of the positivity of $W(\alpha_k,\tau_k)$, we can assume that there exist a sufficiently small $\epsilon_0 > 0$ such that

$$\epsilon_0\|\xi_k\|^2 \leq V(\xi_k,\alpha_k,\tau_k) \leq \epsilon_1\|\xi_k\|^2, \text{ with } \epsilon_1^{-1} = \min_{i\in\mathcal{I}[1,N]} \lambda_{\min}{}_{\tau_k\in\mathcal{I}[\underline{\tau},\bar{\tau}]} W_{i,\tau_k} > 0. \tag{70}$$

Moreover, from (69) with $\omega_k = \mathbf{0}$, we have that

$$\Delta V(\xi_k, \alpha_k, \tau_k) < 2\Psi(\mathbb{K}(\alpha_k)\xi_k)^\top \mathbb{T}(\alpha_k)(\Psi(\mathbb{K}(\alpha_k)\xi_k) - \mathbb{G}(\alpha_k)\xi_k) \leq -\epsilon_2\|\xi_k\|^2 < 0 \quad (71)$$

for some $\epsilon_2 > 0$. Therefore, $V(\xi_k, \alpha_k, \tau_k)$ given in (58) is a Lyapunov function and $\mathcal{R}_\mathcal{E} = \mathcal{L}_\mathcal{V}(\mu)$ is an estimate of the region of attraction of the origin for the closed-loop system (57). That concludes the proof. ∎

3.3 MAIN RESULTS

Before presenting the conditions for the synthesis of the dynamic controller (53), we introduce some matrices that are useful in the development of the results. Based on the approach proposed by (SCHERER, C. et al., 1997), let us define the real matrices $X, Y \in \mathbb{R}^{(\bar{\tau}+1)n\times(\bar{\tau}+1)n}$, $Z, P \in \mathbb{R}^{\sigma n\times(\bar{\tau}+1)n}$, $X_1, X_3, Y_1, Y_3 \in \mathbb{R}^{n\times\sigma n}$, $X_2, Y_2 \in \mathbb{R}^{(\sigma-1)n\times\sigma n}$, $X_4, Y_4 \in \mathbb{R}^{(\bar{\tau}-\sigma)n\times\sigma n}$, and $Z_1, P_1 \in \mathbb{R}^{\sigma n\times\sigma n}$ with the following structures

$$X = \left[\begin{array}{c|c} X_1 & \mathbf{0} \\ X_2 & \\ \hline X_3 & \\ X_4 & \mathbf{I}_{(\bar{\tau}+1-\sigma)n} \end{array}\right], \; Y = \left[\begin{array}{c|c} Y_1 & \mathbf{0} \\ Y_2 & \\ \hline Y_3 & \\ Y_4 & \mathbf{I}_{(\bar{\tau}+1-\sigma)n} \end{array}\right], \; Z = \begin{bmatrix} Z_1 & \mathbf{0} \end{bmatrix}, \text{ and } P = \begin{bmatrix} P_1 & \mathbf{0} \end{bmatrix},$$

such that,

$$U = \begin{bmatrix} X & \bullet \\ Z & \bullet \end{bmatrix}, \quad U^{-1} = \begin{bmatrix} Y & \bullet \\ P & \bullet \end{bmatrix} \text{ and } \Theta = \left[\begin{array}{c|c|c} Y_1 & \mathbf{0} & \mathbf{I}_{\sigma n} \\ Y_2 & & \\ \hline Y_3 & \mathbf{I}_{(\bar{\tau}+1-\sigma)n} & \mathbf{0} \\ Y_4 & & \\ \hline P_1 & \mathbf{0} & \mathbf{0} \end{array}\right]. \quad (72)$$

Therefore, we have

$$U\Theta = \left[\begin{array}{c|c|c} \mathbf{I}_{\sigma n} & \mathbf{0} & X_1 \\ & & X_2 \\ \hline \mathbf{0} & \mathbf{I}_{(\bar{\tau}+1-\sigma)n} & X_3 \\ & & X_4 \\ \hline \mathbf{0}_{\sigma n} & \mathbf{0} & Z_1 \end{array}\right] \text{ and } \hat{U} = \Theta^\top U\Theta = \left[\begin{array}{c|c} Y^\top & F^\top \\ \hline \begin{bmatrix} \mathbf{I}_{\sigma n} & \mathbf{0} \end{bmatrix} & X_1 \\ & X_2 \end{array}\right], \quad (73)$$

where, by construction

$$F = \begin{bmatrix} X_1^\top & X_2^\top & X_3^\top & X_4^\top \end{bmatrix} Y + Z_1^\top P_1. \quad (74)$$

Furthermore, using the partitioning

$$W_{i,j} = \begin{bmatrix} W_1 & W_2 \\ \star & W_3 \end{bmatrix}_{i,j} \text{ with } W_{1i,j} = \begin{bmatrix} W_{1A} & W_{1B} \\ \star & W_{1C} \end{bmatrix}_{i,j} \text{ and } W_{2i,j} = \begin{bmatrix} W_{2A} \\ W_{2B} \end{bmatrix}_{i,j},$$

we obtain

$$\hat{W}_{i,j} = \Theta^\top W_{i,j}\Theta = \begin{bmatrix} Y^\top W_{1i,j}Y + P^\top W_{2i,j}^\top Y & Y^\top \begin{bmatrix} W_{1Ai,j} \\ W_{1Bi,j}^\top \end{bmatrix} + P^\top W_{1Ci,j}^\top \\ +Y^\top W_{2i,j}P + P^\top W_{3i,j}P & \\ \star & W_{1Ai,j} \end{bmatrix}, \\ = \begin{bmatrix} \hat{W}_1 & \hat{W}_2 \\ \star & \hat{W}_3 \end{bmatrix}_{i,j}. \tag{75}$$

With the aid of these matrices, we can provide a solution to Problem 3.1 through the next theorem.

Theorem 3.1 *Suppose that there exist symmetric positive definite matrices $\hat{W}_{i,\tau_k}$, positive definite diagonal matrix S, matrices $\hat{A}_{cij,\tau_k}$, $\hat{\mathfrak{B}}_{cij}$, $\hat{\bar{\mathfrak{B}}}_{cij}$ $\hat{C}_{ci}$, $\hat{\mathfrak{D}}_{ci}$, $\hat{\bar{\mathfrak{D}}}_{ci}$, $\hat{E}_{ci}$, X, Y, F of appropriate dimensions, $\hat{H}_{1i} \in \mathbb{R}^{n_u \times \sigma n}$, $\hat{H}_{2i} \in \mathbb{R}^{n_u \times (\bar{\tau}+1-\sigma)n}$, and $\hat{H}_{3i} \in \mathbb{R}^{n_u \times \sigma n}$, with $i \in \mathcal{I}[1, N]$, $j \in \mathcal{I}[i, N]$ and $\tau_k \in \mathcal{I}[\underline{\tau}, \bar{\tau}]$, and positive scalars δ and μ, such that the following LMIs are feasible.*

$$\left[\begin{array}{c|c|c|c} -\hat{W}_{r,\tau^+} & 0.5\Pi_{1ij} & 0.5\Pi_{2ij} & 0.5\Pi_{3ij} \\ \hline \star & 0.5(\hat{W}_{i,\tau_k} + \hat{W}_{j,\tau_k}) - \hat{U} - \hat{U}^\top & 0.5\Pi_{4ij} & \mathbf{0} \\ \hline \star & \star & -2S & \mathbf{0} \\ \hline \star & \star & \star & -\mathbf{I}_{n_\omega} \end{array}\right] < \mathbf{0}, \tag{76}$$

$$r, i \in \mathcal{I}[1, N];\ j \in \mathcal{I}[i, N];\ \tau^+ \in \mathcal{C}(\tau_k);\ \tau_k \in \mathcal{I}[\underline{\tau}, \bar{\tau}],$$

$$\left[\begin{array}{c|c} \hat{W}_{i,\tau_k} - \hat{U}^\top - \hat{U} & \begin{array}{c} \left(\hat{\mathfrak{D}}_{ci(\ell)}\mathfrak{C} - \hat{H}_{1i(\ell)}\right)^\top \\ \left(\hat{\bar{\mathfrak{D}}}_{ci(\ell)}\bar{\mathfrak{C}} - \hat{H}_{2i(\ell)}\right)^\top \\ \left(\hat{C}_{ci(\ell)} - \hat{H}_{3i(\ell)}\right)^\top \end{array} \\ \hline \star & -\mu\bar{u}_{(\ell)}{}^2 \end{array}\right] < \mathbf{0}, \tag{77}$$

$$\ell \in \mathcal{I}[1, m];\ i \in \mathcal{I}[1, N];\ \tau_k \in \mathcal{I}[\underline{\tau}, \bar{\tau}],$$

and

$$\mu - \delta < 0, \tag{78}$$

where

$$\Pi_{1ij} = \left[\begin{array}{c|c|c} \begin{array}{c}\begin{bmatrix} Y_1^\top & Y_2^\top \end{bmatrix}\left(\mathfrak{A}_{i,\tau_k}+\mathfrak{A}_{j,\tau_k}\right)\\ +2Y_3^\top\begin{bmatrix}\mathbf{0} & \mathbf{I}_n\end{bmatrix}+\hat{\mathfrak{B}}_{cij}\mathfrak{C}\end{array} & \begin{array}{c}\begin{bmatrix} Y_1^\top & Y_2^\top \end{bmatrix}\left(\bar{\mathfrak{A}}_{i,\tau_k}+\bar{\mathfrak{A}}_{j,\tau_k}\right)\\ +Y_4^\top\begin{bmatrix}2\mathbf{I}_{(\bar{\tau}-\sigma)n} & \mathbf{0}\end{bmatrix}+\hat{\bar{\mathfrak{B}}}_{cij}\bar{\mathfrak{C}}\end{array} & \hat{A}_{cij,\tau_k} \\ \hline \begin{bmatrix}\mathbf{0} & 2\mathbf{I}_n\\ \mathbf{0} & \mathbf{0}\end{bmatrix} & \begin{bmatrix}\mathbf{0} & \mathbf{0}\\ 2\mathbf{I}_{(\bar{\tau}-\sigma)n} & \mathbf{0}\end{bmatrix} & \begin{array}{c}\begin{bmatrix}\mathbf{0} & 2\mathbf{I}_n\\ \mathbf{0} & \mathbf{0}\end{bmatrix}\begin{bmatrix}X_1\\ X_2\end{bmatrix}\\ +\begin{bmatrix}\mathbf{0} & \mathbf{0}\\ 2\mathbf{I}_{(\bar{\tau}-\sigma)n} & \mathbf{0}\end{bmatrix}\begin{bmatrix}X_3\\ X_4\end{bmatrix}\end{array} \\ \hline \begin{array}{c}\mathfrak{A}_{i,\tau_k}+\mathfrak{A}_{j,\tau_k}\\ +\begin{bmatrix}\left(B_i\hat{\mathfrak{D}}_{cj}+B_j\hat{\mathfrak{D}}_{ci}\right)\mathfrak{C}\\ \mathbf{0}\end{bmatrix}\end{array} & \begin{array}{c}\bar{\mathfrak{A}}_{i,\tau_k}+\bar{\mathfrak{A}}_{j,\tau_k}\\ +\begin{bmatrix}\left(B_i\hat{\bar{\mathfrak{D}}}_{cj}+B_j\hat{\bar{\mathfrak{D}}}_{ci}\right)\bar{\mathfrak{C}}\\ \mathbf{0}\end{bmatrix}\end{array} & \begin{array}{c}\left(\mathfrak{A}_{i,\tau_k}+\mathfrak{A}_{j,\tau_k}\right)\begin{bmatrix}X_1^\top & X_2^\top\end{bmatrix}^\top\\ +\left(\bar{\mathfrak{A}}_{i,\tau_k}+\bar{\mathfrak{A}}_{j,\tau_k}\right)\begin{bmatrix}X_3^\top & X_4^\top\end{bmatrix}^\top\\ +\begin{bmatrix}B_i\hat{C}_{cj}+B_j\hat{C}_{ci}\\ \mathbf{0}\end{bmatrix}\end{array} \end{array}\right],$$

$$\Pi_{2i} = \left[\begin{array}{c} -\left(\hat{E}_{ci}+\hat{E}_{cj}\right)\\ \hline \mathbf{0}\\ \hline \begin{bmatrix}-\left(B_i+B_j\right)S\\ \mathbf{0}\end{bmatrix}\end{array}\right],\ \Pi_{3i} = \left[\begin{array}{c} Y_1^\top\left(B_{\omega i}+B_{\omega j}\right)\\ \hline \mathbf{0}\\ \hline \begin{bmatrix}B_{\omega i}+B_{\omega j}\\ \mathbf{0}\end{bmatrix}\end{array}\right],\ \Pi_{4i} = \left[\begin{array}{c} \left(\hat{H}_{1i}+\hat{H}_{1j}\right)^\top\\ \hline \left(\hat{H}_{2i}+\hat{H}_{2j}\right)^\top\\ \hline \left(\hat{H}_{3i}+\hat{H}_{3j}\right)^\top\end{array}\right],\ \textit{and}$$

$$\hat{U} = \left[\begin{array}{c|c} Y^\top & F^\top\\ \hline \begin{bmatrix}\mathbf{I}_{\sigma n} & \mathbf{0}\end{bmatrix} & \begin{array}{c}X_1\\ X_2\end{array}\end{array}\right].$$

Then, by choosing non-singular matrices P_1 and Z_1 such that (74) holds, we have that the saturating LPV system (47) under the dynamic output-feedback controller (53) with

matrices defined by

$$
\begin{aligned}
&\mathfrak{D}_{ci} = \hat{\mathfrak{D}}_{ci},\ \bar{\mathfrak{D}}_{ci} = \hat{\bar{\mathfrak{D}}}_{ci},\\
&C_{ci} = \left(\hat{C}_{ci} - \hat{\mathfrak{D}}_{cj}\mathfrak{C}\begin{bmatrix}X_1\\X_2\end{bmatrix} - \hat{\bar{\mathfrak{D}}}_{cj}\bar{\mathfrak{C}}\begin{bmatrix}X_3\\X_4\end{bmatrix}\right)Z_1^{-1},\\
&\mathfrak{B}_{cij} = P_1^{-\top}\left(\hat{\mathfrak{B}}_{cij} - Y_1^{\top}\left(B_i\hat{\mathfrak{D}}_{cj} + B_j\hat{\mathfrak{D}}_{ci}\right)\right),\ \bar{\mathfrak{B}}_{cij} = P_1^{-\top}\left(\hat{\bar{\mathfrak{B}}}_{cij} - Y_1^{\top}\left(B_i\hat{\bar{\mathfrak{D}}}_{cj} + B_j\hat{\bar{\mathfrak{D}}}_{ci}\right)\right),\\
&A_{c_{ij,\tau_k}} = P_1^{-\top}\left(\hat{A}_{cij,\tau_k} - \left(\begin{bmatrix}Y_1^{\top} & Y_2^{\top}\end{bmatrix}\left(\mathfrak{A}_{i,\tau_k} + \mathfrak{A}_{j,\tau_k}\right) + Y_3^{\top}\begin{bmatrix}0 & \mathbf{I}_n\end{bmatrix} + \hat{\mathfrak{B}}_{cij}\mathfrak{C}\right)\begin{bmatrix}X_1\\X_2\end{bmatrix}\right.\\
&\qquad + \left(\begin{bmatrix}Y_1^{\top} & Y_2^{\top}\end{bmatrix}\left(\bar{\mathfrak{A}}_{i,\tau_k} + \bar{\mathfrak{A}}_{j,\tau_k}\right) + Y_4^{\top}\begin{bmatrix}\mathbf{I}_{(\bar{\tau}-\sigma)n} & 0\end{bmatrix} + \hat{\bar{\mathfrak{B}}}_{cij}\bar{\mathfrak{C}}\right)\begin{bmatrix}X_3\\X_4\end{bmatrix}\\
&\qquad \left. + Y_1^{\top}\left(B_iC_{cj} + B_jC_{ci}\right)Z_1\right)Z_1^{-1},\\
&E_{ci} = P_1^{-\top}\left(\hat{E}_{ci}S^{-1} - Y_1^{\top}B_i\right),
\end{aligned}
\tag{79}
$$

is ISS, verifying:

1. *for all $\omega_k \neq 0$, with $\omega_k \in \mathcal{W}(\delta)$, and for all ξ_0 belonging to the set $\mathcal{R}_{\mathcal{E}0} = \mathcal{L}_{\mathcal{V}}(\beta) \subseteq \mathcal{R}_0$, with $\beta^{-1} = \mu^{-1} - \delta^{-1}$, the trajectories of the closed-loop system (57) do not leave the set $\mathcal{R}_{\mathcal{E}} = \mathcal{L}_{\mathcal{V}}(\mu) \subseteq \mathcal{R}_{\mathcal{A}}$, for all $k > 0$;*

2. *for all $\omega_k = 0$, the set $\mathcal{R}_{\mathcal{E}}$ is a region of asymptotic stability for the closed-loop system (57), for all $k > 0$.*

Proof: By supposing the feasibility of (76), from block $(2,2)$, it follows that $\hat{U} + \hat{U}^{\top} > 0$, consequently, $\hat{U}$ is non-singular. Therefore, from (74), we have X and Y non-singular and we can write $\hat{U}$ as

$$
\begin{aligned}
\hat{U} &= \left[\begin{array}{cc|c} Y^{\top} & & F^{\top}\\ \hline \mathbf{I}_{\sigma n} & 0 & X_1\\ & & X_2 \end{array}\right],\\
&= \left[\begin{array}{cc|c} \mathbf{I}_{(\bar{\tau}+1)n} & & Y^{\top}\\ \hline 0 & & \mathbf{I}_{\sigma n}\ \ 0 \end{array}\right]\left[\begin{array}{cc|c} 0 & & F^{\top} - Y^{\top}\begin{bmatrix}X_1^{\top} & X_2^{\top} & X_3^{\top} & X_4^{\top}\end{bmatrix}^{\top}\\ \hline \mathbf{I}_{(\bar{\tau}+1)n} & & \begin{bmatrix}X_1^{\top} & X_2^{\top} & X_3^{\top} & X_4^{\top}\end{bmatrix}^{\top} \end{array}\right],
\end{aligned}
\tag{80}
$$

which allows us to conclude that $\left(F - \begin{bmatrix}X_1^{\top} & X_2^{\top} & X_3^{\top} & X_4^{\top}\end{bmatrix}Y\right)$ is also non-singular. As a result, it is always possible to choose non-singular matrices P_1 and Z_1, such that (74) is satisfied. This shows that the gains (79) are well-defined.

Moreover, by considering $H_i = \begin{bmatrix}\hat{H}_{1i} & \hat{H}_{2i} & \hat{H}_{3i}\end{bmatrix}$, the matrices (72)-(75) and the change of variables $\hat{A}_{cij,\tau_k}$, $\hat{\mathfrak{B}}_{cij}$, $\hat{\bar{\mathfrak{B}}}_{cij}$ $\hat{C}_{ci}$, $\hat{\mathfrak{D}}_{ci}$, $\hat{\bar{\mathfrak{D}}}_{ci}$, $\hat{E}_{ci}$ according to (79), pre- and post-multiply (76) by $\mathtt{diag}\{\Theta^{-\top}, \Theta^{-\top}, \mathbf{I}_{n_u}, \mathbf{I}_{n_\omega}\}$ and its transpose, respectively, to obtain (59)

and, likewise, pre- and post-multiply (77) by $\mathtt{diag}\{\Theta^{-\top}, 1\}$ and its transpose, respectively, to obtain (60). Thus, from Theorem 3.1, these two equivalences allow to conclude the proof. ∎

Remark 3.1 *The design of the dynamic controller (53) through Theorem 3.1 imposes for given X, Y and F, to compute non-singular matrices P_1 and Z_1 satisfying (74) or, equivalently, $Z_1^\top P_1 = F - \begin{bmatrix} X_1^\top & X_2^\top & X_3^\top & X_4^\top \end{bmatrix} Y$. However, the choice of these matrices can be performed in different ways, for instance, we can set $P_1 = \phi \mathbf{I}_{\sigma n}$, for any scalar ϕ, and compute $Z_1^\top = \left(F - \begin{bmatrix} X_1^\top & X_2^\top & X_3^\top & X_4^\top \end{bmatrix} Y\right) \phi^{-1}$, or even use a matrix decomposition, such as LU and QR to determine them.*

Remark 3.2 *Equation (57) allows understanding the closed-loop system as equivalent to an augmented delay-free LPV system controlled by a parameter-dependent state-feedback controller. Thus, we can impose some structures on $\mathbb{K}(\alpha_k)$ such that the respective control law uses only a subset of the augmented state ξ_k. For instance, one may choose $\mathbb{K}_{c1}(\alpha_k) = \begin{bmatrix} \mathbb{K}_0(\alpha_k) & \mathbf{0} & \cdots & \mathbf{0} & \mathbf{0} \end{bmatrix}$, that feeds back only x_k, or $\mathbb{K}_{c2}(\alpha_k) = \begin{bmatrix} \mathbb{K}_0(\alpha_k) & \mathbf{0} & \cdots & \mathbf{0} & \mathbb{K}_{\bar{\tau}}(\alpha_k) & \mathbf{0} \end{bmatrix}$, where x_k and $x_{k-\bar{\tau}}$ are feedback. Such a constraint on the gain $\mathbb{K}(\alpha_k)$ can be done by imposing null matrices on $\mathfrak{C}$, $\bar{\mathfrak{C}}$, $\mathfrak{B}_c$, $\bar{\mathfrak{B}}_c$, $\mathfrak{D}_c$, and $\bar{\mathfrak{D}}_c$ in the positions corresponding to the delayed states that are not feedback.*

Remark 3.3 *The numerical complexity of the proposed LMI conditions are related with their number of scalar variables, $\mathcal{K}$, and their number of rows, $\mathcal{R}$. By denoting $\hat{\tau} = \bar{\tau} - \underline{\tau} + 1$, we have that $\mathcal{K} = (0.5((\bar{\tau}+1+\sigma)n+1)\hat{\tau} + n_u)(\bar{\tau}+1+\sigma)nN + ((2n + 0.5n_yN(N+1))(\bar{\tau}+1) + (0.5N(N+1)\hat{\tau}+1)\sigma n + 2n_uN)\sigma n + (n_u + n_yN(\bar{\tau}+1))n_u + 2$ and $\mathcal{R} = 0.5(2(\bar{\tau}+1+\sigma)n+n_u+n_\omega)(\hat{\tau}^2-(\hat{\tau}-1-\Delta\tau_{\max})(\hat{\tau}-\Delta\tau_{\max}))N^2(N+1)+((\bar{\tau}+1+\sigma)n+1)n_uN\hat{\tau}+1$. Thus, observe that the number of rows is reduced as the maximal variation rate of the delay, $\Delta\tau_{\max}$, is reduced.*

3.3.1 Optimization design procedures

In this section, some convex optimization procedures are defined to match different control objectives for the closed-loop system.

3.3.1.1 Maximization of disturbance tolerance (δ^{-1})

Suppose that the closed-loop LPV system (47) is in equilibrium, i.e $\xi_0 = \mathbf{0}$, which implies that $\delta^{-1} = \mu^{-1}$. Thus, the problem of maximization of the disturbance tolerance can be stated as:

$$\mathcal{O}_3 : \begin{cases} \min & \mu, \\ \text{subject to} & \text{LMIs (76) and (77).} \end{cases} \tag{81}$$

3.3.1.2 Maximization of the estimate of the region of attraction $\mathcal{R}_{\mathcal{E}}$

Consider that the closed-loop LPV system (47) is not subject to disturbance input, i.e. $\omega_k = 0$, $\forall k > 0$. To ensure an estimate of the region of attraction for the system as big as possible, we can minimize a scalar η such that $\eta - \mathtt{tr}\left(W_{i,\tau_k}^{-1}\right) \geq 0$ for all $i \in \mathcal{I}[1, N]$ and $\tau_k \in \mathcal{I}[\underline{\tau}, \bar{\tau}]$. By rewriting W_{i,τ_k}^{-1} in terms of $\hat{W}_{i,\tau_k}^{-1}$ conforming to (75) and setting $x_{c,k} = 0$, we have similarly

$$\eta - \mathtt{tr}\left(\begin{bmatrix} Y & \begin{bmatrix} \mathbf{I}_{\sigma n} & \mathbf{0} \end{bmatrix}^{\top} \end{bmatrix} \hat{W}_{i,\tau_k}^{-1} \begin{bmatrix} Y & \begin{bmatrix} \mathbf{I}_{\sigma n} & \mathbf{0} \end{bmatrix}^{\top} \end{bmatrix}^{\top}\right) \geq 0, \tag{82}$$

for all $i \in \mathcal{I}[1, N]$ and $\tau_k \in \mathcal{I}[\underline{\tau}, \bar{\tau}]$. With the aid of the Schur complement, the previous condition can be expressed in the form of LMIs as follows:

$$\left[\begin{array}{c|cc} \eta \mathbf{I}_{(\bar{\tau}+1)n} & Y & \begin{bmatrix} \mathbf{I}_{\sigma n} & \mathbf{0} \end{bmatrix}^{\top} \\ \hline \star & \multicolumn{2}{c}{\hat{W}_{i,\tau_k}} \end{array}\right] \geq \mathbf{0}, \tag{83}$$
$$i \in \mathcal{I}[1, N];\ \tau_k \in \mathcal{I}[\underline{\tau}, \bar{\tau}].$$

Therefore, the optimization procedure can be summarized as:

$$\mathcal{O}_4 : \begin{cases} \min & \eta, \\ \text{subject to} & \text{LMIs (76), (77), and (83).} \end{cases} \tag{84}$$

3.4 NUMERICAL EXAMPLES

In this section, we present two examples to illustrate our proposal and also to compare it with similar approaches in the literature. In the first example, we focus on the problem of designing a controller such that the set of admissible disturbance signals is maximized. In the second one, we exploit the problem of designing a controller that maximizes the estimate of the region of attraction.

3.4.1 Example 1

Initially, we propose to investigate the scalar system (47) with matrices $A = 2(1 + \vartheta_k)$, $A_d = -0.1(1 + \vartheta_k)$, $B = 1(1 + \vartheta_k)$, $B_\omega = 0.1(1 + \vartheta_k)$ and $C = 0.1$, parameter varying $|\vartheta_k| \leq 0.1$, time-varying delay $\tau_k \in \mathcal{I}[0, 7]$ and symmetric saturation limit $\bar{u} = 0.7$ to make clear our approach.

Maximization of disturbance tolerance: The objective is to design a dynamic output feedback controller that maximizes the allowed energy disturbance, δ^{-1}, thus, ensuring that the trajectories of the closed-loop system remain in the estimated region of attraction. We have run the optimization procedure $\mathcal{O}_3$ given in (81) for maximum

delay values $\bar{\tau} \in \mathcal{I}[1, 7]$ and order of the dynamic output-feedback controller in the range n to $(\bar{\tau}+1)n$, i. e., for $\sigma \in \mathcal{I}[1, \bar{\tau}+1]$. Additionally, we supposed a slow variation of the delay by taking $\Delta\tau_{\max} = 1$, which means that among two consecutive instants, the delay must remain in its current value, increase by one, or reduce by one, but always keeping $\tau_k \in \mathcal{I}[0, 7]$.

Figure 7 shows seven plots with the outputs of the optimizations performed. The plots relate the maximum tolerable disturbance energy (δ^{-1}) to the controller order, which is given by σn. Therefore, the horizontal axis of Figure 1, σ, is proportional to the controller order. We note that:

1. In all plots, one for each maximum delay $\bar{\tau} \in \mathcal{I}[1,\ 7]$, it is clear the increase of the tolerable energy disturbance with the increase of σ; and thus the controller order.

2. For a constant order of the controller, σn, the higher $\bar{\tau}$, the smaller the tolerable energy disturbance.

In both cases, it is clear that our proposal, allowing the designer to choose the controller order, improves the achieved results. For instance, in case 1, if the controller order double from 3 ($\sigma = 3$) to 6 ($\sigma = 6$), the tolerable disturbance energy grows more than twice. Furthermore, to avoid the reduction of the maximum admissible energy mentioned in case 2, the increase of σ (and thus the controller order) seems to be a viable solution to mitigate the degradation provides by maximum delay value.

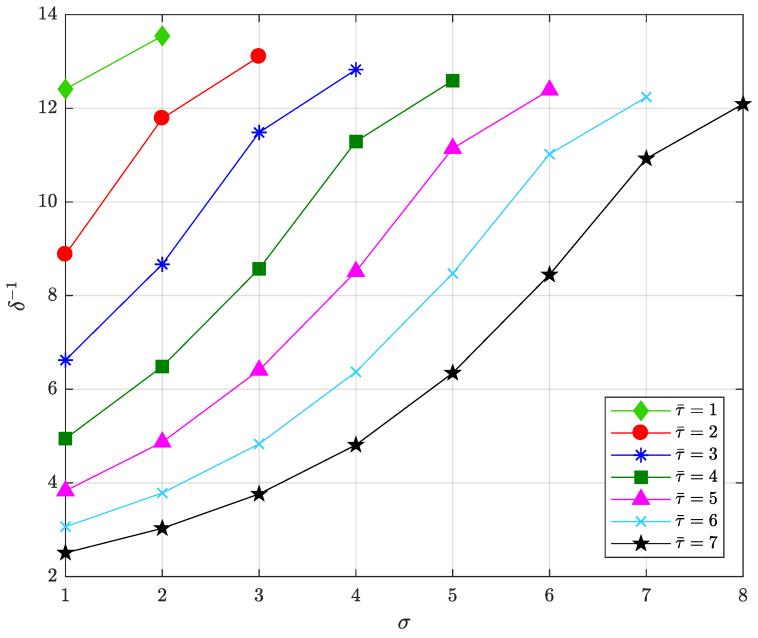

Figure 7 – The maximum tolerable disturbance energy (δ^{-1}) in function of the order of the dynamic controller (σ) for maximum delays $\bar{\tau} = 1$(♦),$\bar{\tau} = 2$(●), $\bar{\tau} = 3$(∗), $\bar{\tau} = 4$(■), $\bar{\tau} = 5$(▲), $\bar{\tau} = 6$(×) and $\bar{\tau} = 7$(⋆).

Next, the time-domain behavior of the closed-loop system is illustrated by a set of simulations performed with $\bar{\tau} = 1$, $\sigma = 1$ (that is, controller order equal to 1). By using the optimization procedure $\mathcal{O}_3$ given in (81), we get the controller data

$$\begin{bmatrix} A_{c11,0} & A_{c12,0} & A_{c21,0} & A_{c22,0} \\ A_{c11,1} & A_{c12,1} & A_{c21,1} & A_{c22,1} \end{bmatrix} = \begin{bmatrix} 0.0315 & 0.0378 & 0.0378 & 0.0718 \\ 0.0124 & 0.0249 & 0.0248 & 0.0264 \end{bmatrix} \text{ and}$$

$$\begin{bmatrix} \mathfrak{B}_{c11} & \mathfrak{B}_{c12} & \mathfrak{B}_{c21} & \mathfrak{B}_{c22} \\ \bar{\mathfrak{B}}_{c11} & \bar{\mathfrak{B}}_{c12} & \bar{\mathfrak{B}}_{c21} & \bar{\mathfrak{B}}_{c22} \end{bmatrix} = \begin{bmatrix} -297.9333 & -250.2424 & -250.2424 & -155.8974 \\ 3.7075 & 1.1032 & 1.1032 & -2.4359 \end{bmatrix}$$

that replaced in (54) yields $A_c(\alpha_k, \tau_k)$, $B_{c0}(\alpha_k)$, and $B_{c1}(\alpha_k)$, and

$$\begin{bmatrix} C_{c1} \\ C_{c2} \end{bmatrix} = \begin{bmatrix} -2.5982 \\ -3.6269 \end{bmatrix} \times 10^{-4}, \quad \begin{bmatrix} \mathfrak{D}_{c1} & \mathfrak{D}_{c2} \\ \bar{\mathfrak{D}}_{c1} & \bar{\mathfrak{D}}_{c2} \end{bmatrix} = \begin{bmatrix} -14.5418 & -17.5271 \\ 0.4183 & 0.5261 \end{bmatrix},$$

and $E_{c1} = E_{c2} = -69.7898$, that replaced in (54) yields $C_c(\alpha_k)$, $D_{c0}(\alpha_k)$, $D_{c1}(\alpha_k)$ and $E_c(\alpha_k)$. Such a controller allows a maximum energy disturbance of $\delta^{-1} = 12.4069$, i.e. $\|\omega_k\|_2 = 3.5223$. Thus, we generate a set of disturbance signals of structure $\omega_k = \begin{bmatrix} \omega_1 & \omega_2 & \omega_3 & \mathbf{0}_{1,17} \end{bmatrix}$, where ω_1, ω_2, and ω_3 were determined from a straight line in the plan $k \times \omega_k$ that touches the ordinate axis in the points corresponding to 5% to 70% of the maximum admissible energy, and the abscissa at $k = 4$, which ensures a worst case perturbation with energy bounded by $\sqrt{\delta^{-1}}$. For each sequence ω_k, we have run ten simulations with α_k and τ_k randomly chosen. The state response in the augmented space $x_k \times x_{k-1} \times x_{c,k}$ can be seen in Figure 8, where we can see the confinement of the trajectories in the estimate of the region of attraction, which is given by the intersection of the ellipsoidal sets defined from the matrices $W_{1,0}^{-1}$, $W_{2,0}^{-1}$, $W_{1,1}^{-1}$ and $W_{2,1}^{-1}$. In addition, we plot in Figure 9 the closed-loop temporal response of some of these cases. Note that although the control signals assume values close to saturation, none of them saturates.

The maximization of the energy allowed for disturbance signals can also be investigated under differently structured gains $\mathbb{K}(\alpha_k)$, by following Remark 3.2. The computed bounds are presented through a radar graphic in Figure 10, in which different controller orders and maximum delays were also considered. Note that each gain structure is represented by a line-type: solid lines correspond to the gain that feeds back the current and all delayed outputs, $\mathbb{K}(\alpha_k)$; dashed lines correspond to the gain that feeds back both the current output and the most delayed output, $\mathbb{K}_{c2}(\alpha_k)$; and dash-dotted lines correspond to the gain that feeds back only the current output, $\mathbb{K}_{c1}(\alpha_k)$. The colors of the lines indicate the controller order: blue for $\sigma = 1$, red for $\sigma = 2$, and green for $\sigma = 3$. And, the axis are associated with the maximum delays in the list $\bar{\tau} \in \{2,\ 4,\ 6\}$. In all cases, we fixed $\Delta\tau_{\max} = 1$.

From these experiments, we note that the disturbance tolerance is improved whenever the gain feeds back more delayed outputs (solid lines), for a same controller

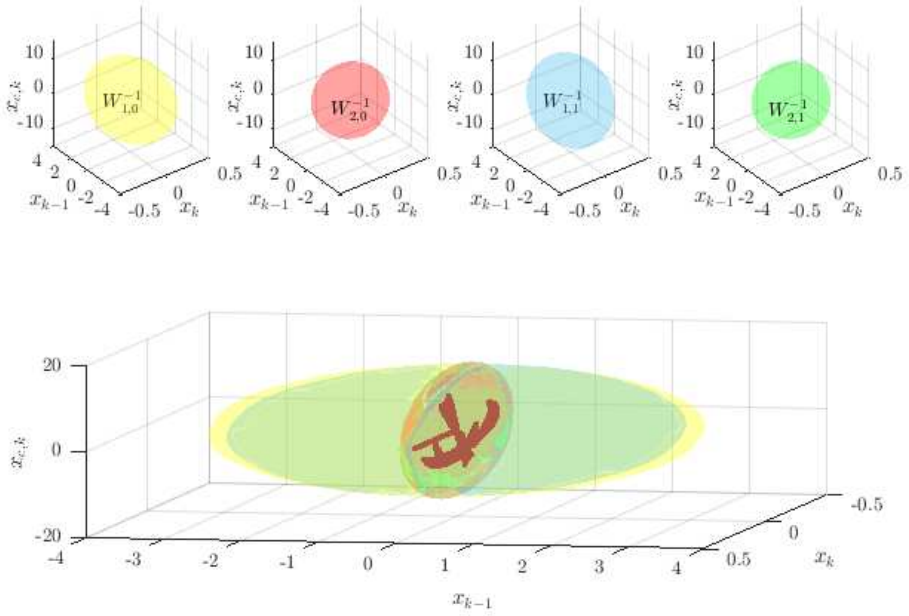

Figure 8 – Top: Ellipsoidal regions achieved by $\xi_k^\top W_{i,j}^{-1} \xi_k$, $i, j \in \mathcal{I}[1,2]$. Bottom: Intersection of the ellipsoids presented in the top, yielding the estimate of the region of attraction, $\mathcal{R}_\mathcal{E}$, of LPV system under exogenous signals ω_k.

order. For instance, considering $\sigma = 2$ (red lines) and $\bar{\tau} = 4$ axis, we have improved the admissible disturbance energy by 11.3% when the outputs $y_k, \ldots, y_{k-4}$ are used (solid red lines, gain $\mathbb{K}(\alpha_k)$) instead only y_k (dash-dotted lines, gain $\mathbb{K}_{c1}(\alpha_k)$).

Moreover, Figure 10 illustrates that increasing the controller order or the number of delayed outputs used in the feedback, results in an improvement on the robustness, allowing higher values of energy disturbance signals. Indeed, our synthesis proposal improves the robustness of the closed-loop system while ensures its local input-to-state stability.

3.4.2 Example 2

Consider the system (4) with null input disturbance, matrices

$$A_1 = \begin{bmatrix} -1.04 & 0.52 \\ 0.21 & 0.31 \end{bmatrix}, \; A_2 = \begin{bmatrix} -1.08 & 0.48 \\ 0.19 & 0.29 \end{bmatrix}, \; A_{d1} = \begin{bmatrix} 0.10 & -0.08 \\ 0 & 0.21 \end{bmatrix},$$
$$A_{d2} = \begin{bmatrix} 0.10 & -0.12 \\ 0 & 0.19 \end{bmatrix}, B_1 = \begin{bmatrix} 2.02 \\ 1.01 \end{bmatrix}, \; B_2 = \begin{bmatrix} 1.98 \\ 0.99 \end{bmatrix}, \; C = \begin{bmatrix} -0.5 & 1 \end{bmatrix}, \tag{85}$$

symmetric saturation limit $\bar{u} = 10$, $\underline{\tau} = 1$, and $\bar{\tau} \in \mathcal{I}[1,\ 6]$.

Maximization of the estimate of the region of attraction $\mathcal{R}_\mathcal{E}$: We have estimated the regions of attraction, by using the optimization procedure $\mathcal{O}_4$ given in (84), for maximum delay values $\bar{\tau} \in \mathcal{I}[1,6]$ and order of the dynamic output-feedback controller

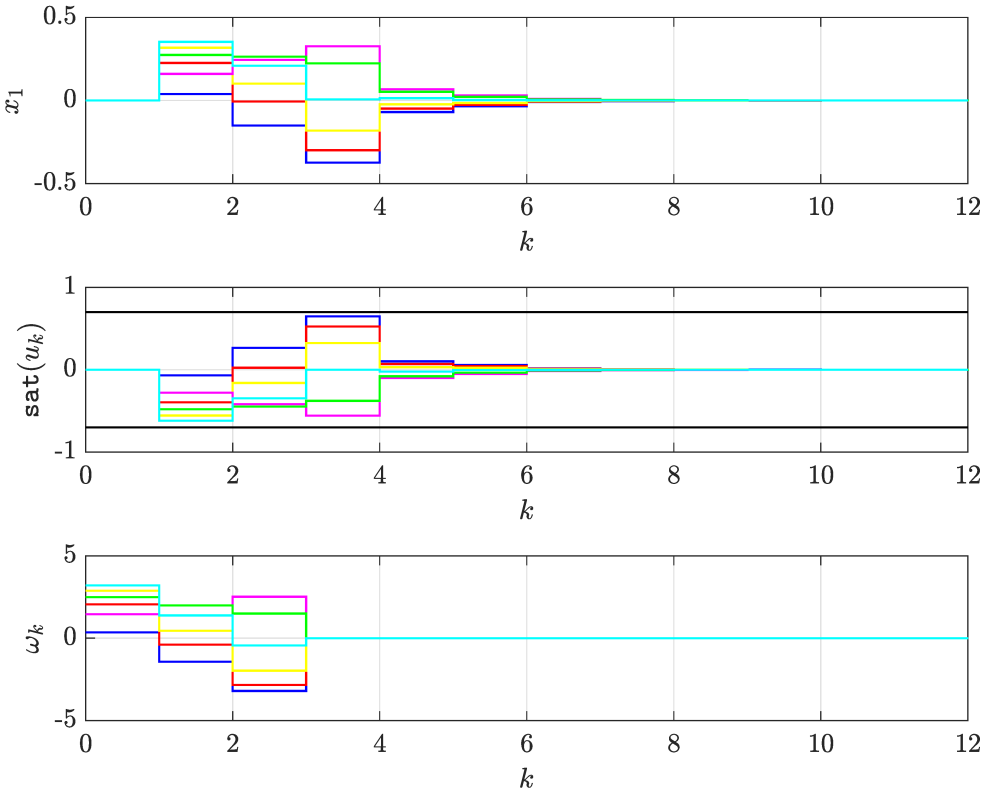

Figure 9 – The closed-loop temporal response for six different disturbance signals.

ranging from n up to $(\bar{\tau}+1)n$. Also, we set again $\Delta\tau_{\max} = 1$, which characterizes a slow variation of the delay. To compare the size of the regions obtained, we calculated the projection area of $\mathcal{R}_{\mathcal{E}}$ on the plan x_k. Figure 11 shows the achieved results, where we can note that *i)* the greater the order of the dynamical controller (σn), the greater the estimated attraction region; and *ii)* such an area has a significant increase whenever the controller's order approaches highest possible order $(\bar{\tau}+1)n$, or equivalently $\sigma = \bar{\tau}+1$.

Moreover, we have compared the estimates of the region of attraction achieved by the optimization procedure $\mathcal{O}_4$ with the estimates achieved by the approach in (SONG, G.; WANG, Z., 2013). Notice that, in (SONG, G.; WANG, Z., 2013) the characterization of the region of attraction is based on the set $\Gamma_\mu = \{\psi_{\xi,k}, k \in \mathcal{I}[-\bar{\tau}, 0] : \max \|\psi_{\xi,k}\|_2 \leq \mu\}$ with $\mu > 0$ for uncertain norm-bounded systems. So to compare the estimates, we compute the cuts of our region of attraction on the sub-spaces defined by the delayed states of the closed-loop system.

Because the conditions in (SONG, G.; WANG, Z., 2013) are bi-linear on parameters J and ε_0, the choice of these parameters may affect the results. Following the guidelines in (SONG, G.; WANG, Z., 2013), we search on these parameters and the best results were found with $J = 10(A^\top A - \mathbf{I})^{-1}$, $\varepsilon_o = 20$, with $A = (A_1 + A_2)/2$ corresponding to the nominal system. The graphical representations of the cuts of both regions

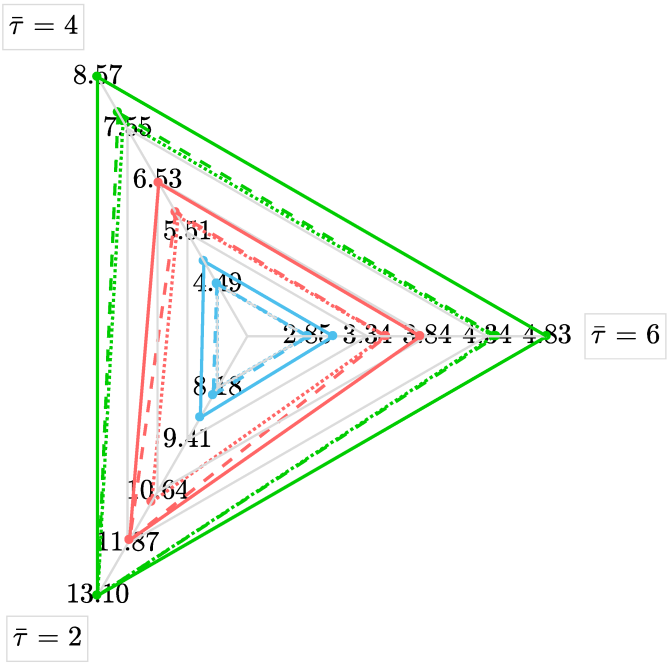

Figure 10 – The maximum tolerable disturbance energy (δ^{-1}) for dynamic controller of order $\sigma = 1$ (blue), $\sigma = 2$ (red) and $\sigma = 3$ (green) and maximum delay $\bar{\tau} = \{2, 4, 6\}$ considering gain structures $\mathbb{K}(\alpha_k)$ (–), $\mathbb{K}_{\bar{\tau}}(\alpha_k)$ (- -) and $\mathbb{K}_0(\alpha_k)$ (:).

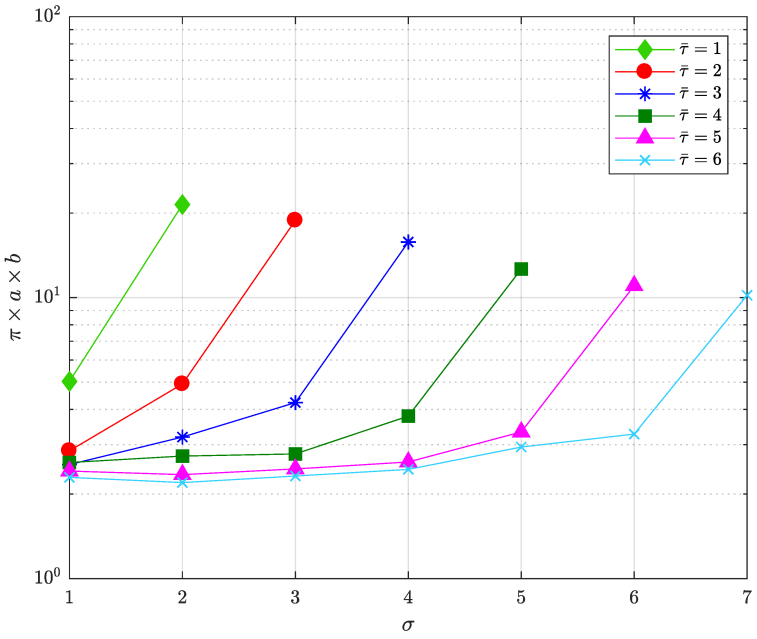

Figure 11 – The projection area on the axis x_k in function of the order of the dynamic controller (σ) for maximum delays $\bar{\tau} = 1$(♦), $\bar{\tau} = 2$(●), $\bar{\tau} = 3$(∗), $\bar{\tau} = 4$(■), $\bar{\tau} = 5$(▲) and $\bar{\tau} = 6$(×).

in each subspace (in this case, plans on the state-space) are shown in Figure 12. The

internal circle corresponds to the achievements of the approach done by (SONG, G.; WANG, Z., 2013). Therefore, it is clear that our approach leads to a larger set of initial conditions than the approach in (SONG, G.; WANG, Z., 2013).

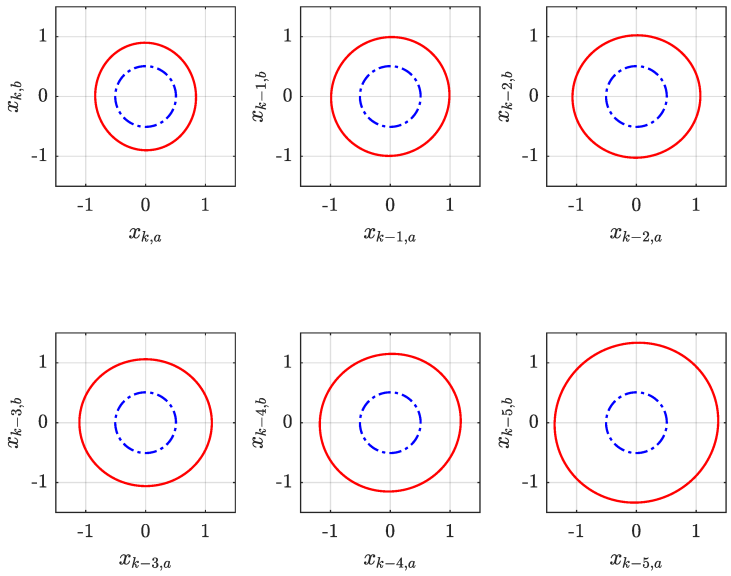

Figure 12 – Comparison between the estimates of region of attraction obtained through our approach (–) and (SONG, G.; WANG, Z., 2013) (–.).

Additionally, Table 2 presents comparisons from the cuts of the $\mathcal{R}_{\mathcal{E}}$ with the plans x_k, x_{k-1}, ..., x_{k-5}. In such a Table, the first column is the maximum delay value. In the second one, we present the radius of the circle obtained by the approach in (SONG, G.; WANG, Z., 2013). It is worth saying that such a radius is the same in all considered plans because of the nature of the initial conditions set characterization ($\|\psi_{\xi,0}\| \leq \mu_{max}$). In the sequence, there are columns concerning the cuts of the $\mathcal{R}_{\mathcal{E}}$ by the plans x_k, x_{k-1}, ..., x_{k-6}. We show the semi-axes, indicated by a and b, of the ellipses found in each cut for each case. The last column of Table 2 presents the percentage area increase provided by our approach (with area $\mathcal{S}_{x_k}$) in the plan x_k when compared with the one achieved by (SONG, G.; WANG, Z., 2013) (with area $\mathcal{S}_{\mu_{max}}$). The reader can note that our method is always superior, and as the maximum delay grows, our approach leads to even better results, achieving 225.4% greater than that in (SONG, G.; WANG, Z., 2013) for $\bar{\tau} = 6$. Furthermore, by the size of the semi-axes a and b in the plans x_{k-1}, ..., x_{k-6} it is clear that the area of those cuts, $\mathcal{S}_{x_{k-1}}$, ..., $\mathcal{S}_{x_{k-6}}$ is even more bigger than the measures on x_k-plan; thus showing that our approach yields to a quite large set of initial conditions.

Finally, it is also worth mentioning that we have verified that our approach yields feasible solutions for the optimization procedure $\mathcal{O}_4$ even with $\underline{\tau} = 0$. However, the

Table 2 – Measures of the axes of the ellipses (cuts) and the radius of the circles (μ_{max}) of the estimates of the regions of attraction.

$\bar{\tau}$	(SONG, G.; WANG, Z., 2013)		Theorem 3.1							$\left(\frac{\mathcal{S}_{x_k}}{\mathcal{S}_{\mu_{max}}} - 1\right) \times 100\%$
	μ_{max}		x_k	x_{k-1}	x_{k-2}	x_{k-3}	x_{k-4}	x_{k-5}	x_{k-6}	
1	0.9672	*a*	1.2792	1.3010	-	-	-	-	-	64.9
		b	1.2062	1.2836						
2	0.7946	*a*	1.0893	1.1712	1.3515	-	-	-	-	78.9
		b	1.0375	1.1320	1.3366					
3	0.6794	*a*	0.9645	1.0750	1.1541	1.3131	-	-	-	95.4
		b	0.9353	1.0339	1.1297	1.2978				
4	0.5613	*a*	0.9210	1.0469	1.1096	1.1661	1.3598	-	-	155.2
		b	0.8732	1.0055	1.0649	1.1442	1.3369			
5	0.5077	*a*	0.8996	1.0032	1.0700	1.1074	1.1848	1.3754	-	194.0
		b	0.8424	0.9799	1.0230	1.0607	1.1447	1.3293		
6	0.4714	*a*	0.8856	0.9631	1.0485	1.0777	1.1160	1.1894	1.3713	225.4
		b	0.8165	0.9586	1.0008	1.0246	1.0726	1.1542	1.3408	

conditions in (SONG, G.; WANG, Z., 2013) do not apply in such a case.

3.5 CONCLUDING REMARKS

This chapter has investigated the regional stabilization in the input-to-state sense of discrete-time LPV systems with time-varying delays subject to saturating actuators and exogenous signals. The main contributions can be listed as *i)* convex delay-dependent conditions to design parameter-dependent dynamic output-feedback controllers with anti-windup action; *ii)* the proposed procedure allows setting the dynamic controller order as an integer multiple of the original system's one; *iii)* the proposed controller enables the user feeds back not only the current output but also the delayed ones; *iv)* the control design is performed by taking into account the maximum variation of the delay between two consecutive instants, yielding less conservative conditions; *v)* the provided methodology allows the design considering optimization problems aiming at increasing the energy bound of the admissible disturbances and the size of the estimate of attraction region.

Through numerical examples, the efficiency of the design method has been illustrated. The novelty of choosing the controller order, for example, allowed achieving better estimates of the region of attraction and higher tolerances to disturbances signals. Similar behavior was also verified whenever the delayed outputs were included in the feedback control action. As in the last chapter, it was also possible to observe a certain conservatism in the simulation results, since even for disturbance signals with the maximum allowed energy, the state trajectories did not reach the edges of the estimate of the region of attraction. Also, in the absence of disturbance signals, the control signal did not saturate for initial conditions in the edges of the estimate of the region of attraction. However, it is worth emphasizing again that the conditions hold for any α_k and τ_k sequences, and finding the worst ones to be used in the simulations is not that simple.

4 EVENT-TRIGGERED DYNAMIC OUTPUT-FEEDBACK CONTROL CO-DESIGN

In this chapter, an event-triggered dynamic output-feedback control design methodology is proposed for discrete-time LPV systems subject to saturating actuators inserted into a communication network with limited bandwidth. Two independent event triggering schemes are designed to determine whether the current signals should be transmitted *a)* from the sensor to the controller and *b)* from the controller to the actuator. As a result, the communication resources can be significantly saved. Both emulation-based approach and co-design of the event-triggering parameters and the controller matrices are addressed.

Based on the Lyapunov stability theory, the proposed conditions stated in the form of linear matrix inequalities (LMIs) ensure the regional asymptotic stability of the closed-loop system for every initial condition belonging to the estimate of the region of attraction. Some optimization procedures are also formulated to effectively reduce the update rate of the output and control signals through communication channels, considering or not a given region of admissible initial conditions. Finally, numerical examples are employed to testify to the validity of the proposal. The results presented here are based on the work (DE SOUZA et al., 2020b). Also, similar approaches can be found in (DE SOUZA et al., 2020c, 2020a, 2020d).

4.1 PROBLEM STATEMENT

Consider the class of discrete-time LPV systems subject to saturating actuators inserted into a communication network represented by

$$\begin{aligned} x_{k+1} &= A(\alpha_k)x_k + B(\alpha_k)\mathtt{sat}(\hat{u}_k), \\ y_k &= Cx_k, \end{aligned} \tag{86}$$

where $x_k \in \mathbb{R}^n$ is the state vector, $\hat{u}_k \in \mathbb{R}^{n_u}$ is the most recent transmitted value of the control input u_k, $y_k \in \mathbb{R}^{n_p}$ is the measured output, and $\mathtt{sat}(u_k)$ is the standard symmetric saturation function defined as

$$\mathtt{sat}(u_{k(\ell)}) = \mathtt{sign}(u_{k(\ell)})\min(|u_{k(\ell)}|, \bar{u}_{(\ell)}), \tag{87}$$

with $\bar{u}_{(\ell)} > 0$, $\ell \in \mathcal{I}[1, n_u]$, denoting the symmetric level relative to the ℓ^{th} control input. The vector of time-varying parameters $\alpha_k \in \mathbb{R}^N$, which is assumed measured and available on-line (BRIAT, 2015), lies in the unitary simplex given by

$$\Lambda \triangleq \left\{ \alpha_k \in \mathbb{R}^N : \sum_{i=1}^{N} \alpha_{k(i)} = 1,\ \alpha_{k(i)} \geq 0, i \in \mathcal{I}[1, N] \right\}. \tag{88}$$

Thus, the parameter-dependent matrices $A(\alpha_k) \in \mathbb{R}^{n\times n}$, $B(\alpha_k) \in \mathbb{R}^{n\times n_u}$ can be written as a convex combination of N known vertices according to

$$\begin{bmatrix} A(\alpha_k) & B(\alpha_k) \end{bmatrix} = \sum_{i=1}^{N} \alpha_{k(i)} \begin{bmatrix} A_i & B_i \end{bmatrix}. \tag{89}$$

To regionally stabilize system (86), we propose the following event-triggered parameter-dependent dynamic output-feedback controller with anti-windup action:

$$\begin{aligned} x_{c,k+1} &= A_c(\alpha_k)x_{c,k} + B_c(\alpha_k)\hat{y}_k - E_c(\alpha_k)\Psi(\hat{u}_k), \\ u_k &= C_c(\alpha_k)x_{c,k} + D_c(\alpha_k)\hat{y}_k, \end{aligned} \tag{90}$$

where $x_{c,k} \in \mathbb{R}^n$ is the controller state vector, $\hat{y}_k \in \mathbb{R}^{n_y}$ is the most recent transmitted value of the measured output y_k and $\Psi(\hat{u}_k)$ is the dead-zone nonlinearity applied over the transmitted control signal $\hat{u}_k$, i.e. $\Psi(\hat{u}_k) = \hat{u}_k - \mathtt{sat}(\hat{u}_k)$. The controller matrices $A_c(\alpha_k) \in \mathbb{R}^{n\times n}$, $B_c(\alpha_k) \in \mathbb{R}^{n\times n_y}$, $E_c(\alpha_k) \in \mathbb{R}^{n\times n_u}$, $C_c(\alpha_k) \in \mathbb{R}^{n_u\times n}$, and $D_c(\alpha_k) \in \mathbb{R}^{n_u\times n_y}$, in the same way as those of the system, are represented in the polytopic form according to the following assumption:

Assumption 4.1 *The controller matrices (90) are supposed to have the following structure:*

$$\begin{bmatrix} A_c(\alpha_k) & B_c(\alpha_k) \end{bmatrix} = 0.5 \sum_{i=1}^{N}\sum_{j=i}^{N} (1+\rho_{ij})\alpha_{k(i)}\alpha_{k(j)} \begin{bmatrix} A_{cij} & B_{cij} \end{bmatrix},$$

$$\begin{bmatrix} C_c(\alpha_k) & D_c(\alpha_k) \end{bmatrix} = \sum_{i=1}^{N} \alpha_{k(i)} \begin{bmatrix} C_{ci} & D_{ci} \end{bmatrix}, \; E_c(\alpha_k) = \sum_{i=1}^{N} \alpha_{k(i)} E_{ci},$$

with $\alpha_k \in \Lambda$ *and* ρ_{ij} *satisfying*

$$\rho_{ij} = \begin{cases} 1, & \text{if } i \neq j, \\ 0, & \text{otherwise}. \end{cases}$$

By admitting a communication network with limited bandwidth, two independent ETMs are introduced on the sensor-to-controller and controller-to-actuator channels to reduce the transmission activity while preserving the stability and certain performance index for the closed-loop system, as shown in Figure 13. Periodically, they make the decision, based on event-triggering rules, whether the current output and the current control input should be transmitted through the network or not. Note that, in this case, we are assuming a perfect matching between the scheduling parameters of the controller and plant.

Output-based ETM: The decision for output updates is made according to the following rule:

$$\hat{y}_k := \begin{cases} y_k, & \text{if } \|\hat{y}_{k-1} - y_k\|^2_{Q_{\Delta y}} > \|y_k\|^2_{Q_y}, \\ \hat{y}_{k-1}, & \text{otherwise}, \end{cases} \tag{91}$$

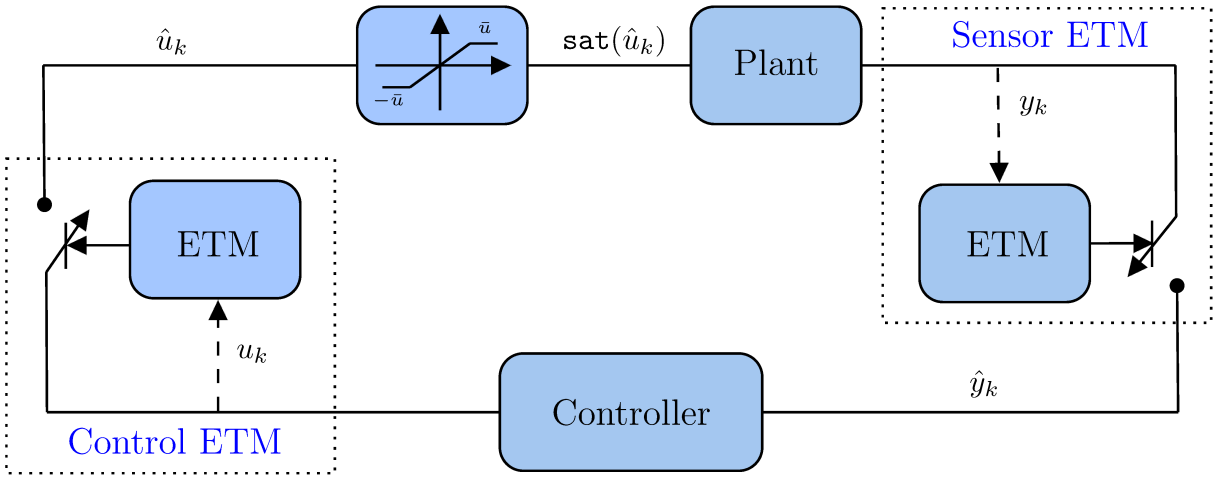

Figure 13 – Event-triggering closed-loop system.

where the symmetric positive definite matrices $Q_{\Delta y}$ and $Q_y \in \mathbb{R}^{n_y \times n_y}$ are variables to be designed. Thus, if (91) holds at step k, then $\hat{y}_k$ is updated to y_k, because the error $\|\hat{y}_{k-1} - y_k\|^2_{Q_{\Delta y}}$ is too big to guarantee stability and a certain performance index for the closed-loop system. On the other hand, if (91) does not hold at step k, then $\hat{y}_k$ keeps its value from the previous instant $\hat{y}(k-1)$, that is, $\hat{y}_k$ is not updated, because the error $\|\hat{y}_{k-1} - y_k\|^2_{Q_{\Delta y}}$ is small enough to guarantee stability and a certain performance index for the closed-loop system.

Control-based ETM: The decision for control updates is made according to the following rule:

$$\hat{u}_k := \begin{cases} u_k, & \text{if } \|\hat{u}_{k-1} - u_k\|^2_{Q_{\Delta u}} > \|u_k\|^2_{Q_u}, \\ \hat{u}_{k-1}, & \text{otherwise,} \end{cases} \tag{92}$$

where the symmetric positive definite matrices $Q_{\Delta u}$ and $Q_u \in \mathbb{R}^{n_u \times n_u}$ are variables to be designed. Thus, if (92) holds at step k, then $\hat{u}_k$ is updated to u_k, because the error $\|\hat{u}_{k-1} - u_k\|^2_{Q_{\Delta u}}$ is too big to guarantee stability and a certain performance index for the closed-loop system. On the other hand, if (92) does not hold at step k, then $\hat{u}_k$ keeps its value from the previous instant $\hat{u}(k-1)$, that is, $\hat{u}_k$ is not updated, because the error $\|\hat{u}_{k-1} - u_k\|^2_{Q_{\Delta u}}$ is small enough to guarantee stability and a certain performance index for the closed-loop system.

Note that, the matrices $Q_{\Delta y}$, Q_y, $Q_{\Delta u}$, and Q_u act as weights on the terms associated with the triggering conditions. Their choice has a direct impact on the event-triggering policy, and, therefore, on how much the data transmission rate can be reduced.

The main difference between this approach and the ones published in (DE SOUZA et al., 2020c, 2020d, 2020a) is related to the investigated event-triggering strategies. (DE SOUZA et al., 2020c, 2020a) consider only one ETM for transmitting the output signal, however, the weighted norm of the control input is taking into account

in the triggering function. The idea behind this more elaborated triggering function is to use more information about the system's behavior to decide whether or not to transmit the signals. By using the same idea, (DE SOUZA et al., 2020d) expands the results for the case with two ETMs, as in this chapter, however, due to the increased complexity of the problem addressed, only the emulation-based approach is developed.

Thus, the problems we intend to solve in this chapter can be stated as follows.

Problem 4.1 (Emulation problem) *Given the dynamic output feedback controller (90), which regionally stabilizes the saturating LPV system (86) in the absence of communication networks, design the two independent event-triggering conditions (91) and (92) to reduce the number of data transmissions on the sensor-to-controller and controller-to-actuator channels, respectively, while preserving the stability of the closed-loop system.*

Problem 4.2 (Co-design problem) *For the saturating LPV system (86), co-design the parameter-dependent dynamic output-feedback controller (90) and the two independent event-triggering conditions (91) and (92) ensuring the regional asymptotic stability of the closed-loop system, while reducing the number of data transmissions on the sensor-to-controller and controller-to-actuator channels.*

An implicit objective in solving problems 4.1 and 4.2 is to characterize an estimate of the basin of attraction of the origin of the closed-loop system $\mathcal{R}_{\mathcal{E}} \subseteq \mathcal{R}_{\mathcal{A}}$.

4.2 PRELIMINARY RESULTS

The saturating LPV system (86) in closed-loop with the dynamic output-feedback controller (90) can be represented by the following model:

$$\begin{aligned} \zeta_{k+1} &= \mathbb{A}(\alpha_k)\zeta_k - \mathbb{B}(\alpha_k)\Psi(\hat{u}_k) + \mathbb{E}_y(\alpha_k)e_{y,k} + \mathbb{E}_u(\alpha_k)e_{u,k}, \\ u_k &= \mathbb{K}(\alpha_k)\zeta_k + D_c(\alpha_k)e_{y,k}, \\ y_k &= \mathbb{C}\zeta_k, \end{aligned} \tag{93}$$

where $\zeta_k = \begin{bmatrix} x_k^\top & x_{c,k}^\top \end{bmatrix}^\top \in \mathbb{R}^{2n}$ is the augmented state, $e_{y,k} \in \mathbb{R}^{n_y}$ is the error between the latest transmission $\hat{y}_k$ and the latest sampling y_k, i.e. $e_{y,k} = \hat{y}_k - y_k$, and $e_{u,k} \in \mathbb{R}^{n_u}$ is the error between the latest transmission $\hat{u}_k$ and the latest sampling u_k, i.e. $e_{u,k} = \hat{u}_k - u_k$. The parameter-dependent matrices $\mathbb{A}(\alpha_k)$, $\mathbb{B}(\alpha_k)$, $\mathbb{E}_y(\alpha_k)$, $\mathbb{E}_u(\alpha_k)$, and $\mathbb{K}(\alpha_k)$ verify from Assumption 4.1:

$$\begin{bmatrix} \mathbb{A}(\alpha_k) & \mathbb{E}_y(\alpha_k) \end{bmatrix} = 0.5 \sum_{i=1}^{N} \sum_{j=i}^{N} (1 + \rho_{ij}) \alpha_{k(i)} \alpha_{k(j)} \begin{bmatrix} \mathbb{A}_{ij} & \mathbb{E}_{yij} \end{bmatrix},$$

$$\begin{bmatrix} \mathbb{B}(\alpha_k) & \mathbb{E}_u(\alpha_k) & \mathbb{K}(\alpha_k)^\top \end{bmatrix} = \sum_{i=1}^{N} \alpha_{k(i)} \begin{bmatrix} \mathbb{B}_i & \mathbb{E}_{ui} & \mathbb{K}_i^\top \end{bmatrix},$$

with $\alpha_k \in \Lambda$, $\rho_{ij} = 1$ if $i \neq j$ and $\rho_{ij} = 0$ otherwise, and

$$\mathbb{A}_{ij} = \begin{bmatrix} A_i + A_j + (B_i D_{cj} + B_j D_{ci})C & B_i C_{cj} + B_j C_{ci} \\ B_{cij} C & A_{cij} \end{bmatrix}, \ \mathbb{B}_i = \begin{bmatrix} B_i \\ E_{ci} \end{bmatrix}, \ \mathbb{E}_{ui} = \begin{bmatrix} B_i \\ \mathbf{0} \end{bmatrix},$$
$$\mathbb{E}_{yij} = \begin{bmatrix} B_i D_{cj} + B_j D_{ci} \\ B_{cij} \end{bmatrix}, \ \mathbb{K}_i = \begin{bmatrix} D_{ci} C & C_{ci} \end{bmatrix}, \text{ and } \mathbb{C} = \begin{bmatrix} C & \mathbf{0} \end{bmatrix}.$$

Note that if y_k is updated at instant k, then from (91) it follows that $e_{y,k} = \hat{y}_k - y_k = y_k - y_k = \mathbf{0}$, and if y_k is not updated at instant k, then from (91) we have that $e_{y,k} = \hat{y}_k - y_k = \hat{y}_{k-1} - y_k$. In other words, the following inequality is always satisfied:

$$\|e_{y,k}\|^2_{Q_{\Delta y}} \leq \|y_k\|^2_{Q_y}. \tag{94}$$

Similarly, if u_k is updated at instant k, then from (92) it follows that $e_{u,k} = \hat{u}_k - u_k = u_k - u_k = \mathbf{0}$, and if u_k is not updated at instant k, then from (92) we have that $e_{u,k} = \hat{u}_k - u_k = \hat{u}_{k-1} - u_k$. Consequently, the following condition always holds

$$\|e_{u,k}\|^2_{Q_{\Delta u}} \leq \|u_k\|^2_{Q_u}. \tag{95}$$

To investigate the regional asymptotic stability of the closed-loop system (93), we use the following candidate Lyapunov function

$$V(\zeta_k, \alpha_k) = \zeta_k^\top W^{-1}(\alpha_k)\zeta_k, \ W(\alpha_k) = \sum_{i=1}^{N} \alpha_{k(i)} W_i, \tag{96}$$

with $\mathbf{0} < W_i = W_i^\top \in \mathbb{R}^{2n \times 2n}$ and $\alpha_k \in \Lambda$. In this case, the level set associated to $V(\zeta_k, \alpha_k)$ is defined as $\mathcal{R}_\mathcal{E} = \mathcal{L}_\mathcal{V}(1) = \{\zeta_k \in \mathbb{R}^{2n} : V(\zeta_k, \alpha_k) \leq 1\}$ and its calculation is done in a similar way to the one presented in Lemma 2.2, that is

$$\mathcal{R}_\mathcal{E} = \mathcal{L}_\mathcal{V}(1) = \bigcap_{\forall \alpha_k \in \Lambda} \mathcal{E}(W(\alpha_k)^{-1}, 1) \ = \bigcap_{i \in \mathcal{I}[1,N]} \mathcal{E}(W_i^{-1}, 1), \tag{97}$$

where $\mathcal{E}(W(\alpha_k)^{-1}, 1)$ denotes the ellipsoidal sets represented by

$$\mathcal{E}(W_i^{-1}, 1) = \left\{ \zeta_k \in \mathbb{R}^{2n} : \zeta_k^\top W_i^{-1} \zeta_k \leq 1, \ i \in \mathcal{I}[1, N] \right\}. \tag{98}$$

In addition, to deal with the saturation effects, we use the following lemma directly derived from (TARBOURIECH et al., 2011, Lemma 1.6) by considering u_k given in (90) and $\nu_k = \hat{u}_k - \mathbb{G}(\alpha_k)\zeta_k$.

Lema 4.1 *Consider u_k given by (90), $\bar{u} \in \mathbb{R}^{n_u}$, $\bar{u} > \mathbf{0}$, and a matrix $\mathbb{G}(\alpha_k) = \sum_{i=1}^{N} \alpha_{k(i)} \mathbb{G}_i$, $\mathbb{G}_i \in \mathbb{R}^{n_u \times 2n}$, $\mathcal{I}[1, N]$, $\alpha_k \in \Lambda$, such that*

$$\mathcal{S}(\bar{u}) \triangleq \left\{ x_k \in \mathbb{R}^{2n} : |\mathbb{G}_{(\ell)}(\alpha_k)\zeta_k| \leq \bar{u}_{(\ell)}, \ \ell \in \mathcal{I}[1, n_u] \right\}. \tag{99}$$

If $x_k \in \mathcal{S}(\bar{u})$, then for any diagonal positive definite matrix $\mathbb{T} \in \mathbb{R}^{n_u \times n_u}$, $\alpha_k \in \Lambda$, the following inequality is verified

$$\Psi(\hat{u}_k)^\top \mathbb{T}(\Psi(\hat{u}_k) - (\mathbb{K}(\alpha_k) - \mathbb{G}(\alpha_k))\zeta_k - D_c(\alpha_k)e_{y,k} - e_{u,k}) \leq 0. \tag{100}$$

4.3 EMULATION-BASED APPROACH

In this section, we provide a solution to Problem 4.1. In this case, we assume that the dynamic output-feedback controller (90), which can regionally stabilize the system (86) in the absence of communication networks, is available and we design the parameters of the event-triggering rules (91) and (92) that minimize the transmission activity on the communication channels.

Theorem 4.1 *Consider the closed-loop system (93) with given controller matrices A_{cij}, B_{cij}, C_{ci}, D_{ci}, and E_{ci}. Suppose that there exist symmetric positive definite matrices $W_i \in \mathbb{R}^{2n\times 2n}$, $Q_{\Delta u}$, $\hat{Q}_u \in \mathbb{R}^{n_u\times n_u}$, $Q_{\Delta y}$, $\hat{Q}_y \in \mathbb{R}^{n_y\times n_y}$, a positive definite diagonal matrix $S \in \mathbb{R}^{n_u\times n_u}$, matrices $H_i \in \mathbb{R}^{n_u\times 2n}$ and $U \in \mathbb{R}^{2n\times 2n}$, with $i \in \mathcal{I}[1,N]$ and $j \in \mathcal{I}[i,N]$, such that the following LMIs are feasible.*

$$\left[\begin{array}{c|c|c|c|c|c|c} U+U^\top \\ -0.5(W_i+W_j) & \star & \star & \star & \star & \star & \star \\ \hline \mathbf{0} & Q_{\Delta u} & \star & \star & \star & \star & \star \\ \hline \mathbf{0} & \mathbf{0} & Q_{\Delta y} & \star & \star & \star & \star \\ \hline 0.5(H_i+H_j \\ -\mathbb{K}_i U-\mathbb{K}_j U) & -\mathbf{I}_{n_u} & -0.5(D_{ci}+D_{cj}) & 2S & \star & \star & \star \\ \hline 0.5\mathbb{A}_{ij}U & 0.5(\mathbb{E}_{uj}+\mathbb{E}_{uj}) & 0.5\mathbb{E}_{yij} & -0.5(\mathbb{B}_i+\mathbb{B}_j)S & \hat{P}_r & \star & \star \\ \hline 0.5(\mathbb{K}_i+\mathbb{K}_j)U & \mathbf{0} & 0.5(D_{ci}+D_{cj}) & \mathbf{0} & \mathbf{0} & \hat{Q}_u & \star \\ \hline \mathbb{C}U & \mathbf{0} & \mathbf{0} & \mathbf{0} & \mathbf{0} & \mathbf{0} & \hat{Q}_y \end{array}\right] > \mathbf{0},$$

$$r, i \in \mathcal{I}[1,N], j \in \mathcal{I}[i,N], \tag{101}$$

$$\begin{bmatrix} U+U^\top - W_i & \star \\ H_{i(\ell)} & \bar{u}^2_{(\ell)} \end{bmatrix} > \mathbf{0}, \quad i \in \mathcal{I}[1,N], \ell \in \mathcal{I}[1,n_u]. \tag{102}$$

Then, the closed-loop system (93) *subject to the ETMs (91) and (92) with matrices $Q_{\Delta u}$, $Q_u = \hat{Q}_u^{-1}$, $Q_{\Delta y}$, and $Q_y = \hat{Q}_y^{-1}$ is regionally asymptotically stable. Moreover, the region $\mathcal{R}_\mathcal{E} = \mathcal{L}_\mathcal{V}(1) \subseteq \mathcal{R}_\mathcal{A}$, computed in (97)-(98), is an estimate of the region of attraction of the origin for the closed-loop system.*

Proof: First, by supposing the feasibility of (102), multiply its left-hand side by $\alpha_{k(i)}$ and sum it up to $i \in \mathcal{I}[1,N]$. Then, replace $H(\alpha_k)$ by $\mathbb{G}(\alpha_k)U$, use the fact that $[W(\alpha_k) - U]^\top W^{-1}(\alpha_k)[W(\alpha_k) - U] \geq \mathbf{0}$ to replace block (1,1) by $U^\top W^{-1}(\alpha_k)U$, thus obtaining

$$\begin{bmatrix} U^\top W^{-1}(\alpha_k)U & \star \\ \mathbb{G}(\alpha_k)_{(\ell)}U & \bar{u}^2_{(\ell)} \end{bmatrix} > \mathbf{0}. \tag{103}$$

With the regularity of U, we can pre- and post-multiply (103) by $\mathtt{diag}\{U^{-\top}, 1\}$ and its transpose, respectively, to get

$$\begin{bmatrix} W^{-1}(\alpha_k) & \star \\ \mathbb{G}(\alpha_k)_{(\ell)} & \bar{u}^2_{(\ell)} \end{bmatrix} > 0. \tag{104}$$

Finally, applying Schur's complement and pre- and post-multiplying the resulting inequality by $\zeta_k^\top$ and ζ_k, respectively, we have that

$$-\zeta_k^\top W(\alpha_k)^{-1}\zeta_k + \zeta_k^\top \mathbb{G}(\alpha_k)_{(\ell)}^\top (\bar{u}^2_{(\ell)})^{-1}\mathbb{G}(\alpha_k)_{(\ell)}\zeta_k \leq 0, \tag{105}$$

which, from (96) and (99), ensures the inclusion $\mathcal{R}_\mathcal{E} = \mathcal{L}_\mathcal{V}(1) \subseteq \mathcal{S}(\bar{u})$ and, consequently, Lemma 4.1 applies. Therefore, any trajectory of the closed-loop system (93) starting in $\mathcal{R}_\mathcal{E}$ remains in $\mathcal{S}(\bar{u})$.

Moreover, if (101) is also satisfied, multiply its left-hand side by $\alpha_{k+1(r)}$, $\alpha_{k(i)}$, and $\alpha_{k(j)}$, and sum it up to $r, i \in \mathcal{I}[1, N]$ and $j \in \mathcal{I}[i, N]$. Then, replace $H(\alpha_k)$, $\hat{Q}_y$, and $\hat{Q}_u$ by $\mathbb{G}(\alpha_k)U$, Q_y^{-1}, and Q_u^{-1}, respectively, and use again the fact that $U^\top + U - W(\alpha_k) \leq U^\top W^{-1}(\alpha_k)U$ to obtain

$$\begin{bmatrix} U^\top W^{-1}(\alpha_k)U & \star & \star & \star & \star & \star & \star \\ \mathbf{0} & Q_{\Delta u} & \star & \star & \star & \star & \star \\ \mathbf{0} & \mathbf{0} & Q_{\Delta y} & \star & \star & \star & \star \\ -(\mathbb{K}(\alpha_k) - \mathbb{G}(\alpha_k))U & -\mathbf{I}_{n_u} & -D_c(\alpha_k) & 2S & \star & \star & \star \\ \mathbb{A}(\alpha_k)U & \mathbb{E}_u(\alpha_k) & \mathbb{E}_y(\alpha_k) & -\mathbb{B}(\alpha_k)S & W(\alpha_{k+1}) & \star & \star \\ \mathbb{K}(\alpha_k)U & \mathbf{0} & D_c(\alpha_k) & \mathbf{0} & \mathbf{0} & Q_u^{-1} & \star \\ \mathbb{C}U & \mathbf{0} & \mathbf{0} & \mathbf{0} & \mathbf{0} & \mathbf{0} & Q_y^{-1} \end{bmatrix} > 0. \tag{106}$$

With the regularity of U, we can pre- and post-multiply (106) by $\mathtt{diag}\{U^{-\top}, \mathbf{I}_{n_u}, \mathbf{I}_{n_y}, S^{-1}, \mathbf{I}_{2n}, \mathbf{I}_{n_u}, \mathbf{I}_{n_y}\}$ and its transpose, respectively, to get

$$\begin{bmatrix} W^{-1}(\alpha_k) & \star & \star & \star & \star & \star & \star \\ \mathbf{0} & Q_{\Delta u} & \star & \star & \star & \star & \star \\ \mathbf{0} & \mathbf{0} & Q_{\Delta y} & \star & \star & \star & \star \\ -S^{-1}(\mathbb{K}(\alpha_k) - \mathbb{G}(\alpha_k)) & -S^{-1} & -S^{-1}D_c(\alpha_k) & 2S^{-1} & \star & \star & \star \\ \mathbb{A}(\alpha_k) & \mathbb{E}_u(\alpha_k) & \mathbb{E}_y(\alpha_k) & -\mathbb{B}(\alpha_k) & W(\alpha_{k+1}) & \star & \star \\ \mathbb{K}(\alpha_k) & \mathbf{0} & D_c(\alpha_k) & \mathbf{0} & \mathbf{0} & Q_u^{-1} & \star \\ \mathbb{C} & \mathbf{0} & \mathbf{0} & \mathbf{0} & \mathbf{0} & \mathbf{0} & Q_y^{-1} \end{bmatrix} > 0. \tag{107}$$

Next, applying Schur's complement, we have that

$$\begin{bmatrix} W^{-1}(\alpha_k) + \mathbb{C}^\top Q_y \mathbb{C} \\ +\mathbb{K}(\alpha_k)^\top Q_u \mathbb{K}(\alpha_k) & \star & \star & \star \\ \mathbf{0} & Q_{\Delta u} & \star & \star \\ \mathbf{0} & \mathbf{0} & Q_{\Delta y} & \star \\ -S^{-1}(\mathbb{K}(\alpha_k) - \mathbb{G}(\alpha_k)) & -S^{-1} & -S^{-1}D_c(\alpha_k) & 2S^{-1} \end{bmatrix} + \begin{bmatrix} \mathbb{A}(\alpha_k)^\top \\ \mathbb{E}_u(\alpha_k)^\top \\ \mathbb{E}_y(\alpha_k)^\top \\ -\mathbb{B}(\alpha_k)^\top \end{bmatrix} W^{-1}(\alpha_{k+1}) \times \begin{bmatrix} \mathbb{A}(\alpha_k) & \mathbb{E}_u(\alpha_k) & \mathbb{E}_y(\alpha_k) & -\mathbb{B}(\alpha_k) \end{bmatrix} > \mathbf{0}. \quad (108)$$

Then, pre- and post-multiplying (108) by the augmented vector $\begin{bmatrix} \zeta_k^\top & e_{u,k}^\top & e_{y,k}^\top & \Psi(\hat{u}_k)^\top \end{bmatrix}$ and its transpose, respectively, and replacing $\mathbb{A}(\alpha_k)x_k + \mathbb{E}_u(\alpha_k)e_{u,k} + \mathbb{E}_y(\alpha_k)e_{y,k} - \mathbb{B}(\alpha_k)\Psi(\hat{u}_k)$ by ζ_{k+1} according to (93), results in

$$\begin{aligned} &\zeta_{k+1}^\top W^{-1}(\alpha_{k+1})\zeta_{k+1} - \zeta_k^\top W^{-1}(\alpha_k)\zeta_k - 2\Psi(\hat{u}_k)^\top \mathbb{T}(\Psi(\hat{u}_k) - (\mathbb{K}(\alpha_k) - \mathbb{G}(\alpha_k))\zeta_k \\ &- D_c(\alpha_k)e_{y,k} - e_{u,k}) - e_{u,k}^T Q_{\Delta u} e_{u,k} + u_k^T Q_u u_k - e_{y,k}^T Q_{\Delta y} e_{y,k} + y_k^T Q_y y_k \leq 0. \quad (109) \end{aligned}$$

From (96), we have that $\zeta_{k+1}^\top W^{-1}(\alpha_{k+1})\zeta_{k+1} - \zeta_k^\top W^{-1}(\alpha_k)\zeta_k = V(\zeta_{k+1}, \alpha_{k+1}) - V(\zeta_k, \alpha_k) = \Delta V(\zeta_k, \alpha_k)$. By taking this into account and denoting $S^{-1} = \mathbb{T}$, we conclude that

$$\begin{aligned} \Delta V(\zeta_k, \alpha_k) &< 2\Psi(\hat{u}_k)^\top \mathbb{T}(\Psi(\hat{u}_k) - (\mathbb{K}(\alpha_k) - \mathbb{G}(\alpha_k))x_k - D_c(\alpha_k)e_{y,k} - e_{u,k}) \\ &< e_{u,k}^\top Q_{\Delta u} e_{u,k} - u_k^\top Q_u u_k + e_{y,k}^\top Q_{\Delta y} e_{y,k} - y_k^\top Q_y y_k \leq 0. \quad (110) \end{aligned}$$

By supposing that $\zeta_k \in \mathcal{S}(\bar{u})$, the generalized sector condition presented in Lemma 4.1 ensures the non-positivity of $2\Psi(\hat{u}_k)^\top \mathbb{T}(\Psi(\hat{u}_k) - (\mathbb{K}(\alpha_k) - \mathbb{G}(\alpha_k))\zeta_k - D_c(\alpha_k)e_{y,k} - e_{u,k})$. Also, by inequalities (94) and (95), we have that $e_{u,k}^\top Q_{\Delta u} e_{u,k} - u_k^\top Q_u u_k \leq 0$ and $e_{y,k}^\top Q_{\Delta y} e_{y,k} - y_k^\top Q_y y_k \leq 0$ are always satisfied, respectively. Because of the positivity of $W(\alpha_k)$, we can assume that there exist a sufficiently small $\epsilon_0 > 0$ such that

$$\epsilon_0 \|\zeta_k\|^2 \leq V(\zeta_k, \alpha_k) \leq \epsilon_1 \|\zeta_k\|^2, \text{ with } \epsilon_1^{-1} = \min_{i \in \mathcal{I}[1,N]} \lambda_{\min} W_i > 0. \quad (111)$$

Moreover, we have that

$$\Delta V(\zeta_k, \alpha_k) \leq -\epsilon_2 \|\zeta_k\|^2 < 0. \quad (112)$$

for some $\epsilon_2 > 0$. Therefore, $V(\zeta_k, \alpha_k)$ given in (96) is a Lyapunov function and $\mathcal{R}_\mathcal{E} = \mathcal{L}_\mathcal{V}(1)$ is an estimate of the region of attraction of the origin for the closed-loop system (93). ∎

Remark 4.1 *Theorem 4.1 can be adapted to treat particular cases usually found in the literature, in which there is an event generator in only one of the communication channels (see, for example, (ZHANG, X. M.; HAN, 2014; DE SOUZA et al., 2020c, 2020d; DING et al., 2020)). To consider an event generator only in the channel between*

the sensor and the controller, it is necessary to delete the second and the sixth lines and columns of the LMI (101). On the other hand, to admit an event generator only in the channel between the controller and the actuator, we have to delete the third and the seventh lines and columns of the LMI (101).

4.4 CO-DESIGN APPROACH

In the previous section, the dynamic output-feedback controller is supposed to be known and capable to regionally stabilize the system (86) without communication networks. Therefore, only the ETMs are designed by Theorem 4.1. The disadvantage is that the control performance of the closed-loop system may be constrained by the previously selected controller. To overcome such a restriction, a co-design of the dynamic controller and the ETMs is proposed in this section, thus providing a solution to Problem 4.2.

Let us start by introducing some matrices useful to the developments. Thus, as in the previous chapter, we use matrices X, Y, P, and $Z \in \mathbb{R}^{n\times n}$ to define

$$U = \begin{bmatrix} X & \bullet \\ Z & \bullet \end{bmatrix}, \quad U^{-1} = \begin{bmatrix} Y & \bullet \\ P & \bullet \end{bmatrix}, \quad \Theta = \begin{bmatrix} Y & \mathbf{I}_n \\ P & \mathbf{0} \end{bmatrix}, \tag{113}$$

which yield

$$U\Theta = \begin{bmatrix} \mathbf{I}_n & X \\ \mathbf{0} & Z \end{bmatrix} \text{ and } \hat{U} = \Theta^\top U\Theta = \begin{bmatrix} Y^\top & F^\top \\ \mathbf{I}_n & X \end{bmatrix}, \tag{114}$$

where, by construction, we have

$$F^\top = Y^\top X + P^\top Z. \tag{115}$$

By partitioning matrix $W_i = \begin{bmatrix} W_{11i} & \star \\ W_{21i} & W_{22i} \end{bmatrix}$, one obtains:

$$\hat{W}_i = \Theta^\top W_i \Theta = \begin{bmatrix} \hat{W}_{11i} & \star \\ \hat{W}_{21i} & \hat{W}_{22i} \end{bmatrix}, \tag{116}$$

with $\hat{W}_{11i} = Y^\top W_{11i} Y + P^\top W_{21i} Y + Y^\top W_{21i}^\top P + P^\top W_{22i} P$, $\hat{W}_{21i} = W_{11i}^\top Y + W_{12i} P$, and $\hat{W}_{22i} = W_{11i}$.

With the aid of these matrices, we can provide a solution to Problem 4.2 through the next theorem.

Theorem 4.2 *Consider there exist symmetric positive definite matrices $\hat{W}_i \in \mathbb{R}^{2n\times 2n}$, $Q_{\Delta u}$, $\hat{Q}_u \in \mathbb{R}^{n_u\times n_u}$, $Q_{\Delta y}$, $\hat{Q}_y \in \mathbb{R}^{n_y\times p}$, a positive definite diagonal matrix $S \in \mathbb{R}^{n_u\times n_u}$, and matrices $\hat{A}_{cij}$, $\hat{B}_{cij}$, $\hat{C}_{ci}$, $\hat{D}_{ci}$, $\hat{E}_{ci}$, X, Y and M of appropriate dimensions, with*

$i \in \mathcal{I}[1, N]$ and $j \in \mathcal{I}[i, N]$, such that the following LMIs are feasible.

$$\left[\begin{array}{c|c|c|c|c|c|c} \hat{U} + \hat{U}^\top \\ -0.5(\hat{W}_i + \hat{W}_j) & \star & \star & \star & \star & \star & \star \\ \hline \mathbf{0} & Q_{\Delta u} & \star & \star & \star & \star & \star \\ \hline \mathbf{0} & \mathbf{0} & Q_{\Delta y} & \star & \star & \star & \star \\ \hline 0.5(H_i + H_j - \Pi_{1ij}) & -\mathbf{I}_{n_u} & -0.5(\hat{D}_{ci} + \hat{D}_{cj}) & 2S & \star & \star & \star \\ \hline 0.5\Pi_{2ij} & 0.5\Pi_{3ij} & 0.5\Pi_{4ij} & 0.5\Pi_{5ij} & \hat{W}_r & \star & \star \\ \hline 0.5\Pi_{1ij} & \mathbf{0} & 0.5(\hat{D}_{ci} + \hat{D}_{cj}) & \mathbf{0} & \mathbf{0} & \hat{Q}_u & \star \\ \hline \begin{bmatrix} C & CX \end{bmatrix} & \mathbf{0} & \mathbf{0} & \mathbf{0} & \mathbf{0} & \mathbf{0} & \hat{Q}_y \end{array}\right] > \mathbf{0}, \tag{117}$$

$$r, i \in \mathcal{I}[1, N], j \in \mathcal{I}[i, N]$$

$$\begin{bmatrix} \hat{U} + \hat{U}^\top - \hat{W}_i & \star \\ H_{i(\ell)} & \bar{u}^2_{(\ell)} \end{bmatrix} > \mathbf{0}, \tag{118}$$
$$i \in \mathcal{I}[1, N], \ell \in \mathcal{I}[1, n_u],$$

with

$$\Pi_{1ij} = \begin{bmatrix} (\hat{D}_{ci} + \hat{D}_{cj})C & \hat{C}_{ci} + \hat{C}_{cj} \end{bmatrix},$$

$$\Pi_{2ij} = \begin{bmatrix} Y^\top(A_i + A_j) + \hat{B}_{cij}C & \hat{A}_{cij} \\ A_i + A_j + (B_i\hat{D}_{cj} + B_j\hat{D}_{cj})C & (A_i + A_j)X + (B_i\hat{C}_{cj} + B_j\hat{C}_{ci}) \end{bmatrix},$$

$$\Pi_{3ij} = \begin{bmatrix} Y^\top(B_i + B_j) \\ B_i + B_j \end{bmatrix}, \ \Pi_{4ij} = \begin{bmatrix} \hat{B}_{cij} \\ B_i\hat{D}_{cj} + B_j\hat{D}_{ci} \end{bmatrix}, \ \Pi_{5ij} = \begin{bmatrix} -(\hat{E}_{ci} + \hat{E}_{cj}) \\ -(B_j + B_i)S \end{bmatrix}, \ \hat{U} = \begin{bmatrix} Y^\top & F^\top \\ \mathbf{I}_n & X \end{bmatrix}.$$

Then, by choosing non-singular matrices P and Z such that (115) holds, we have that the saturating LPV system (86) *under the dynamic output-feedback compensator* (90) *with matrices defined by*

$$\begin{aligned} D_{ci} &= \hat{D}_{ci} \\ C_{ci} &= (\hat{C}_{ci} - D_{ci}CX)Z^{-1}, \\ B_{cij} &= (P^{-1})^\top(\hat{B}_{cij} - Y^\top(B_iD_{cj} + B_jD_{ci}), \\ A_{cij} &= (P^{-1})^\top(\hat{A}_{cij} - Y^\top(A_i + A_j + (B_iD_{cj} + B_jD_{ci})C)X - P^\top B_{cij}CX \\ &\quad -Y^\top(B_iC_{cj} + B_jC_{ci})Z)Z^{-1}. \\ E_{ci} &= (P^{-1})^\top(\hat{E}_{ci}S^{-1} - Y^\top B_i) \end{aligned} \tag{119}$$

subject to the ETMs (91) and (92) with matrices $Q_{\Delta u}$, $Q_u = \hat{Q}_u^{-1}$, $Q_{\Delta y}$, and $Q_y = \hat{Q}_y^{-1}$ is regionally asymptotically stable. Moreover, the region $\mathcal{R}_\mathcal{E}$, computed in (97)-(98), is an estimate of the region of attraction of the origin for the closed-loop system.

Proof: By supposing the feasibility of (117), from block (1,1), we have that $\hat{U} + \hat{U}^\top > 0$, and consequently, $\hat{U}$ is non-singular. Therefore, from (114), we have X and Y non-singular and we can write $\hat{U}$ as

$$\begin{bmatrix} Y^\top & F^\top \\ \mathbf{I}_n & X \end{bmatrix} = \begin{bmatrix} \mathbf{I}_n & Y^\top \\ \mathbf{0} & \mathbf{I}_n \end{bmatrix} \begin{bmatrix} \mathbf{0} & F^\top - Y^T X \\ \mathbf{I}_n & X \end{bmatrix}, \tag{120}$$

which allows us to conclude that $(F^\top - Y^\top X)$ is also non-singular. As a result, it is always possible to choose non-singular matrices P and Z, such that (115) is satisfied. This shows that the gains (119) are well-defined.

Moreover, by considering the matrices (113)-(116) and the change of variables $\hat{A}_{cij}$, $\hat{B}_{cij}$, $\hat{C}_i$, $\hat{D}_i$, and $\hat{E}_{ci}$ according to (119), pre- and post-multiply (117) by $\mathtt{diag}\{\Theta^{-\top}, \mathbf{I}_{n_u}, \mathbf{I}_{n_y}, \Theta^{-\top}, \mathbf{I}_{n_u}, \mathbf{I}_{n_y}\}$ and its transpose, respectively, to obtain (101) and, likewise, pre- and post-multiply (118) by $\mathtt{diag}\{\Theta^{-\top}, 1\}$ and its transpose, respectively, to obtain (102). Thus, from Theorem 4.1, these two equivalences allow to conclude the proof. ∎

Note that the Remark 3.1 also applies to Theorem 4.2.

Remark 4.2 *The LMI-conditions proposed in Theorems 4.1 and 4.2 also allow to have triggering parameters dependent on α_k. In this case, it is necessary to replace $Q_{\Delta u}$, $Q_{\Delta y}$, $\hat{Q}_u$ and $\hat{Q}_y$ by $Q_{\Delta ui}$, $Q_{\Delta yi}$, $\hat{Q}_{ui}$, and $\hat{Q}_{yi}$, respectively.*

Remark 4.3 *Theorems 4.1 and 4.2 can be simplified to deal with LTI and non-saturated systems. In the LTI case, it is required to set $r = i = j = 1$, which results in fixed matrices. Notice that, the dynamic and input matrices of the controller, A_c and B_c, are retrieved by setting $A_{c11} = 0.5A_{c11}$ and $B_c = 0.5B_{c11}$, according to Assumption 4.1, with A_{c11} and B_{c11} calculated as in (119). In the non-saturated case, the third line and column of the LMIs (101) and (117) must be deleted, and the LMIs (102) and (118) discarded.*

4.4.1 Optimization design procedures

In this section, some optimization procedures are formulated to improve the closed-loop operation.

4.4.1.1 Minimization of the update rate

The main objective here is to reduce the number of data transmissions on the sensor-to-controller and the controller-to-actuator channels. Let us remark that if

$$\left(\hat{y}_{k-1} - y_k\right)^\top \left(\hat{y}_{k-1} - y_k\right) \lambda_{\max}(Q_{\Delta y}) - y_k^\top y_k \lambda_{\min}(Q_y) \leq 0, \tag{121a}$$

$$\left(\hat{u}_{k-1} - u_k\right)^\top \left(\hat{u}_{k-1} - u_k\right) \lambda_{\max}(Q_{\Delta u}) - u_k^\top u_k \lambda_{\min}(Q_y) \leq 0, \tag{121b}$$

then, the triggering conditions (91) and (92) hold, respectively. Note that, in the worst case, that is, when the conditions become equalities, one gets:

$$\frac{\left(\hat{y}_{k-1} - y_k\right)^\top \left(\hat{y}_{k-1} - y_k\right) \lambda_{\max}(Q_{\Delta y})}{y_k^\top y_k \lambda_{\min}(Q_y)} \leq 1 \text{ and} \tag{122a}$$

$$\frac{\left(\hat{y}_{k-1} - y_k\right)^\top \left(\hat{u}_{k-1} - u_k\right) \lambda_{\max}(Q_{\Delta y})}{u_k^\top u_k \lambda_{\min}(Q_u)} \leq 1, \tag{122b}$$

respectively. Since $\lambda_{\min}(Q_y)^{-1} = \lambda_{\max}(Q_y^{-1})$ and $\lambda_{\min}(Q_u)^{-1} = \lambda_{\max}(Q_u^{-1})$, we can rewrite (122a) and (122b) as

$$\frac{\left(\hat{y}_{k-1} - y_k\right)^\top \left(\hat{y}_{k-1} - y_k\right)}{y_k^\top y_k} \gamma(Q_{\Delta y}, Q_y^{-1}) \leq 1 \text{ and} \tag{123a}$$

$$\frac{\left(\hat{u}_{k-1} - u_k\right)^\top \left(\hat{u}_{k-1} - u_k\right)}{u_k^\top u_k} \gamma(Q_{\Delta u}, Q_u^{-1}) \leq 1, \tag{123b}$$

respectively, with $\gamma(Q_{\Delta y}, Q_y^{-1}) = \lambda_{\max}(Q_{\Delta y})\lambda_{\max}(Q_y^{-1})$ and $\gamma(Q_{\Delta u}, Q_u^{-1}) = \lambda_{\max}(Q_{\Delta u})$ $\lambda_{\max}(Q_u^{-1})$. Thus, the idea is to minimize $\gamma(Q_{\Delta y}, \hat{Q}_y)$ and $\gamma(Q_{\Delta u}, \hat{Q}_u)$ with $\hat{Q}_y = Q_y^{-1}$ and $\hat{Q}_u = Q_u^{-1}$, respectively, so that the minimum time required for the expressions on the left hand-side of (122a) and (122b) to evolve from 0 to 1 is enlarged. However, $\gamma(Q_{\Delta y}, \hat{Q}_y)$, and $\gamma(Q_{\Delta u}, \hat{Q}_u)$ are not convex functions and, therefore, it can be difficult to optimize them. Nevertheless, one can observe that the event-triggering functions depend on all the eigenvalues of $Q_{\Delta y}$, $\hat{Q}_y$, $Q_{\Delta y}$ and $\hat{Q}_y$. So, to formulate a convex objective function, we can minimize the sum of all these eigenvalues, which leads to the following convex optimization procedure:

$$\mathcal{O}_5 : \begin{cases} \min & \mathtt{tr}(Q_{\Delta y} + \hat{Q}_y) + \mathtt{tr}(Q_{\Delta u} + \hat{Q}_u), \\ \text{subject to} & \begin{cases} (101) \text{ and } (102), \\ \quad \text{or} \\ (117) \text{ and } (118), \end{cases} \end{cases} \tag{124}$$

Therefore, using the optimization procedure $\mathcal{O}_5$, the transmission activity is indirectly reduced.

4.4.1.2 Minimization of the update rate for a given region of admissible initial conditions $\mathcal{X}_0$:

Another objective of optimization consists in considering a given region of admissible initial states $\mathcal{X}_0$ for which we can reduce the update rate on the sensor-to-controller and the controller-to-sensor channels. In this case, we should ensure that $\mathcal{X}_0$ is included in the region of attraction of the closed-loop systems, i.e. $\mathcal{X}_0 \subseteq \mathcal{R}_\mathcal{E} \subseteq \mathcal{R}_\mathcal{A}$. If $\mathcal{X}_0$ is specified as an ellipsoid $\mathcal{E}(R, 1)$, defined similarly to (98), then we have that

$$\begin{bmatrix} R & \star \\ \mathbf{I}_{2n} & W_i \end{bmatrix} > \mathbf{0}, \text{ or equivalently} \tag{125a}$$

$$\begin{bmatrix} R & \star \\ \Theta^\top & \hat{W}_i \end{bmatrix} > \mathbf{0}, \tag{125b}$$

with Θ given in (113), for all $i \in \mathcal{I}[1, N]$. However, the LMI (125b) is non-convex due to the presence of the matrix P in Θ. To make it convex, we can consider the partitioning

$R = \begin{bmatrix} R_{11} & \star \\ R_{21} & R_{22} \end{bmatrix}$ and $x_{c,0} = \mathbf{0}$, which allows us to dismiss the rows concerning the position of P in Θ. With that, the inequality (125b) can be rewritten as

$$\left[\begin{array}{c|c} R_{11} & \star \\ \hline Y & \hat{W}_i \\ \mathbf{I}_n & \end{array}\right] > \mathbf{0}, \tag{126}$$

for all $i \in \mathcal{I}[1, N]$. Thus, we have

$$\mathcal{O}_6 : \begin{cases} \min & \mathtt{tr}(Q_{\Delta y} + \hat{Q}_y) + \mathtt{tr}(Q_{\Delta u} + \hat{Q}_u), \\ \text{subject to} & \begin{cases} (101), (102) \text{ and } (125a), \\ \quad \text{or} \\ (117), (118) \text{ and } (126), \end{cases} \end{cases} \tag{127}$$

with $\hat{Q}_y = Q_y^{-1}$ and $\hat{Q}_u = Q_u^{-1}$.

Although both optimization procedures aim at minimizing the data transmission, the optimization procedure $\mathcal{O}_6$ differs from the optimization procedure $\mathcal{O}_5$ by the inclusion of the restrictions (125a) and (126) to take into account a specific region of initial conditions. It is important to point out that, the use of the optimization procedure $\mathcal{O}_6$ leads to deal with a classical trade-off between the size of the estimate of the basin of attraction and the transmission saving. Indeed, it results that the smaller the estimate of the basin of attraction, the greater the transmission saving.

4.5 NUMERICAL EXAMPLES

In this section, we present three examples to illustrate our proposal and also to compare it with other results in the literature. Both the LPV and the LTI cases, with and without saturating actuators, are addressed.

4.5.1 Example 1

Consider the inverted pendulum shown in Figure 14. This system has been extensively investigated in the literature (see, for example, (WU, W. et al., 2014; GROFF et al., 2016; DING et al., 2020)), but without taking into account possible variations in the system parameters. Let us then consider such variations by adding the parameter-varying α_k to the system model, as follows

$$\begin{aligned} x_{k+1} &= \begin{bmatrix} 1.0018 & 0.01 \\ 0.04\alpha_k + 0.36 & 1.0018 \end{bmatrix} x_k + \begin{bmatrix} -0.001 \\ 0.025\alpha_k - 0.184 \end{bmatrix} \mathtt{sat}(\hat{u}_k), \\ y_k &= \begin{bmatrix} 1 & 0 \end{bmatrix} x_k \end{aligned} \tag{128}$$

with $|\alpha_k| \leq 1$ and symmetric saturation limit $\bar{u} = 1$. Note that, this arbitrary variation was added just to test the approach, and, therefore, has no direct physical meaning with the continuous-time system's variables. Our objective here is to made the co-design of the dynamic controller (90) and the two ETMs (91) and (92) for two different given admissible initial conditions region $\mathcal{X}_0$, such that the number of data transmissions in both channels is as low as possible.

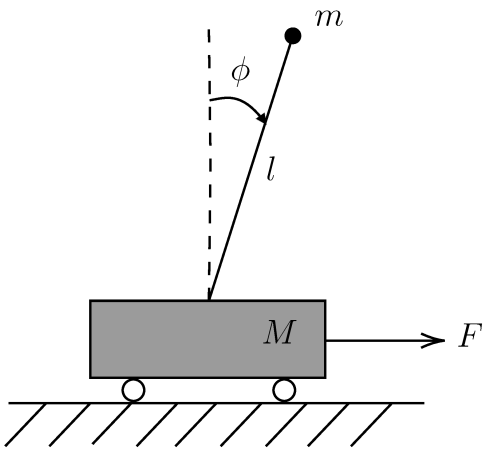

Figure 14 – An inverted pendulum (WU, W. et al., 2014)

For the first case, let us consider a given region of admissible initial conditions $\mathcal{X}_0 = \mathcal{E}(R, 1)$ with $R_{11} = \texttt{diag}\{76, 2\}$ derived from the partitioning of R. By using the optimization procedure $\mathcal{O}_6$ with conditions of Theorem 4.2, we design simultaneously the dynamic controller (90) and the two independent ETMs (91) and (92) such that the update on the sensor-to-controller and the controller-to-actuator channels are minimized. Through this, we got the ETM matrices $Q_{\Delta y} = 18.8382$, $Q_y = 0.2365$, $Q_{\Delta u} = 3.6281$, and $Q_u = 0.0516$ and the following dynamic controller matrices

$$A_{c11} = \begin{bmatrix} 2.0127 & 2.1023 \\ -0.3230 & -0.3377 \end{bmatrix}, A_{c12} = \begin{bmatrix} 0.9254 & -4.9222 \\ -0.1469 & 0.7998 \end{bmatrix},$$
$$A_{c22} = \begin{bmatrix} 0.0834 & -10.4533 \\ -0.0125 & 1.6824 \end{bmatrix}, B_{c11} = \begin{bmatrix} -26.0948 \\ 4.1866 \end{bmatrix},$$
$$B_{c12} = \begin{bmatrix} -22.1621 \\ 3.5556 \end{bmatrix}, B_{c22} = \begin{bmatrix} -16.4072 \\ 2.6323 \end{bmatrix}, E_{c1} = \begin{bmatrix} 0.3900 \\ -0.0626 \end{bmatrix},$$
$$E_{c2} = \begin{bmatrix} 2.5333 \\ -0.4064 \end{bmatrix}, C_{c1} = \begin{bmatrix} -0.2975 \\ -2.1999 \end{bmatrix}^\top, C_{c2} = \begin{bmatrix} -0.1745 \\ -1.4513 \end{bmatrix}^\top,$$
$$D_{c1} = 6.8209, \text{ and } D_{c2} = 7.8238.$$

Figure 15 shows the projection (–) and the cut (–), on the plane defined by the plant states, of the $\mathcal{R}_\mathcal{E}$ obtained, $\mathcal{X}_0$ (–), and also the projections of some convergent (—) and some divergent trajectories (—) starting from the points marked with ∘ and ∗, respec-

tively. Notice that, as required, $\mathcal{R}_{\mathcal{E}}$ contains $\mathcal{X}_0$, i.e. $\mathcal{X}_0 \subset \mathcal{R}_{\mathcal{E}}$. In particular, for the convergent trajectory (—) starting in the initial condition $x_0 = \begin{bmatrix} -0.1480 & -0.4735 & 0 & 0 \end{bmatrix}^\top$ marked with '•', we plot in the Figure 16 the states, the control input, the events of the sensor and the controller, and the parameter-varying as a function of the sampling instants. In the inter-events graph, the events that occur asynchronously in the sensor and in the controller are represented by '○' and '○', respectively, and synchronous by '○'. Thus, we can see the asymptotic stability of the system despite the saturation in the first instant of the simulation. For this case, the update rate between the sensor and controller and between the controller and actuator was 50.33% and 43%, respectively, thus, saving a significant amount of samples to be transmitted. However, the inclusion of $\mathcal{X}_0$ yielded an ETM behavior that appears to have some periodicity despite the asynchronous updates of sensor and control ETMs. Moreover, the asynchronous ETMs save transmissions because only one ETM is active over the network.

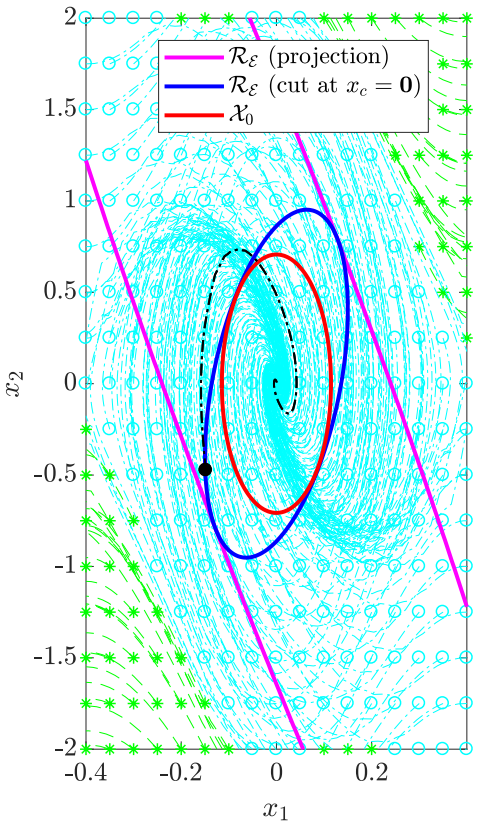

Figure 15 – $\mathcal{R}_{\mathcal{E}}$ and $\mathcal{X}_0 = \mathcal{E}(R, 1)$ with $R_{11} = \texttt{diag}\{76, 2\}$.

Then, for the second case, we carried out the co-design for a region of admissible initial conditions less stringent, given by $\mathcal{X}_0 = \mathcal{E}(R, 1)$ with $R_{11} = \texttt{diag}\{26.60, 0.70\}$ derived from the partitioning of R. For this case, we obtained the ETM matrices $Q_{\Delta y} = 29.5663$, $Q_y = 0.0881$, $Q_{\Delta u} = 5.8971$, and $Q_u = 0.0221$ and the dynamic controller

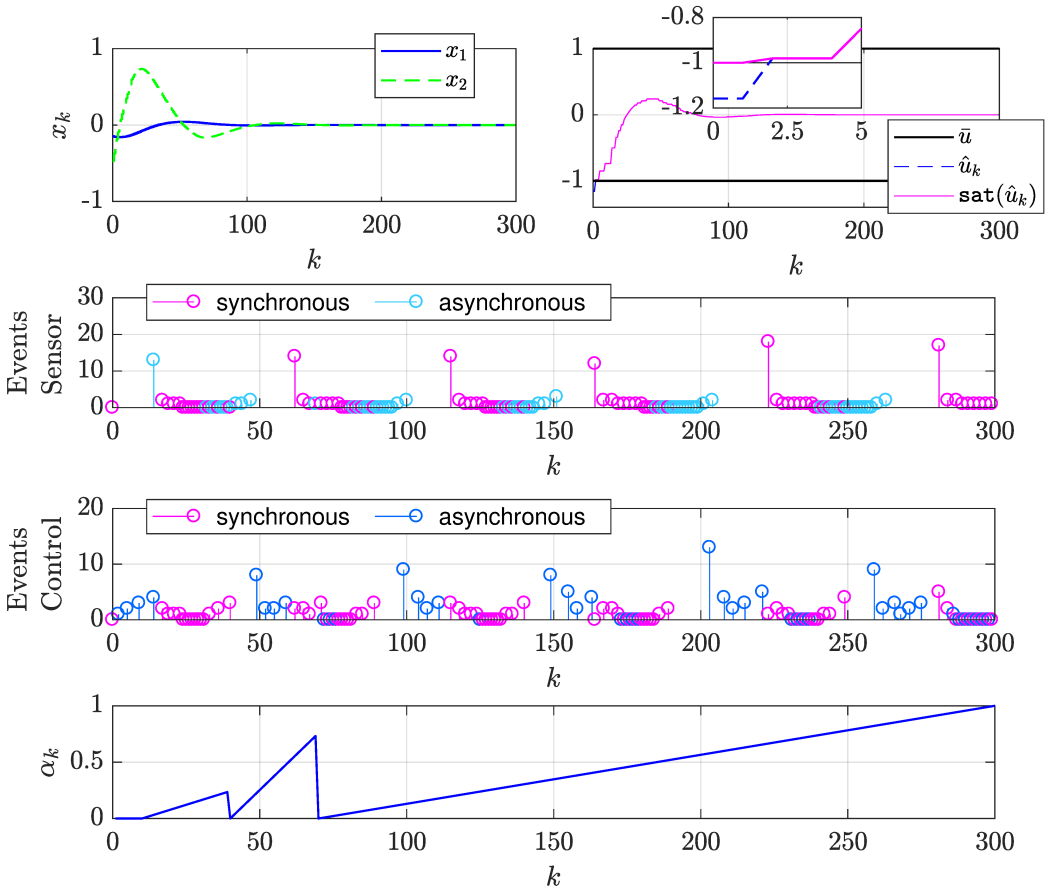

Figure 16 – The closed-loop response of system (128) - $\mathcal{X}_0 = \mathcal{E}(R, 1)$ with $R_{11} = \texttt{diag}\{76, 2\}$.

matrices

$$A_{c11} = \begin{bmatrix} 5.2362 & 20.9969 \\ -0.8710 & -3.4869 \end{bmatrix}, \; A_{c12} = \begin{bmatrix} 2.9999 & 7.3585 \\ -0.5051 & -1.2549 \end{bmatrix},$$

$$A_{c22} = \begin{bmatrix} -0.0841 & -11.4126 \\ 0.0137 & 1.9028 \end{bmatrix}, \; B_{c11} = \begin{bmatrix} -6.4201 \\ 1.0716 \end{bmatrix},$$

$$B_{c12} = \begin{bmatrix} -4.9392 \\ 0.8246 \end{bmatrix}, \; B_{c22} = \begin{bmatrix} -2.7266 \\ 0.4550 \end{bmatrix}, \; E_{c1} = \begin{bmatrix} 3.7979 \\ -0.6337 \end{bmatrix},$$

$$E_{c2} = \begin{bmatrix} 4.3923 \\ -0.7330 \end{bmatrix}, \; C_{c1} = \begin{bmatrix} 1.7658 \\ 9.7753 \end{bmatrix}^\top, \; C_{c2} = \begin{bmatrix} -0.0633 \\ -1.2096 \end{bmatrix}^\top,$$

$$D_{c1} = 5.5867, \text{ and } D_{c2} = 6.2479.$$

Figure 17 presents the projection and the cut, on the plane defined by the plant states, of the $\mathcal{R}_\mathcal{E}$ obtained. For the convergent trajectory (—) starting in the initial condition $x_0 = \begin{bmatrix} -0.2117 & -0.3245 & 0 & 0 \end{bmatrix}^\top$ marked with "•", we simulated the closed-loop response of the system, and the results can be seen in Figure 18. In this case, the update rates between the sensor and controller and between the controller and actuator found were 67.33% and 59.67%, respectively. Therefore, concerning the update rate,

there was a slightly worse performance than the more restrictive (on the plane defined by the plant states) $\mathcal{X}_0$ specification. The ETMs seem to present a more pronounced periodic behavior in this case, which may be connected to the higher transmission rate achieved due to the inclusion of a larger region of initial condition considered here (with respect to that in the previous case). Another effect of including a larger $\mathcal{X}_0$ is the reduction on the asynchronous transmission, supporting the hypothesis of the bigger the region of initial conditions, the smaller the transmissions saving.

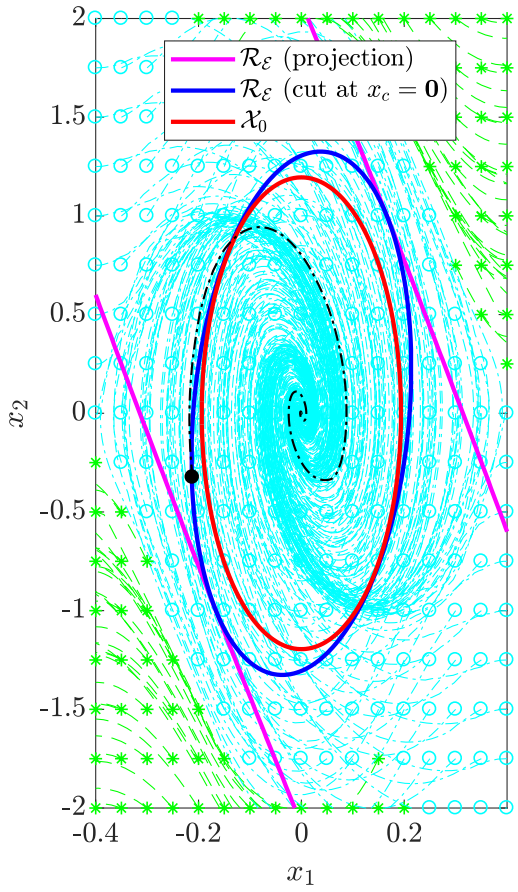

Figure 17 – $\mathcal{R}_\mathcal{E}$ and $\mathcal{X}_0 = \mathcal{E}(R, 1)$ with $R_{11} = \texttt{diag}\{26.60, 0.70\}$.

The inverted pendulum is also investigated in (DING et al., 2020), where the design of event-triggering static and dynamic state stabilizing controllers for discrete-time linear systems with saturating actuators is addressed. The number of updates obtained by (DING et al., 2020) are showed in Table 3, where the initial conditions $x_0 = \begin{bmatrix} 0.2 & 0.8 \end{bmatrix}^\top$ and $x_{c,0} = \begin{bmatrix} 0 & 0 \end{bmatrix}^\top$ were taken to simulate the closed-loop response of the system. Observe that since (DING et al., 2020) does not consider a communication network between the controller and actuator channel, then the system updates the control at all sampling times.

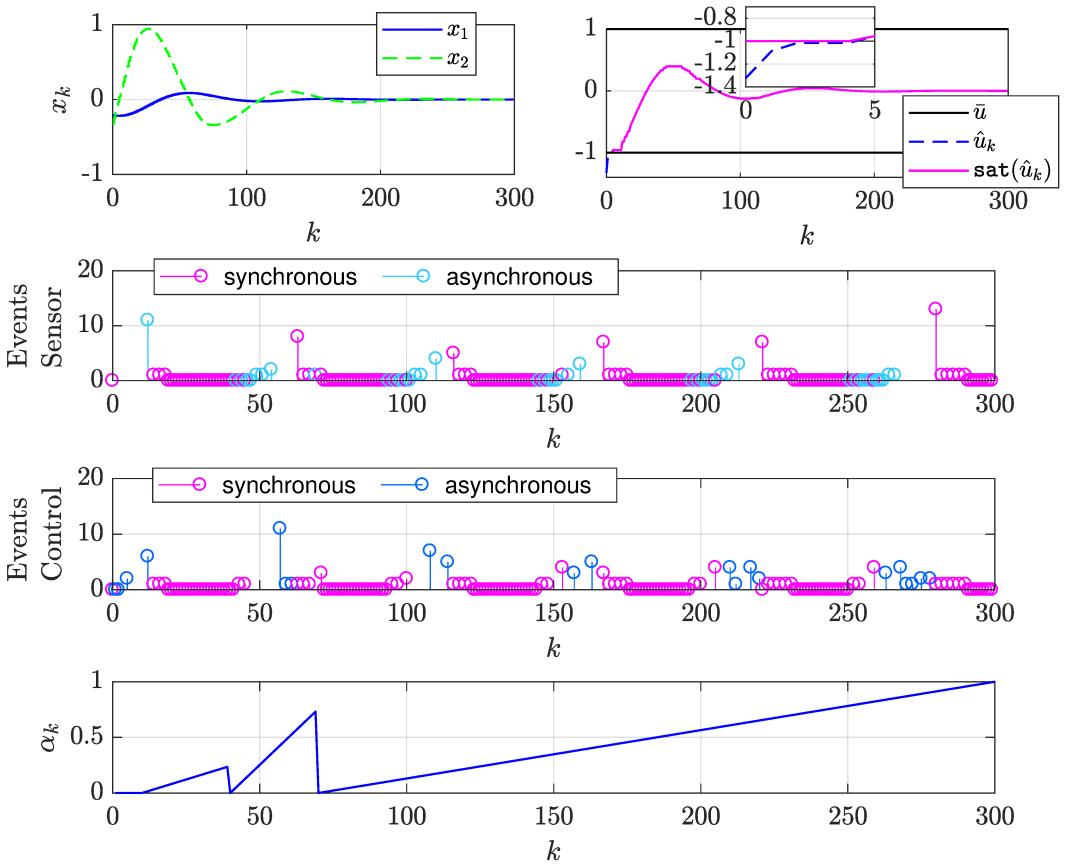

Figure 18 – The closed-loop response of system (128) - $\mathcal{X}_0 = \mathcal{E}(R, 1)$ with $R_{11} = \texttt{diag}\{26.60, 0.70\}$.

Table 3 – Comparison of the number of samplings - Example (128).

Design method	update	
	output	control
Theorem 3.1 in (DING et al., 2020)	67	1000
Theorem 4.1 in (DING et al., 2020)	70	1000
Theorem 4.2	85	232

As the authors in (DING et al., 2020) explore the LTI case with saturation, to compare our approach with theirs, we fix $\alpha_k = 0$, and set $C = \mathbf{I}_2$. Also, we consider a region of admissible initial conditions $\mathcal{X}_0 = \mathcal{E}(R, 1)$ with $R_{11} = \begin{bmatrix} 11.9987 & 0.2318 \\ 0.2318 & 0.5873 \end{bmatrix}$, which is contained in the region of attraction estimated by (DING et al., 2020). Thus, for the co-design, we run the optimization procedure $\mathcal{O}_6$ with conditions of Theorem 4.2, and got the following ETM matrices

$$Q_{\Delta y} = \begin{bmatrix} 1.2955 & 0.9134 \\ 0.9134 & 0.6441 \end{bmatrix}, \; Q_y = \begin{bmatrix} 0.0758 & 0.0106 \\ 0.0106 & 0.0425 \end{bmatrix},$$

$$Q_{\Delta u} = 1.5369, \text{ and } Q_u = 0.0261,$$

and the following dynamic controller matrices

$$A_c = \begin{bmatrix} -6.3069 & -29.0632 \\ 1.5869 & 7.3118 \end{bmatrix},\ B_c = \begin{bmatrix} -0.0264 & -0.0186 \\ 0.0067 & 0.0047 \end{bmatrix},$$
$$E_c = \begin{bmatrix} -0.1133 \\ 0.0288 \end{bmatrix},\ C_c = \begin{bmatrix} -6.6853 \\ -3.1688 \end{bmatrix}^\top,\ \text{and } D_c = \begin{bmatrix} 1.3583 \\ 0.9577 \end{bmatrix}^\top.$$

For the same initial condition, we simulate the closed-loop response of the system and found the updates rates showed in Table 3. Although in the first channel, the update rates obtained by (DING et al., 2020) with Theorem 3.1 and Theorem 4.1 are 21.18% and 17.65% smaller than ours, respectively, in the second channel, they are in both cases 331.03% higher than ours.

4.5.2 Example 2

Consider the following discretized version, with sampling time $T_s = 0.05$ seconds, of the system investigated in (MA et al., 2015).

$$\begin{aligned} x_{k+1} &= \begin{bmatrix} 1 & 0.05 \\ 0.1 & 0.85 \end{bmatrix} x_k + \begin{bmatrix} 0.11 \\ 0.11 \end{bmatrix} \hat{u}_k, \\ y_k &= \begin{bmatrix} -1 & 4 \end{bmatrix} x_k. \end{aligned} \tag{129}$$

Our objective here is to compare our co-design and emulation proposals with the one in (MA et al., 2015). The authors in (MA et al., 2015) address the co-design event-triggered dynamic output-feedback control problem for continuous linear time-invariant (LTI) system. The two independent ETMs are based on a condition that depends on the plant output and the controller output taken at different times. The results obtained by (MA et al., 2015) are presented in Table 4, where the initial conditions $x_0 = x_{c,0} = \begin{bmatrix} 40 & -20 \end{bmatrix}^\top$ were taken to simulate the closed-loop response of the system. Observe that, in the first channel, (MA et al., 2015) got an average sampling time that corresponds to 3 times the sampling time of the system without ETM; and, in the second channel, the average sampling time found corresponds to 3.6 times the sampling time of the system without ETM.

Table 4 – Comparison of the average sampling time - Example (129).

Design method	average sampling time [sec]	
	output	control
Theorem 2 in (MA et al., 2015)	0.15	0.18
Theorem 4.1	0.2303	0.25
Theorem 4.2	0.2303	0.375

First, to compare the co-design approach, we solve the optimization procedure $\mathcal{O}_5$ given in (124) with conditions of Theorem 4.2, and obtain the ETM matrices $Q_{\Delta y} =$

1.5489, $Q_y = 0.7091$, $Q_{\Delta u} = 1.4102$, and $Q_u = 0.6456$ and the following dynamic controller matrices

$$A_c = \begin{bmatrix} 6.1903 & 3.8725 \\ -8.3910 & -5.2462 \end{bmatrix}, \; B_c = \begin{bmatrix} -17.4254 \\ 23.6933 \end{bmatrix},$$
$$C_c = \begin{bmatrix} 0.1654 & 0.1180 \end{bmatrix}, \text{ and } D_c = -1.2314.$$

By simulating the closed-loop response of the system for the same initial conditions, we got the average sampling times presented in Table 4. Note that, in the first channel, we obtained an average sampling time that corresponds to almost 5 times the sampling time of the system without ETM, and in the second channel, the average sampling time found corresponds to 7.5 times the sampling time of the system without ETM. Therefore, we increased the average sampling by 53.87% on the sensor-to-controller channel, and 108.33% on the controller-to-actuator channel, with respect to (MA et al., 2015).

Then, to compare the emulation-approach, we design the ETMs (91) and (92) for both the controller obtained in the co-design and the one obtained by (MA et al., 2015) using the optimization procedure $\mathcal{O}_5$ given in (124) with conditions of Theorem 4.1. For the first case, we have found the same results, and for the second, we got the ETM matrices $Q_{\Delta y} = 1.8588$, $Q_y = 0.2646$, $Q_{\Delta u} = 3.7788$ and $Q_u = 0.5380$. By using these matrices to simulate the closed-loop response of the system, we find the average sampling times presented in Table 4. Thus, using our controller, the sampling average in the control ETM improved 50% in relation to the controller of (MA et al., 2015).

4.5.3 Example 3

Consider the following discretized version, with sampling time $T_s = 0.05$ seconds, of the system investigated in (LIU, D.; YANG, G.-H., 2018)

$$\begin{aligned} x_{k+1} &= \begin{bmatrix} 1 & 0.05 \\ -0.25 & 1 \end{bmatrix} x_k + \begin{bmatrix} 0 \\ 0.05 \end{bmatrix} \hat{u}_k, \\ y_k &= \begin{bmatrix} 1 & 0 \end{bmatrix} x_k. \end{aligned} \tag{130}$$

Our objective is to compare our co-design approach with the one in (LIU, D.; YANG, G.-H., 2018), where a novel exponential stability criterion is applied to provide an algorithm to co-design a dynamic output-feedback controllers and two independent ETMs for continuous linear time-invariant systems with communication delays. The results obtained by (LIU, D.; YANG, G.-H., 2018) are showed in Table 5, where the initial states condition $x_0 = \begin{bmatrix} 1 & 0.2 \end{bmatrix}^\top$ and $x_{c,0} = 0_{1,2}$ were taken to simulated the closed-loop response. By taking into account the procedures described in Remark 4.3 to deal with LTI ($\alpha_k = 0$) and non-saturated system, we run the optimization procedure $\mathcal{O}_5$ given

in (124) with conditions of Theorem 4.2, and got the ETM matrices $Q_{\Delta y} = 2.6910$, $Q_y = 0.6063$, $Q_{\Delta u} = 1.6493$, and $Q_u = 0.3716$ and the following dynamic controller matrices

$$A_c = \begin{bmatrix} 1.0819 & 0.5297 \\ -0.4837 & -0.2445 \end{bmatrix}, \; B_c = \begin{bmatrix} -5.9799 \\ 2.6499 \end{bmatrix},$$
$$C_c = \begin{bmatrix} 0.4254 & 1.1925 \end{bmatrix}, \text{ and } D_c = -2.3619.$$

Table 5 – Comparison of the updates rates - Example (130).

Design Method	Updates rates (%)	
	output	control
(LIU, D.; YANG, G.-H., 2018, Th. 2)	34.50%	38.25%
Theorem 4.2	30.50%	36.25%

For the same initial conditions, we simulated the system's closed-loop response and got the transmission rates showed in Table 5. In this case, we reduced the update rate in 6.15% and 5.23% on the sensor-to-controller and controller-to-actuator channels, respectively, in relation to (LIU, D.; YANG, G.-H., 2018).

4.6 CONCLUDING REMARKS

This chapter has investigated an event-triggering control design method that regionally stabilizes discrete-time LPV systems subject to saturating actuators inserted into a communication network with limited bandwidth. The main contributions can be summarized as: *i)* a convex procedure to design both a parameter-dependent dynamic output-feedback controller with anti-windup action and two event generators; *ii)* the proposed event-triggering policies allows to reduce the transmission of the output measurements and the control input over the communication channels; *iii)* the convex methodology can be simplified to design only an event generator for a given parameter-dependent dynamic output-feedback controller with anti-windup action; *iv)* Some convex optimization problems incorporating the main conditions as constraints permit to minimize the transmission activity over the network by considering or not a given region of admissible initial conditions.

Through numerical examples, the efficacy of the proposal in saving communication resources has been proved. Moreover, it was evident the classical trade-off between the size of the domain of attraction and the transmission reduction, in which the smaller the estimate of the domain of attraction, the higher the transmission reduction. The event-triggering schemes have shown a periodic behavior during certain time intervals, mainly for larger domains of attraction, but still with lower update rates than other approaches in the literature. Finally, it is important to re-emphasize that, the proposed approach requires a perfect matching between the scheduling parameters of the

controller and plant, which can be a conservative assumption in the sense of data transmission economy. To overcome such an issue, in the next chapter, an event-triggering mechanism to transmit the scheduling parameter over the network is introduced.

5 EVENT-TRIGGERED CO-DESIGN UNDER PARAMETER-ERROR

This chapter examines the event-triggered state-feedback control problem of discrete-time LPV systems subject to saturating actuators inserted into a communication network with limited bandwidth. Two independent event-triggering schemes are proposed to economize the communication resources. They indicate whether the current state or the current scheduling parameters should be transmitted from the sensor to the controller or not. In this sense, the controller scheduling parameters can differ from those of the system, which yields a certain degree of robustness concerning parameter deviations.

The convex conditions, given in terms of linear matrix inequalities (LMIs) thanks to the use of the Lyapunov theory, ensure the regional asymptotic stability of the closed-loop system for every initial condition within the estimate of the region of attraction. A convex optimization scheme incorporating these conditions as constraints is also proposed to reduce the amount of data transmission over the network. Finally, through numerical examples, the usefulness of the method is illustrated. The results presented are based on the work (DE SOUZA et al., 2021b).

5.1 PROBLEM STATEMENT

Consider the class of discrete-time LPV systems subject to saturating actuators inserted into a communication network represented by

$$x_{k+1} = A(\alpha_k)x_k + B(\alpha_k)\mathtt{sat}(u_k). \tag{131}$$

where $x_k \in \mathbb{R}^n$ is the state vector, $u_k \in \mathbb{R}^{n_u}$ is the control signal and $\mathtt{sat}(u_k)$ is the standard symmetric saturation function defined as

$$\mathtt{sat}(u_{k(\ell)}) = \mathtt{sign}(u_{k(\ell)})\min(|u_{k(\ell)}|, \bar{u}_{(\ell)}), \tag{132}$$

with $\bar{u}_{(\ell)} > 0$, $\ell \in \mathcal{I}[1, n_u]$, denoting the symmetric amplitude bound relative to the ℓ^{th} control input. The vector of time-varying parameters $\alpha_k \in \mathbb{R}^N$, which is assumed measured and available on-line (BRIAT, 2015), belongs to the unitary simplex given by

$$\Lambda \triangleq \left\{ \alpha_k \in \mathbb{R}^N : \sum_{i=1}^{N} \alpha_{k(i)} = 1,\ \alpha_{k(i)} \geq 0, i \in \mathcal{I}[1, N] \right\}. \tag{133}$$

Thus, the parameter-dependent matrices $A(\alpha_k) \in \mathbb{R}^{n\times n}$, $B(\alpha_k) \in \mathbb{R}^{n\times n_u}$ can be written as a convex combination of N known vertices according to

$$\begin{bmatrix} A(\alpha_k) & B(\alpha_k) \end{bmatrix} = \sum_{i=1}^{N} \alpha_{k(i)} \begin{bmatrix} A_i & B_i \end{bmatrix}. \tag{134}$$

To regionally stabilize system (131), we propose the following event-triggered parameter-dependent state-feedback controller:

$$u_k = K(\hat{\alpha}_k)\hat{x}_k, \tag{135}$$

where $\hat{\alpha}_k$ and $\hat{x}_k$ are the most recently transmitted value of the scheduling parameter and the state vector, respectively. The control gain matrix $K(\hat{\alpha}_k)$, in the same way as the system's matrices, is represented in the polytopic form as

$$K(\hat{\alpha}_k) = \sum_{j=1}^{N} \hat{\alpha}_{k(j)} K_j, \tag{136}$$

with $\hat{\alpha}_k \in \Lambda$ and $K_i \in \mathbb{R}^{n_u \times n}$. Note that, unlike the last chapter, the controller scheduling parameters can differ from those of the system, yielding a certain degree of robustness concerning parameter deviations.

By admitting a communication network with limited bandwidth, two independent ETMs are introduced into the channel between the sensor and controller to reduce the transmission activity while preserving the stability and certain performance index for the closed-loop system, as shown in Figure 19. Periodically, they make the decision, based on event-triggering rules, whether the current state and the current scheduling parameter should be transmitted through the communication channel.

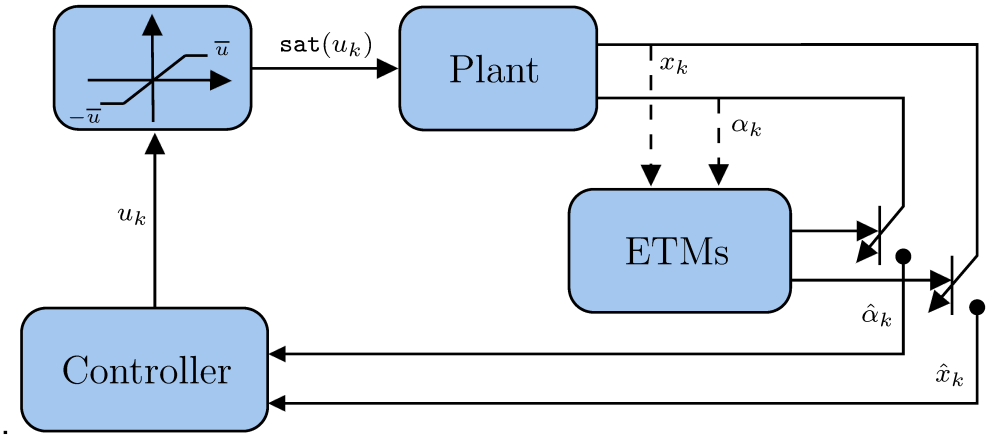

Figure 19 – Event-triggering closed-loop system.

State-based ETM: The decision for state updates is made according to the following rule:

$$\hat{x}_k := \begin{cases} x_k, & \text{if } \|\hat{x}_{k-1} - x_k\|^2_{Q_\Delta(\hat{\alpha}_k)} > \|x_k\|^2_{Q_x(\hat{\alpha}_k)} \\ \hat{x}_{k-1}, & \text{otherwise,} \end{cases} \tag{137}$$

where the positive definite matrices $Q_\Delta(\hat{\alpha}_k) = \sum_{i=1}^{N} \hat{\alpha}_{k(i)} Q_{\Delta i}$, $Q_{\Delta i} \in \mathbb{R}^{n \times n}$ and $Q_x(\hat{\alpha}_k) = \sum_{i=1}^{N} \hat{\alpha}_{k(i)} Q_{xi}$, $Q_{xi} \in \mathbb{R}^{n \times n}$ are variables to be designed, leading to an additional degree of freedom in the co-design. As these matrices acts as weights on the terms of the

event-triggering condition, their computation has a direct impact on the event-triggering policy and, consequently, on the way of reducing the data transmissions.

Note that if (137) holds at step k, then $\hat{x}_k$ is updated to x_k, because the error $\|\hat{x}_{k-1} - x_k\|^2_{Q_\Delta(\hat{\alpha}_k)}$ is too big to guarantee stability and a certain performance index for the closed-loop system. On the other hand, if (137) does not hold at step k, then $\hat{x}_k$ keeps its value from the previous instant $\hat{x}_{k-1}$, that is, $\hat{x}_k$ is not updated, because the error $\|\hat{x}_{k-1} - x_k\|^2_{Q_\Delta(\hat{\alpha}_k)}$ is small enough to guarantee stability and a certain performance index for the closed-loop system.

Scheduling-parameter based ETM: Additionally, we consider that whenever the difference between the last transmitted scheduling parameter $\hat{\alpha}_k$ and the current one α_k multiplied by a given scalar $0 \leq g \leq 1$ reaches the lower bound 0 or the upper bound $1 - g$, then the current sample of α_k is transmitted through the network. Therefore, the policy of the scheduling parameter transmission is based on the violation of the condition

$$0 < \hat{\alpha}_{k(i)} - g\alpha_{k(i)} < 1 - g, \tag{138}$$

for a given $0 \leq g \leq 1$. Following (DA CUNHA et al., 2020, Lemma 2), we note that the last transmitted scheduling parameter, $\hat{\alpha}_k$, can be written as

$$\hat{\alpha}_{k(i)} = g\alpha_{k(i)} + (1 - g)\varphi_{k(i)}, \tag{139}$$

for a vector $\varphi_k \in \mathbb{R}^N$ verifying $\sum_{i=1}^N \varphi_{k(i)} = 1$ and $\varphi_{k(i)} \geq 0$. Therefore, once both sides of inequality (138) are satisfied, equation (139) is ensured. Such a fact can be noted by summing (139) up for $i \in \mathcal{I}[1, N]$ and considering $\alpha_k, \hat{\alpha}_k \in \Lambda$, to obtain

$$\sum_{i=1}^{N} \varphi_{k(i)} = \frac{\sum_{i=1}^N \hat{\alpha}_{k(i)} - g\sum_{i=1}^N \alpha_{k(i)}}{1 - g} = 1. \tag{140}$$

Moreover, taking into account the positivity of $\hat{\alpha}_{k(i)} - g\alpha_{k(i)}$, one has $\varphi_{k(i)} \geq 0$.

Observe that the value of g has a direct influence on the size of the error allowed between the plant and controller parameters, and consequently, on the transmission rate. For g close to 0, the greater the error, the lower the transmission rate. On the other hand, for g close to 1, the lower the error, the greater the transmission rate. In the worst case, when $g = 1$, there is a transmission rate of 100%, where the plant and controller share the same scheduling parameter, then recovering the assumption of parameter sharing in (DE SOUZA et al., 2020d, 2020b; LI, S. et al., 2015; SAADABADI; WERNER, 2020).

The proposed ETM policy (138) differs from the usually found in the literature such as those in (SHANBIN; BUGONG, 2013; LI, S. et al., 2014; GOLABI et al., 2016, 2017). In our approach, the transmission policy depends directly on the scheduling parameters, while in the previous works the decision policy depends on the norm of

the dynamic matrices variations, which is an indirect parameter-based decision, or on some prescribed (small) deviation of the parameter.

In view of this, the problem we intend to solve in this chapter can be stated as follows.

Problem 5.1 *Consider the saturating LPV system (131). For a given scalar* $0 \leq g \leq 1$*, co-design the parameter-dependent state-feedback controller (135) and the two independent event-triggering conditions (137) and (138) that ensure the regional asymptotic stability of the closed-loop system, while reducing the data transmission on the communication network.*

An implicit objective in solving Problem 5.1 is to characterize an estimate of the domain of attraction of the origin, $\mathcal{R}_{\mathcal{E}}$, for the closed-loop system.

5.2 PRELIMINARY RESULTS

The saturating LPV system (131) in closed-loop with the state-feedback controller (135) can be represented by the following model:

$$x_{k+1} = (A(\alpha_k) + B(\alpha_k)K(\hat{\alpha}_k))x_k + B(\alpha_k)K(\hat{\alpha}_k)e_{x,k} - B(\alpha_k)\Psi(K(\hat{\alpha}_k)\hat{x}_k), \tag{141}$$

where $e_{x,k} \in \mathbb{R}^{n\times n}$ is the error between the latest transmission $\hat{x}_k$ and the latest sampling x_k, i.e. $e_{x,k} = \hat{x}_k - x_k$. By considering the polytopic form of the matrices, the system (141) can also be described as:

$$x_{k+1} = \sum_{i=1}^{N} \alpha_{k(i)} \big((A_i + B_i \sum_{j=1}^{N} \hat{\alpha}_{k(j)} K_j)x_k + B_i \sum_{j=1}^{N} \hat{\alpha}_{k(j)} K_j e_{x,k} - B_i \Psi(K(\hat{\alpha}_k)\hat{x}_k)\big). \tag{142}$$

Also, by using (139) and doing some manipulations, we have that:

$$\begin{aligned} x_{k+1} = &\sum_{i=1}^{N}\sum_{j=1}^{N} \rho_{ij}\alpha_{k(i)}\alpha_{k(j)} 0.5\big((A_i + A_j)x_k - (B_i + B_j)\Psi(u_k) + g(B_iK_j + B_jK_i)(x_k + e_{x,k})\big) \\ &+ \sum_{q=1}^{N}\sum_{i=1}^{N}\sum_{j=i}^{N} \rho_{ij}\alpha_{k(i)}\alpha_{k(j)}\varphi_{k(q)} 0.5(1-g)(B_iK_q + B_jK_q)(x_k + e_{x,k}). \end{aligned} \tag{143}$$

with $\rho_{ij} = 1$ when $i = j$ and $\rho_{ij} = 2$ otherwise.

Note that if x_k is updated at instant k, then from (137), it follows that $e_{x,k} = \hat{x}_k - x_k = x_k - x_k = 0$, and if x_k is not updated at instant k, then from (137), we have that $e_{x,k} = \hat{x}_k - x_k = \hat{x}_{k-1} - x_k$. Thus, the following inequality is always satisfied:

$$\|e_{x,k}\|^2_{Q_\Delta(\hat{\alpha}_k)} \leq \|x_k\|^2_{Q_x(\hat{\alpha}_k)}. \tag{144}$$

To investigate the regional asymptotic stability of the closed-loop system (141), we use the following candidate Lyapunov function

$$V(x_k, \hat{\alpha}_k) = x_k^\top P(\hat{\alpha}_k) x_k, \;\; P(\hat{\alpha}_k) = \sum_{i=1}^{N} \hat{\alpha}_{k(i)} P_i, \tag{145}$$

with $0 < P_i = P_i^\top \in \mathbb{R}^{2n \times 2n}$ and $\hat{\alpha}_k \in \Lambda$. The level set associated to $V(x_k, \hat{\alpha}_k)$ is defined as $\mathcal{R}_\mathcal{E} = \mathcal{L}_\mathcal{V}(1) = \{x_k \in \mathbb{R}^n : V(x_k, \hat{\alpha}_k) \leq 1\}$ and its calculation can be done as follows

$$\mathcal{R}_\mathcal{E} = \mathcal{L}_\mathcal{V}(1) = \bigcap_{\forall \hat{\alpha}_k \in \Lambda} \mathcal{E}(P(\hat{\alpha}_k), 1) \;\; = \bigcap_{i \in \mathcal{I}[1,N]} \mathcal{E}(P_i, 1), \tag{146}$$

where $\mathcal{E}(P(\hat{\alpha}_k), 1)$ denotes the ellipsoidal sets represented by

$$\mathcal{E}(P_i, 1) = \left\{ x_k \in \mathbb{R}^n : x_k^\top P_i x_k \leq 1, \;\; i \in \mathcal{I}[1, N] \right\}. \tag{147}$$

In addition, to deal with the saturation effects, we use the following Lemma directly derived from (TARBOURIECH et al., 2011, Lemma 1.6) by considering u_k given in (135) and $\nu_k = u_k - G(\hat{\alpha}_k) x_k$.

Lema 5.1 *Consider u_k given by (135), $\bar{u} \in \mathbb{R}^{n_u}$, $\bar{u} > 0$, and a matrix $G(\hat{\alpha}_k) = \sum_{i=1}^{N} \hat{\alpha}_{k(i)} G_i$, $G_i \in \mathbb{R}^{n_u \times n}$, $i \in \mathcal{I}[1, N]$, $\hat{\alpha}_k \in \Lambda$, such that*

$$\mathcal{S}(\bar{u}) \triangleq \{x_k \in \mathbb{R}^n : |G_{(\ell)}(\hat{\alpha}_k) x_k| \leq \bar{u}_{(\ell)}, \;\; \ell \in \mathcal{I}[1, n_u]\}. \tag{148}$$

If $x_k \in \mathcal{S}(\bar{u})$, then for any positive definite diagonal matrix $T(\hat{\alpha}_k) = \sum_{i=1}^{N} \hat{\alpha}_{k(i)} T_i$, $T_i \in \mathbb{R}^{n_u \times n_u}$, $i \in \mathcal{I}[1, N]$, $\hat{\alpha}_k \in \Lambda$, the following inequality is verified.

$$\Psi(K(\hat{\alpha}_k)\hat{x}_k)^\top T(\hat{\alpha}_k) \big(\Psi(K(\hat{\alpha}_k)\hat{x}_k) - (K(\hat{\alpha}_k) - G(\hat{\alpha}_k)) x_k - K(\hat{\alpha}_k) e_{x,k} \big) \leq 0. \tag{149}$$

5.3 MAIN RESULTS

The following theorem solves Problem 5.1 by providing convex conditions to design the state-feedback controller (135) and the two event-triggering mechanisms (137) and (138) that ensure the regional asymptotic stability of the closed-loop system with a reduced number of data transmission on the communication network.

Theorem 5.1 *Suppose there exist symmetric positive definite matrices $W_i \in \mathbb{R}^{n \times n}$, $\bar{Q}_{\Delta i} \in \mathbb{R}^{n \times n}$ and $\bar{Q}_{xi} \in \mathbb{R}^{n \times n}$, a positive definite diagonal matrices $S_i \in \mathbb{R}^{m \times m}$, matrices $Z_i \in \mathbb{R}^{m \times n}$, $Y_i \in \mathbb{R}^{m \times n}$ and $U \in \mathbb{R}^{n \times n}$, with $i \in \mathcal{I}[1, N]$, and a given scalar $0 \leq g \leq 1$,*

such that the following LMIs are feasible.

$$\left[\begin{array}{c|c|c|c} 0.5g(W_i+W_j+\bar{Q}_{xi}+\bar{Q}_{xj}) & \star & \star & \star \\ +\tilde{g}(W_q+\bar{Q}_{xq})-U-U^\top & & & \\ \hline \mathbf{0} & -0.5g(\bar{Q}_{\Delta i}+\bar{Q}_{\Delta j}) & \star & \star \\ & -\tilde{g}\bar{Q}_{xq} & & \\ \hline 0.5g(Y_i+Y_j-Z_i-Z_j) & 0.5g(Y_i+Y_j) & -g(S_i+S_j) & \star \\ +\tilde{g}(Y_q-Z_q) & +\tilde{g}Y_q & -2\tilde{g}S_q & \\ \hline 0.5(A_i+A_j)U & 0.5g(B_iY_j+B_jY_i) & -0.5g(B_iS_j+B_jS_i) & -gW_r \\ +0.5g(B_iY_j+B_jY_i) & +0.5\tilde{g}(B_i+B_j)Y_q & -0.5\tilde{g}(B_i+B_j)S_q & -\tilde{g}W_s \\ +0.5\tilde{g}(B_i+B_j)Y_q & & & \end{array}\right] < \mathbf{0},$$

$$i,q,r,s \in \mathcal{I}[1,N], j \in \mathcal{I}[i,N], \tag{150}$$

and

$$\left[\begin{array}{c|c} gW_i+\tilde{g}W_q-U-U^\top & \star \\ \hline gZ_{i(\ell)}+\tilde{g}Z_{q(\ell)} & -\bar{u}_{(\ell)}{}^2 \end{array}\right] < \mathbf{0}, \tag{151}$$

$$i,q \in \mathcal{I}[1,N], \ell \in \mathcal{I}[1,m].$$

with $\tilde{g} = (1-g)$. Then, the saturating LPV system (131) under the state-feedback controller (135) with gain matrix defined by

$$K_i = Y_iU^{-1} \tag{152}$$

subject to the ETMs (137) and (138) with matrices $Q_{\Delta i} = U^{-\top}\bar{Q}_{\Delta i}U^{-1}$ and $Q_{xi} = U^{-\top}\bar{Q}_{xi}U^{-1}$, is regionally asymptotically stable. Moreover, the region $\mathcal{R}_\mathcal{E} = \mathcal{L}_\mathcal{V}(1) \subseteq \mathcal{R}_\mathcal{A}$ is an estimate of the region of attraction of the origin for the closed-loop system.

Proof: First, by supposing the feasibility of (151), multiply its left-hand side by $\alpha_{k(i)}$ and $\varphi_{k(q)}$, sum it up to $i,q \in \mathcal{I}[1,N]$, and replace Z_i by G_iU, to obtain

$$\left[\begin{array}{c|c} \sum_{i=1}^N \alpha_{k(i)}gW_i + \sum_{q=1}^N \varphi_{k(q)}(1-g)W_q - U - U^\top & \star \\ \hline \left(\sum_{i=1}^N \alpha_{k(i)}gG_{i(\ell)} + \sum_{q=1}^N \varphi_{k(q)}(1-g)G_{q(\ell)}\right)U & -\bar{u}_{(\ell)}{}^2 \end{array}\right] < \mathbf{0}. \tag{153}$$

Then, replace $\sum_{q=1}^{N} \varphi_{k(q)}(1-g)$ by $\sum_{q=1}^{N} \hat{\alpha}_{k(q)} - \sum_{q=1}^{N} \alpha_{k(q)} g$, according to (139). Note that, in this step, the matrices W and G become function only of the parameter $\hat{\alpha}_k$. By assuming that $W(\hat{\alpha}_k) = P^{-1}(\hat{\alpha}_k)$ and using the fact that $\left[P^{-1}(\hat{\alpha}_k) - U\right]^{\top} P(\hat{\alpha}_k) \times \left[P^{-1}(\hat{\alpha}_k) - U\right] \geq \mathbf{0}$ to replace block (1,1) of the resulting inequality by $-U^{\top} P(\hat{\alpha}_k) U$, we have that

$$\left[\begin{array}{c|c} -U^{\top} P(\hat{\alpha}_k) U & \star \\ \hline G_{(\ell)}(\hat{\alpha}_k) U & -\bar{u}_{(\ell)}{}^2 \end{array}\right] < \mathbf{0}. \tag{154}$$

With the regularity of U, we can pre- and post multiply (154) by $\mathtt{diag}\{U^{-\top}, 1\}$ and its transpose, respectively, to get

$$\left[\begin{array}{c|c} -P(\hat{\alpha}_k) & \star \\ \hline G_{(\ell)}(\hat{\alpha}_k) & -\bar{u}_{(\ell)}{}^2 \end{array}\right] < \mathbf{0}. \tag{155}$$

Finally, applying Schur complement and pre- and post multiplying the resulting inequality by $x_k^{\top}$ and x_k, respectively, we have that

$$-x_k^{\top} P(\hat{\alpha}_k) x_k + x_k^{\top} G(\hat{\alpha}_k)_{(\ell)}^{\top} \bar{u}_{(\ell)}^2 G(\hat{\alpha}_k)_{(\ell)} x_k < 0, \tag{156}$$

which ensures the inclusion $\mathcal{R}_{\mathcal{E}} \subseteq \mathcal{S}(\bar{u})$ and, consequently, Lemma 5.1 applies. Therefore, any trajectory of the closed-loop system stating inside $\mathcal{R}_{\mathcal{E}}$ remains in $\mathcal{S}(\bar{u})$.

Moreover, by supposing the feasibility of (150), multiply its left-hand side by $\alpha_{k+1(r)}$, $\alpha_{k(i)}$, $\alpha_{k(j)}$, $\varphi_{k+1(s)}$ and $\varphi_{k(q)}$, sum it up to $r, s, q, i \in \mathcal{I}[1, N]$ and $j \in \mathcal{I}[i, N]$, and replace Y_i, Z_i, $\bar{Q}_{\Delta i}$ and $\bar{Q}_{xi}$ by $K_i U^{-1}$, $G_i U$, $U^{\top} Q_{\Delta i} U$ and $U^{\top} Q_{xi} U$, respectively, to obtain (157), which can be rewritten, after some algebraic manipulations, as (158).

$$
\begin{bmatrix}
\begin{array}{c} 0.5\sum_{i=1}^{N}\sum_{j=i}^{N}\rho_{ij}\alpha_{k(i)}\alpha_{k(j)}g(W_i+W_j+U^\top(Q_{xi}+Q_{xj})U) \\ +\sum_{q=1}^{N}\varphi_{k(q)}(1-g)(W_q+U^\top Q_{xq}U)-U-U^\top \end{array} & \star \\
\hline
\mathbf{0} & \begin{array}{c} -0.5\sum_{i=1}^{N}\sum_{j=i}^{N}\rho_{ij}\alpha_{k(i)}\alpha_{k(j)}gU^\top(Q_{\Delta i}+Q_{\Delta j})U \\ -\sum_{q=1}^{N}\varphi_{k(q)}(1-g)U^\top Q_{\Delta q}U \end{array} \\
\hline
\begin{array}{c} 0.5\sum_{i=1}^{N}\sum_{j=i}^{N}\rho_{ij}\alpha_{k(i)}\alpha_{k(j)}g(K_i+K_j-G_i-G_j)U \\ +\sum_{q=1}^{N}\varphi_{k(q)}(1-g)(K_q-G_q)U \end{array} & \begin{array}{c} 0.5\sum_{i=1}^{N}\sum_{j=i}^{N}\rho_{ij}\alpha_{k(i)}\alpha_{k(j)}g(K_i+K_j)U \\ +\sum_{q=1}^{N}\varphi_{k(q)}(1-g)K_qU \end{array} \\
\hline
\begin{array}{c} 0.5\sum_{i=1}^{N}\sum_{j=i}^{N}\sigma_{ij}\alpha_{k(i)}\alpha_{k(j)}(A_i+A_j+g(B_iK_j+B_jK_i))U \\ +0.5\sum_{i=1}^{N}\sum_{j=i}^{N}\sum_{q=1}^{N}\rho_{ij}\alpha_{k(i)}\alpha_{k(j)}\varphi_{k(q)}(1-g)(B_i+B_j)K_qU \end{array} & \begin{array}{c} 0.5\sum_{i=1}^{N}\sum_{j=i}^{N}\rho_{ij}\alpha_{k(i)}\alpha_{k(j)}g(B_iK_j+B_jK_i)U \\ +0.5\sum_{i=1}^{N}\sum_{j=i}^{N}\sum_{q=1}^{N}\rho_{ij}\alpha_{k(i)}\alpha_{k(j)}\varphi_{k(q)}(1-g)(B_i+B_j)K_qU \end{array}
\end{bmatrix}
$$

$$
\begin{bmatrix}
\star & \star \\
\hline
\star & \star \\
\hline
-\sum_{i=1}^{N}\sum_{j=i}^{N}\rho_{ij}\alpha_{k(i)}\alpha_{k(j)}g(S_i+S_j) & \star \\
-2\sum_{q=1}^{N}\varphi_{k(q)}(1-g)S_q & \\
\hline
-0.5\sum_{i=1}^{N}\sum_{j=i}^{N}\rho_{ij}\alpha_{k(i)}\alpha_{k(j)}g(B_iS_j+B_jS_i) & -\sum_{r=1}^{N}\alpha_{k+1(r)}gW_r \\
-0.5\sum_{i=1}^{N}\sum_{j=i}^{N}\sum_{q=1}^{N}\rho_{ij}\alpha_{k(i)}\alpha_{k(j)}\varphi_{k(q)}(1-g)(B_i+B_j)S_q & -\sum_{r=i}^{N}\varphi_{k+1(s)}(1-g)W_s
\end{bmatrix}
< \mathbf{0}. \quad (157)
$$

$$
\begin{bmatrix}
\begin{array}{c}\sum_{j=1}^{N}\alpha_{k(j)}g(W_j+U^\top Q_{xj}U)\\ +\sum_{q=1}^{N}\varphi_{k(q)}(1-g)(W_q+U^\top Q_{xq}U)-U-U^\top\end{array} & \star \\
\hline
\mathbf{0} & \begin{array}{c}-\sum_{j=1}^{N}\alpha_{k(j)}g(U^\top Q_{\Delta j}U)\\ -\sum_{q=1}^{N}\varphi_{k(q)}(1-g)U^\top Q_{\Delta q}U\end{array} \\
\hline
\begin{array}{c}\sum_{j=1}^{N}\alpha_{k(j)}g(K_j-G_j)U\\ +\sum_{q=1}^{N}\varphi_{k(q)}(1-g)(K_q-G_q)U\end{array} & \begin{array}{c}0.5\sum_{j=1}^{N}\alpha_{k(j)}gK_iU\\ +\sum_{q=1}^{N}\varphi_{k(q)}(1-g)K_qU\end{array} \\
\hline
\begin{array}{c}\sum_{i=1}^{N}\sum_{j=1}^{N}\alpha_{k(i)}\alpha_{k(j)}(A_i+gB_iK_j)U\\ +\sum_{i=1}^{N}\sum_{q=1}^{N}\alpha_{k(i)}\varphi_{k(q)}(1-g)B_iK_qU\end{array} & \begin{array}{c}\sum_{i=1}^{N}\sum_{j=1}^{N}\alpha_{k(i)}\alpha_{k(j)}gB_iK_jU\\ +\sum_{i=1}^{N}\sum_{q=1}^{N}\alpha_{k(i)}\varphi_{k(q)}(1-g)B_iK_qU\end{array}
\end{bmatrix}
$$

$$
\begin{bmatrix}
\star & \star \\
\hline
\star & \star \\
\hline
\begin{array}{c}-2\sum_{j=1}^{N}\alpha_{k(j)}gS_j\\ -2\sum_{q=1}^{N}\varphi_{k(q)}(1-g)S_q\end{array} & \star \\
\hline
\begin{array}{c}-\sum_{i=1}^{N}\sum_{j=1}^{N}\alpha_{k(i)}\alpha_{k(j)}gB_iS_j\\ -\sum_{i=1}^{N}\sum_{q=1}^{N}\alpha_{k(i)}\varphi_{k(q)}(1-g)B_iS_q\end{array} & \begin{array}{c}-\sum_{r=1}^{N}\alpha_{k+1(r)}gW_r\\ -\sum_{r=i}^{N}\varphi_{k+1(s)}(1-g)W_s\end{array}
\end{bmatrix} < 0. \quad (158)
$$

Then, replace $\sum_{q=1}^{N}\varphi_{k(q)}(1-g)$ by $\sum_{q=1}^{N}\hat{\alpha}_{k(q)}-\sum_{q=1}^{N}\alpha_{k(q)}g$, according to (139). Note that, in this step, the matrices W, Q_x, Q_Δ, G, S, and K become function only of the parameter $\hat{\alpha}_k$. By assuming that $W(\hat{\alpha}_k)=P^{-1}(\hat{\alpha}_k)$ and using the fact that $-U^\top P(\hat{\alpha}_k)U\leq P^{-1}(\hat{\alpha}_k)-U-U^\top$, we have that

$$
\begin{bmatrix}
-U^\top\big(P(\hat{\alpha}_k)-Q_x(\hat{\alpha}_k)\big)U & \star & \star & \star \\
\hline
\mathbf{0} & -U^\top Q_\Delta(\hat{\alpha}_k)U & \star & \star \\
\hline
(K(\hat{\alpha}_k)-G(\hat{\alpha}_k))U & K(\hat{\alpha}_k) & -2S(\hat{\alpha}_k) & \star \\
\hline
\big(A(\alpha_k)+B(\alpha_k)K(\hat{\alpha}_k)\big)U & B(\alpha_k)K(\hat{\alpha}_k)U & -B(\alpha_k)S(\hat{\alpha}_k) & -P^{-1}(\hat{\alpha}_{k+1})
\end{bmatrix} < 0. \quad (159)
$$

With the regularity of U, we can pre- and post multiply (159) by $\mathtt{diag}\{U^{-\top}, U^{-\top}, S^{-1}(\hat{\alpha}_k), \mathbf{I}_n\}$ and its transpose, respectively, to get

$$\left[\begin{array}{c|c|c|c} -P(\hat{\alpha}_k)+Q_x(\hat{\alpha}_k) & \star & \star & \star \\ \hline \mathbf{0} & -Q_\Delta(\hat{\alpha}_k) & \star & \star \\ \hline S^{-1}(\hat{\alpha}_k)(K(\hat{\alpha}_k)-G(\hat{\alpha}_k)) & S^{-1}(\hat{\alpha}_k)K(\hat{\alpha}_k) & -2S^{-1}(\hat{\alpha}_k) & \star \\ \hline (A(\alpha_k)+B(\alpha_k)K(\hat{\alpha}_k)) & B(\alpha_k)K(\hat{\alpha}_k) & -B(\alpha_k) & -P^{-1}(\hat{\alpha}_{k+1}) \end{array}\right] < \mathbf{0}. \quad (160)$$

Next, applying Schur complement, we have that

$$\left[\begin{array}{c|c|c} -P(\hat{\alpha}_k)+Q_x(\hat{\alpha}_k) & \star & \star \\ \hline \mathbf{0} & -Q_\Delta(\hat{\alpha}_k) & \star \\ \hline S^{-1}(\hat{\alpha}_k)(K(\hat{\alpha}_k)-G(\hat{\alpha}_k)) & S^{-1}(\hat{\alpha}_k)K(\hat{\alpha}_k) & -2S^{-1}(\hat{\alpha}_k) \end{array}\right] + \begin{bmatrix} (A(\alpha_k)+B(\alpha_k)K(\hat{\alpha}_k))^\top \\ (B(\alpha_k)K(\hat{\alpha}_k))^\top \\ -B(\alpha_k)^\top \end{bmatrix}$$
$$\times P(\hat{\alpha}_{k+1}) \begin{bmatrix} (A(\alpha_k)+B(\alpha_k)K(\hat{\alpha}_k)) & B(\alpha_k)K(\hat{\alpha}_k) & -B(\alpha_k) \end{bmatrix} < \mathbf{0}. \quad (161)$$

Then, pre- and post multiplying (161) by the augmented vector $\begin{bmatrix} x_k^\top & e_{x,k}^\top & \Psi(K(\hat{\alpha}_k)\hat{x}_k)^\top \end{bmatrix}$ and its transpose, respectively, and replacing $\big(A(\alpha_k)$ $+B(\alpha_k)K(\hat{\alpha}_k)\big)x_k + B(\alpha_k)K(\hat{\alpha}_k))e_{x,k} - B(\alpha_k)\Psi(K(\hat{\alpha}_k))x_k)$ by x_{k+1}, according to (141), results in

$$x_{k+1}^\top P(\hat{\alpha}_{k+1})x_{k+1} - x_k^\top P(\hat{\alpha}_k)x_k - 2\Psi(K(\hat{\alpha}_k)\hat{x}_k)^\top T(\hat{\alpha}_k)(\Psi(K(\hat{\alpha}_k)\hat{x}_k) - (K(\hat{\alpha}_k)-G(\hat{\alpha}_k))x_k$$
$$- K(\hat{\alpha}_k)e_{x,k}) - e_{x,k}^\top Q_\Delta(\hat{\alpha}_k)e_{x,k} + x_k^\top Q_x(\hat{\alpha}_k)x_k \leq 0. \quad (162)$$

From (145), we have that $x_{k+1}^\top P(\hat{\alpha}_{k+1})x_{k+1} - x_k^\top P(\hat{\alpha}_k)x_k = V(x_{k+1}, \hat{\alpha}_{k+1}) - V(x_k, \hat{\alpha}_k) = \Delta V(x_k, \hat{\alpha}_k)$. By taking this into account and denoting $S^{-1}(\hat{\alpha}_k) = T(\hat{\alpha}_k)$, we conclude that

$$\Delta V(x_k, \hat{\alpha}_k) < 2\Psi(K(\hat{\alpha}_k)\hat{x}_k)^\top T(\hat{\alpha}_k)(\Psi(K(\hat{\alpha}_k)\hat{x}_k) - (K(\hat{\alpha}_k)-G(\hat{\alpha}_k))x_k$$
$$- K(\hat{\alpha}_k)e_{x,k}) < e_{x,k}^\top Q_\Delta(\hat{\alpha}_k)e_{x,k} - x_k^\top Q_x(\hat{\alpha}_k)x_k \leq 0. \quad (163)$$

By supposing that $x_k \in \mathcal{S}(\bar{u})$, the generalized sector condition presented in Lemma 5.1 ensures the non-positivity of $2\Psi(K(\hat{\alpha}_k)\hat{x}_k)^\top T(\hat{\alpha}_k)(\Psi(K(\hat{\alpha}_k)\hat{x}_k) - (K(\hat{\alpha}_k)-G(\hat{\alpha}_k))x_k - K(\hat{\alpha}_k)e_{x,k})$. Also, from inequality (144), we have that $e_{x,k}^\top Q_\Delta(\hat{\alpha}_k)e_{x,k}$ $-x_k^\top Q_x(\hat{\alpha}_k)x_k \leq 0$ is always satisfied. Because of the positivity of $P(\hat{\alpha_k})$, we can assume that there exist a sufficiently small $\epsilon_0 > 0$ such that

$$\epsilon_0\|x_k\|^2 \leq V(x_k, \hat{\alpha_k}) \leq \epsilon_1\|x_k\|^2, \text{ with } \epsilon_1 = \max_{i\in\mathcal{I}[1,N]} \lambda_{\max} P_i > 0. \quad (164)$$

Moreover, we have that

$$\Delta V(x_k, \hat{\alpha_k}) \leq -\epsilon_2 \|x_k\|^2 < 0. \tag{165}$$

for some $\epsilon_2 > 0$. Therefore, $V(x_k, \hat{\alpha}_k)$ given in (145) is a Lyapunov function and $\mathcal{R}_{\mathcal{E}} = \mathcal{L}_{\mathcal{V}}(1)$ is an estimate of the region of attraction of the origin for the closed-loop system (141). That concludes the proof. ∎

Observe that g parameter may affect the feasibility of the LMIs condition in Theorem 5.1 and a search on this parameter over the interval $0 \leq g \leq 1$ can be used to improve the ETM performance. In general, the feasibility of condition (150) and (151) is easier to verify for $g = 1$, since this case corresponds to consider a full transmission rate and no parameter error. Examples presented later illustrate such a possibility.

5.3.1 Optimization design procedure

This section aims to propose an optimization procedure that indirectly reduces the number of state signal updates. By looking at the event-triggering condition (137), we can see that it is a relative measure of the deviation between the last sampled state and the current state with $Q_{\Delta i}$ and Q_{xi} acting as weights on this measure. Thus, we have that the "smaller" $Q_{\Delta i}$ and the "larger" Q_{xi} are, the more the current state is allowed to deviate from the last sampled one and the fewer transmissions events are expected. However, the matrices $Q_{\Delta i}$ and Q_{xi} do not appear as decision variables in the conditions of Theorem 5.1, due to the congruence transformation required to formulate them in terms of LMIs. To overcome such an issue, we propose the following restrictions:

$$\left[\begin{array}{c|c} g\bar{Q}_{xi} + (1-g)\bar{Q}_{xq} & \star \\ \hline U & g\hat{Q}_{xi} + (1-g)\bar{Q}_{xq} \end{array}\right] > 0, \tag{166}$$

$$\left[\begin{array}{c|c} g\hat{Q}_{\Delta i} + (1-g)\bar{Q}_{xq} & \star \\ \hline \mathbf{I}_n & \begin{array}{c} U + U^\top - g\bar{Q}_{\Delta i} \\ -(1-g)\bar{Q}_{\Delta q} \end{array} \end{array}\right] > 0. \tag{167}$$

$$i, q \in \mathcal{I}[1, N]; j \in \mathcal{I}[i, N].$$

The first one enforces the lower bound $Q_{xi} > \hat{Q}_{xi}^{-1}$ through the direct application of the Schur's complement, and the second enforces the upper bound $Q_{\Delta i} < \hat{Q}_{\Delta i}$ through the direct application of Lemma 1 in (SEURET; GOMES DA SILVA JR, 2012). In this case, the fact to minimize the pair $(\hat{Q}_{\Delta i}, \hat{Q}_{xi})$ effectively minimizes the pair $(Q_{\Delta i}, Q_{xi})$.

Therefore, we have the following optimization procedure:

$$\mathcal{O}_7 : \begin{cases} \min & \sum_{i=1}^{N} \mathtt{tr}(\hat{Q}_{\Delta i} + \hat{Q}_{xi}), \\ \text{subject to} & (150), (151), (166) \text{ and } (167). \end{cases} \tag{168}$$

It is important to highlight that the transmission activity of the scheduling parameter is associated with the choice of the scalar g. As discussed earlier, the closer g is to zero, the smaller the transmission activity. This will be evident in the examples that follow.

5.4 NUMERICAL EXAMPLES

In this section, we present illustrative examples, borrowed from the literature (HEEMELS et al., 2010; LI, S. et al., 2014, 2015), to show the effectiveness of our proposal.

5.4.1 Example 1

Consider the saturating LPV system

$$x_{k+1} = \begin{bmatrix} 0.25 & 1 & 0 \\ 0 & 0.1 & 0 \\ 0 & 0 & 0.6 + \vartheta_k \end{bmatrix} x_k + \begin{bmatrix} 1 - 0.8\vartheta_k \\ 0 \\ 1 - \vartheta_k \end{bmatrix} \mathtt{sat}(u_k), \tag{169}$$

where the time-varying parameter $0 \leq \vartheta_k 0.5$ and the symmetric saturation limit is $\bar{u} = 0.5$. In this case, we can take $\alpha_{k(1)} = 1 - 2\vartheta_k$ and $\alpha_{k(2)} = 2\vartheta_k$ with $A_1 = A(0)$, $B_1 = B(0)$, $A_2 = A(0.5)$ and $B_2 = B(0.5)$.

First, we are interested in investigating the influence of parameter g (see (138)) in the update rate of the scheduling parameter and the state. With this purpose, for $g = 0.1, 0.2, \ldots, 1$, we use the optimization procedure $\mathcal{O}_7$ given in (168) to design the control gains and the event-triggering parameters. For each case, we simulate the closed-loop response for 1000 initial conditions belonging to $\mathcal{R}_{\mathcal{E}}$ and α_k chosen randomly. The average update rate (%) of the scheduling parameter, marked with $\times$, and the state, marked with ■, as a function of g are illustrated in Figure 20. We can see that as g approaches to 1, the update rate increases until it reaches 100% for $g = 1$, i.e. $\hat{\alpha}_k = \alpha_k$. In such a case, we also have the smallest update rate of the states, which is expected as the controller is better adjusted to the conditions of the plant.

For one of these cases, $g = 0.8$, we plot in Figure 21, the estimate of the region of attraction $\mathcal{R}_{\mathcal{E}}$ (light purple line) along with all the trajectories of the states (colored dots). One can see that the trajectories do not leave the domain of attraction, as expected.

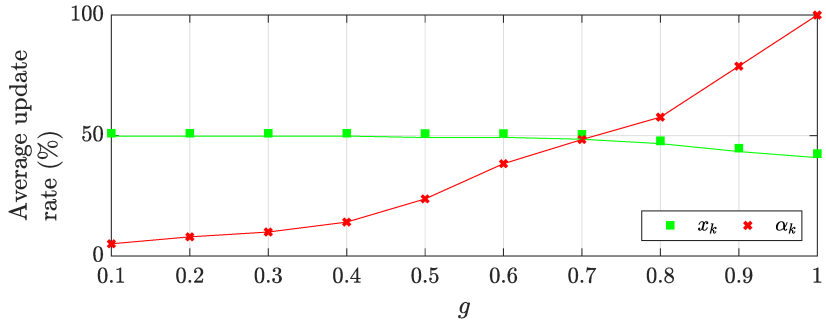

Figure 20 – Average update rate of the scheduling parameter and the state.

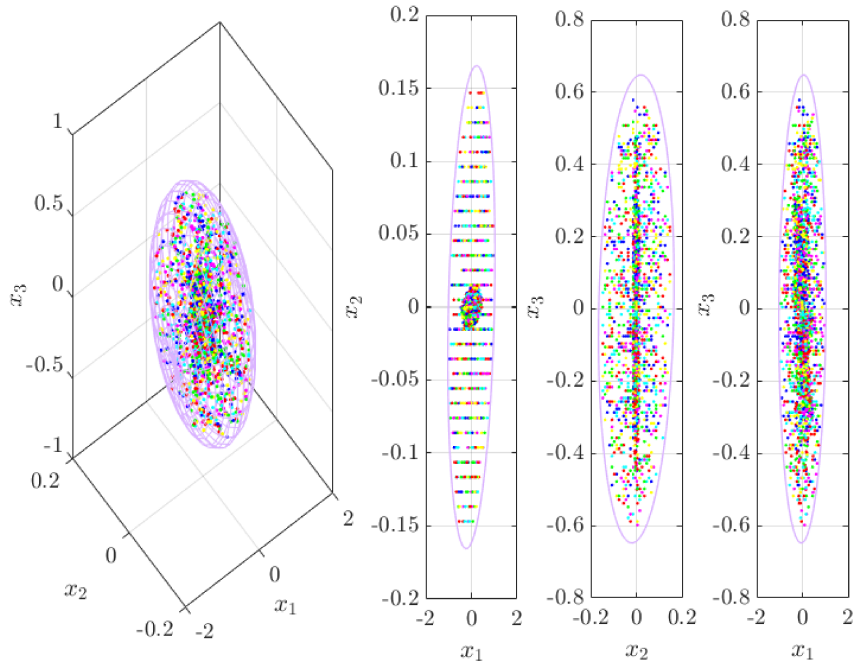

Figure 21 – The estimate of the region of attraction $\mathcal{R}_{\mathcal{E}}$ for $g = 0.8$.

In addition, we plot for a specific initial condition $x_0 = \begin{bmatrix} -0.0351 & -0.0253 & -0.5887 \end{bmatrix}^\top$, the closed-loop temporal response and the inter-event interval of the event generators, as seen in figures 22 and 23, respectively. In the first one, we can observe that the states converge to origin despite the saturation of the actuator in the first two instants of simulation. In the second, we have (on the bottom) the inter-event interval of the scheduling parameter, marked with $\times$, and the state, marked with ■. Note that both mechanisms are independent, although one can affect the other indirectly, as discussed previously. Moreover, we have (on the top) the difference between $\hat{\alpha}_k$ and α_k, which is marked with • ($\times$) when its value is inside (outside) the region of validity imposed by Lemma 139, traced with black lines. With g close to 1, the smaller the error allowed between $\hat{\alpha}_k$ and α_k, and therefore, the higher the update rate. The control gain and the

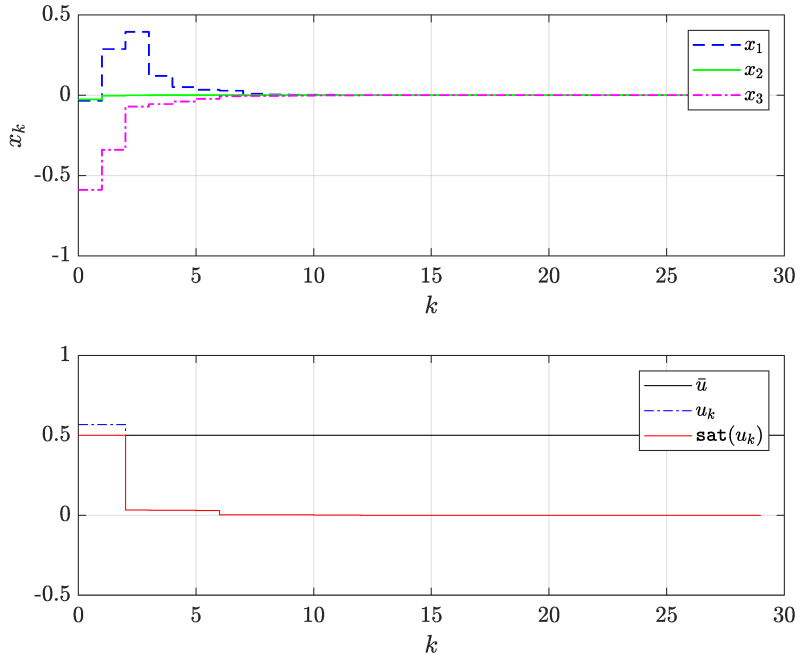

Figure 22 – The closed-loop temporal response for $x_0 = \begin{bmatrix}-0.0351 & -0.0253 & -0.5887\end{bmatrix}^\top$.

event-triggering parameters used for this simulation were

$$K_1 = \begin{bmatrix}-0.0536 & -0.0837 & -0.1480\end{bmatrix}$$
$$K_2 = \begin{bmatrix}-0.0885 & -0.2223 & -1.0458\end{bmatrix}$$

and

$$Q_{\Delta 1} = \begin{bmatrix} 0.0328 & 0.0529 & 0.1064 \\ 0.0529 & 0.0895 & 0.2117 \\ 0.1064 & 0.2117 & 0.7273 \end{bmatrix}, \quad Q_{\Delta 2} = \begin{bmatrix} 0.0131 & 0.0324 & 0.1492 \\ 0.0324 & 0.0804 & 0.3736 \\ 0.1492 & 0.3736 & 1.7519 \end{bmatrix},$$
$$Q_{x1} = \begin{bmatrix} 0.8472 & -0.0343 & 0.0403 \\ -0.0343 & 2.1130 & 0.0365 \\ 0.0403 & 0.0365 & 1.2695 \end{bmatrix}, \quad Q_{x1} = \begin{bmatrix} 0.8357 & -0.0572 & 0.0860 \\ -0.0572 & 2.0484 & 0.1050 \\ 0.0860 & 0.1050 & 0.6704 \end{bmatrix}.$$

5.4.2 Example 2

By assuming that the LPV system (169) is not subject to any restriction on the input signal, we compare our approach with (GOLABI et al., 2016, 2017). The authors in (GOLABI et al., 2016) consider the problem of the co-design of an event-triggering condition and a state-feedback controller for LPV systems. The proposed ETM sends information on states and scheduling variables simultaneously to the controller when needed. On the other hand, the authors in (GOLABI et al., 2017) propose an event-triggered reference tracking control design method for LPV systems, in which are de-

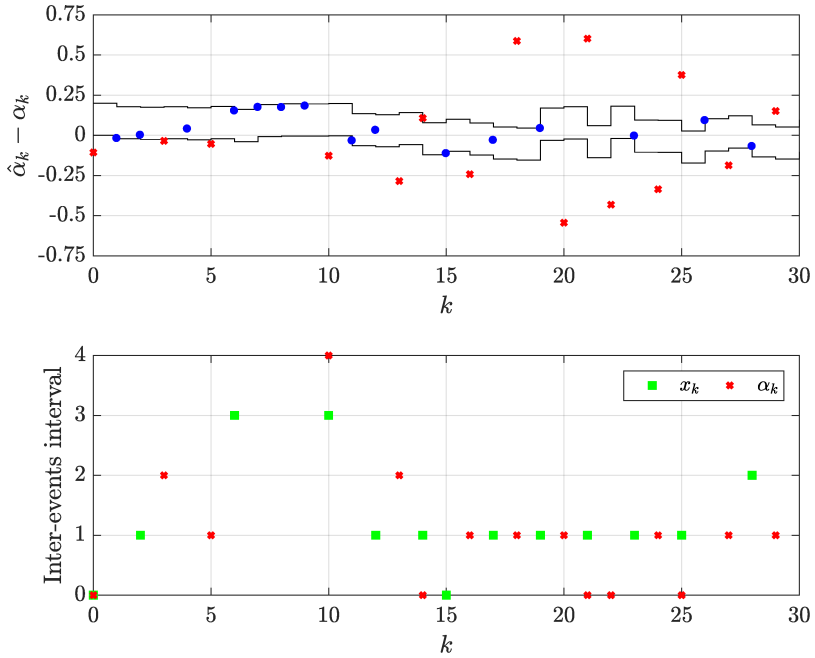

Figure 23 – Inter-event interval of the event generators.

signed a state-feedback controller and three separate ETMs for transmitting the state, the scheduling variables, and the controller output over the network.

By solving Theorem 1 in (GOLABI et al., 2016), we design the control gains $K_1 = \begin{bmatrix} -0.095 & -0.373 & -0.368 \end{bmatrix}$ and $K_2 = \begin{bmatrix} -0.179 & -0.728 & -1.205 \end{bmatrix}$ and the triggering parameter $\sigma = \sigma_x^{-1} = 0.048$. Also, by disregarding the reference tracking setup, we solve Theorem 2 in (GOLABI et al., 2017) with the scheduling parameter error threshold $\delta_0 = 0.05$, obtaining the control gains $K_1 = \begin{bmatrix} -0.032 & -0.111 & -0.322 \end{bmatrix}$ and $K_2 = \begin{bmatrix} -0.030 & -0.1388 & -1.071 \end{bmatrix}$ and triggering parameters $\sigma_\Psi = 0.0226$ and $\sigma_u = 0.0250$. We use the data of both approaches to simulate the system's closed-loop response for $x_0 = \begin{bmatrix} 1 & -1 & -0.5 \end{bmatrix}^\top$ and 1000 values of α_k generated randomly. The results are presented in Table 6.

The same procedure was performed using our approach for some values of $0 \leq g \leq 1$. The results are also shown in Table 6. One can see that the average update rates of the states and the scheduling parameter obtained by (GOLABI et al., 2016) and (GOLABI et al., 2017) are higher than ours in almost all cases. Note that, although (GOLABI et al., 2017) considers a third ETM for the control output, such a mechanism had a high transmission rate. For $g = 0.2$, for instance, the transmission activity of (GOLABI et al., 2016) and (GOLABI et al., 2017) are about 731% and 877% greater than ours w.r.t. the scheduling parameter, respectively, and about 36% and 104% greater than ours w.r.t the state, respectively.

Table 6 – Percentage of transmission rate achieved by the proposed method and those from 1-(GOLABI et al., 2017) and 2-(GOLABI et al., 2016).

	1	2	Theorem 5.1				
			g				
			0.2	0.4	0.6	0.8	1.0
α_k(%)	78.33	66.66	8.02	14.42	38.22	57.56	100
x_k(%)	100	66.66	49.05	49.05	55.41	47.50	42.68
u_k(%)	98.4	-	-	-	-	-	-

5.4.3 Example 3

By assuming that the LPV system (169) is not subject to any restriction on the input signal, and has a fixed matrix of control i.e. $B_1 = B_2 = B(0)$, we compare our approach with (SHANBIN; BUGONG, 2013). The authors in (SHANBIN; BUGONG, 2013) propose the co-design of an ETM and a state-feedback controller for LPV systems where the parameters are not exactly known, but estimated parameters satisfying certain level are known. The robustness of the proposed event-triggered control system w.r.t the uncertainty of the parameter is indicated by the scalar δ_0 according to the inequality $\|\Delta A(\alpha_k, \hat{\alpha}_k)x_k\|^2 \leq \delta_0^2\|x_k\|^2$, with $\Delta A(\alpha_k, \hat{\alpha}_k) = A(\alpha_k) - A(\hat{\alpha}_k)$. Thus, we solve Theorem 1 in (SHANBIN; BUGONG, 2013) with $\delta_0 = 0.1$ and the triggering parameter $\eta = 1$, obtaining the control gains $K_1 = \begin{bmatrix} -0.095 & -0.354 & -0.414 \end{bmatrix}$ and $K_2 = \begin{bmatrix} -0.091 & -0.335 & -0.768 \end{bmatrix}$. By using the ETM and the controller designed, we simulated the closed-loop response for $x_0 = \begin{bmatrix} 1 & -1 & -0.5 \end{bmatrix}^\top$ and 1000 values of $\Delta A(\alpha_k, \hat{\alpha}_k)$, generated randomly within the allowed range, obtaining an average update rate of x_k equal to 84.11, as indicated in Table 7. Note that, from the values of $\Delta A(\alpha_k, \hat{\alpha}_k)$ and $\hat{\alpha}_k$, we can determine α_k. We used these values of α_k to establish a fair comparison with (SHANBIN; BUGONG, 2013).

To compare our approach with that proposed by (SHANBIN; BUGONG, 2013), we measured, for some values of $0 \leq g \leq 1$, the robustness of our event-triggered control system and computed the average update rate of both x_k and α_k. The robustness of our method was determined by computing the following scalar $\delta : \delta = \max_k \left\{ \sqrt{\|\Delta A(\alpha_k, \hat{\alpha}_k)x_k\|^2 / \|x_k\|^2} \right\}$ among the instants of simulation. The results are shown in Table 7. As we can see, for values of g smaller than 0.8, our approach is more robust to the variation of parameters than (SHANBIN; BUGONG, 2013), almost 4 times for $g = 0.2$. In addition, we found an average update rate of x_k smaller than (SHANBIN; BUGONG, 2013) in all cases. For $g = 0.8$, for instance, we obtained a rate 35% smaller, approximately. As (SHANBIN; BUGONG, 2013) does not consider an ETM to sent the information about the scheduling parameter over the network, these data are not comparable.

Table 7 – Relative robustness (δ/δ_0) achieved by the proposed method and that from (SHANBIN; BUGONG, 2013) and the percentage of transmission rate.

	(SHANBIN; BUGONG, 2013)	Theorem 5.1				
		g				
		0.2	0.4	0.6	0.8	1.0
δ/δ_0	1	3.86	2.87	1.95	0.96	0
α_k(%)	-	4.80	10.90	44.40	74.75	100
x_k(%)	84.11	55.63	55.61	55.59	53.86	40.21

5.5 CONCLUDING REMARKS

This chapter has presented a methodology to design an event-triggered state-feedback control for discrete-time LPV systems subject to saturating actuators inserted in a communication network with limited bandwidth. The main contributions can be listed as *i)* a convex procedure to design both a state-feedback controller and two event-generators; *ii)* the proposed event-triggering policies permit to reduce the transmission of states and scheduling variables in the sensor-to-controller channel; *iii)* the proposed controller depends on scheduling parameters that may differ from those of the plant, yielding a certain degree of robustness concerning parameter deviations *iv)* Some optimization problems incorporating the main conditions as constraints allow to effectively reduce the update rate of the states through the communication network.

By using numerical examples, the effectiveness of the approach in reducing the transmission activity over the network has been demonstrated. In particular, for the transmission of the scheduling parameters, very small update rates were achieved, thanks to the new methodology presented.

6 CONCLUSION

This thesis has presented new approaches for the problem of regional stabilization of two classes of discrete-time linear parameter varying systems with input constraints. The first class consisted of systems with time-varying delay in the states subject to saturating actuators and exogenous signals. The second one concerned the systems with saturating actuators inserted into a communication network with limited bandwidth. The proposed convex conditions were based on parameter-dependent Lyapunov functions, which yielded linear matrix inequality (LMI) based formulations. Convex optimizations procedures incorporating these conditions were also established to achieve different control objectives, such as maximization of the estimate of the region of attraction, minimization of the disturbance tolerance, and minimization of the transmission activity on the communication channels. Numerical examples borrowed from the literature allowed us to describe the effectiveness of our approach compared to other literature methods.

At first, in Chapter 2, we depicted some results related to the first class of systems. As one of the contributions of this thesis, we designed in this chapter parameter-dependent state-feedback controllers ensuring the input-to-state stability of the closed-loop for a set of admissible initial conditions and a set of admissible disturbance signals. The approach permits, with the use of the augmented delay-free switched representation of the closed-loop system, to design one of three possible control gain structures, which are: *i)* the one that feeds all states, *ii)* the one that feeds only the current state and *iii)* the one that feeds both the current and the most delayed state. Comparisons, in terms of the size of the domain of attraction and the maximum energy allowed for the disturbance signals, between such gains and also the robust one were performed at the end of the chapter. It was evident that the full parameter-dependent gain achieved the best results in all cases, which was expected. Although the other parameter-dependent gains feed back less delayed states, they still got better results compared to the robust one. For the design of these controllers, limited delay variation rates were considered, which resulted in higher tolerances to disturbances signals.

Chapter 3 also presented some results regarding the first class of systems. The contribution reported in the chapter followed as an extension of the previous one, where the augmented delay-free switched representation was used in the synthesis of parameter-dependent dynamic output-feedback controllers with an anti-windup term. One of the relevant characteristics of the proposed dynamic controller is that its order can vary from the actual system's order to the augmented delay-free switched system's. Such a characteristic proved to be relevant in obtaining bigger domains of attraction and higher tolerances to disturbances signals for higher order controllers. Although it is the designer's choice, it is important to stress that the higher the controller's order, the

higher the numerical complexity, consequently, computational effort, then establishing a trade-off between these variables.

In Chapters 4, we focused on the second class of systems. The contribution stated in the chapter consisted of designing two event-triggering mechanisms and a dynamic output-feedback controller with anti-windup action ensuring the regional asymptotic stability of the closed-loop system. The transmission activity on the sensor-to-controller and controller-to-actuator channels was indirectly reduced thanks to the proposed optimization procedures. One of them even allowed the minimization of the update rate for a given admissible initial conditions region. Through numerical examples, the update rates for two different admissible initial conditions regions were evaluated. It was evident the existing trade-off between the size of the domain of attraction and the transmission saving, in which the smaller the domain of attraction, the higher the transmission saving.

Finally, Chapter 5 was also dedicated to the second class of systems. The contribution of the chapter is related to the synthesis of two event-triggering mechanisms and a state-feedback controller ensuring the regional asymptotic stability of the closed-loop system. The proposed ETMs were specified to reduce the data transmission of the states and scheduling parameters at the sensor node. Thus, unlike the last chapter, we assumed that the controller scheduling parameter can differ from that of the system, which is more realistic, yielding a certain degree of robustness concerning the parameter deviations. Through numerical examples, we have shown the efficiency of our approach in saving the limited network resources, mainly with regard to the transmission of the scheduling parameters.

6.1 PERSPECTIVES

Among some possible extensions to the work presented in this thesis, the following directions can be mentioned:

- Study a more general parameter dependence, for instance, the polynomial one. Such a direction should impose to consider other methods as those based on sum-of-squares (WU, F.; PRAJNA, 2005).

- Expand the approach to introduce discretization errors in the system modeling. As the present work considers a discrete-time framework for analysis and control, discretization issues are not addressed. Thus, it would be interesting to investigate discretization procedures to present a more general formulation, like that proposed by (BRAGA et al., 2015).

- Study more involving event-triggering mechanisms, such as dynamic ones. According to (GIRARD, 2014), the guaranteed lower bound on inter-execution times

using a dynamic event generator cannot be smaller than that obtained for a classical static event generator. So, the use of a dynamic event-generator could further improve the results obtained in this work, eliminating, for instance, the periodic behavior seen in the examples in Chapter 4.

- Consider other imperfections typical of networked control systems such as network-induced delays. In the present work, it was considered that the communication channel can transmit information quickly enough that this problem can be disregarded. However, that is not always the case, and tools to consider the effect of this delay in such context are an important open topic.

6.2 PUBLICATIONS

Before this document, the contributions of the research throughout this Ph.D. include the following papers, published in journals:

- **ISS Robust Stabilization of State-Delayed Discrete-time Systems with Bounded Delay Variation and Saturating Actuators**. de Souza, C., Leite, V. J. S., Castelan, E. B., and Silva, L. F. P. *IEEE Transactions on Automatic Control*, 2018;
- **Dynamic controllers for local input-to-state stabilization of discrete-time linear parameter-varying systems with delay and saturating actuators**. de Souza, C., Castelan, E. B., and Leite, V. J. S. *International Journal of Robust and Nonlinear Control*, 2020;
- **Emulation-based Dynamic Output-Feedback Control of Saturating Discrete-time LPV Systems**. de Souza, C., Leite, V. J. S., Tarbouriech, S., and Castelan, E. B. *IEEE Control Systems Letters*, 2020;
- **Co-design of an Event-triggered Dynamic Output Feedback Controller for Discrete-time LPV Systems with Constraints**. de Souza, C., Tarbouriech, S., Leite, V. J. S., and Castelan, E. B. *Journal of The Franklin Institute*, 2020;
- **Event-triggered Policy for DOF stabilization of discrete-time LPV Systems under input Constraints**. de Souza, C., Leite, V. J. S., Tarbouriech, S., and Castelan, E. B. *System & Control Letters*, 2020;
- **Regional Input-to-State Stabilization of Fuzzy State-Delayed Discrete-Time Systems with Saturating Actuators**, Silva, L. F. P., Leite, V. J. S., Castelan, E. B., and de Souza, C. *Information Sciences*, 2020;

the following papers, published in conference proceeding:

- **ISS Stabilization of Discrete-time LPV Systems with Interval Time-varying State Delay and Saturating Actuators**. de Souza, C., Leite, V. J. S., Castelan, E. B., and Silva, L. F. P. *2nd IFAC Workshop on Linear Parameter Varying Systems LPVS*, 2018;

- **Input-to-state stabilization of discrete-time LPV systems with bounded time-varying state delay and saturating actuators through a dynamic controller**. de Souza, C., Castelan, E. B., and Leite, V. J. S. 58*th Conference on Decision and Control (CDC) - Nice, France*, 2019;

- **Avaliação de duas condições para a estabilização entrada-estado de sistemas LPV discretos no tempo com atraso eatuadores saturantes**. de Souza, C.; Leite, V. J. S., and Castelan, E. B. 14^{o} Simpósio Brasileiro de Automação Inteligente - Ouro Preto, Minas Gerais, Brasil, 2019;

- **Event-triggered Dynamic Output-Feedback Controller for Discrete-time LPV Systems with Constraints**. de Souza, C., Tarbouriech, S., Castelan, E. B., and Leite, V. J. S. *24th International Symposium on Mathematical Theory of Networks and Systems - Cambridge, UK*, 2020;

- **Emulation-based Dynamic Output-Feedback Control of Saturating Discrete-time LPV Systems**. de Souza, C., Leite, V. J. S., Tarbouriech, S., and Castelan, E. B. *2021 American Control Conference - New Orleans, USA*, 2020;

the following book chapter:

- **Control Strategy for Time-Delay Systems: Part I: Concepts and Theories. Chapter 10: Control of constrained discrete-time systems with time-varying state delay**. Leite, V. J. S., Castelan, E. B., Silva, L. F. P., and de Souza, C. *Elsevier* 2020.

and the following paper submitted to a journal:

- **A new approach for the event-triggered control of discrete-time saturating LPV systems**, de Souza, C., Leite, V. J. S., Tarbouriech, S., Castelan, E. B., and Silva, L. F. P. Submitted to *IEEE transactions on Automatic Control*, 2020;

REFERÊNCIAS

ABDELRAHIM, M.; POSTOYAN, R.; DAAFOUZ, J.; NEŠIĆ, D. Co-design of output feedback laws and event-triggering conditions for linear systems. In: IEEE. 53RD IEEE Conference on Decision and Control. Los Angeles, CA, USA: [s.n.], 2014. P. 3560–3565.

ASTRÖM, K. J.; WITTENMARK, B. **Computer-controlled systems: theory and design**. New York, USA: Prentice-Hall, 1984.

BEMPORAD, A.; HEEMELS, M.; JOHANSSON, M. **Networked control systems**. London, UK: Springer, 2010. v. 406.

BORGERS, D. P.; DOLK, V. S.; HEEMELS, W. P. M. H. Riccati-based design of event-triggered controllers for linear systems with delays. **IEEE Transactions on Automatic Control**, IEEE, v. 63, n. 1, p. 174–188, 2017.

BOYD, S.; EL GHAOUI, L.; FERON, E.; BALAKRISHNAN, V. **Linear matrix inequalities in systems and control theory**. Philadelphia, PA, USA: SIAM Studies for Industrial in Applied Mathematics, 1994.

BRAGA, M. F.; MORAIS, C. F.; TOGNETTI, E. S.; OLIVEIRA, R.C.L.F.; P.L.D.PERES. Discretization and event triggered digital output feedback control of LPV systems. **Systems** & **Control Letters**, Elsevier, v. 86, p. 54–65, 2015.

BRIAT, C. **Linear parameter-varying and time-Delay systems: analysis, observation, filtering** & **control**. Berlin, Heidelberg: Springer, 2015. v. 3.

BRIAT, C.; SENAME, O.; LAFAY, J.-F. Design of LPV observers for LPV time-delay systems: an algebraic approach. **International Journal of Control**, Taylor & Francis, v. 84, n. 9, p. 1533–1542, 2011.

CAO, Y. Y.; LIN, Z.; SHAMASH, Y. Set invariance analysis and gain-scheduling control for LPV systems subject to actuator saturation. **Systems** & **Control Letters**, Elsevier, v. 46, n. 2, p. 137–151, 2002.

CASTELAN, E. B.; LEITE, V. J. S.; MIRANDA, M. F.; MORAES, V. M. Synthesis of output feedback controllers for a class of nonlinear parameter-varying discrete-time

systems subject to actuators limitations. In: IEEE. 2010 American Control Conference (ACC). Baltimore, MD, USA: [s.n.], 2010. P. 4235–4240.

CHEN, W. H.; GUAN, Z. H.; LU, X. Delay-dependent guaranteed cost control for uncertain discrete-time systems with delay. **IEEE Proceedings-Control Theory and Applications**, IET, v. 150, n. 4, p. 412–416, 2003.

CORSO, J.; CASTELAN, E. B.; MORENO, U. F.; PIERI, De E. R. Controle dependente de parâmetros para uma classe de sistemas não-lineares incertos com atuadores saturantes. **SBA: Controle** & **Automação Sociedade Brasileira de Automatica**, SciELO Brasil, v. 20, n. 2, p. 119–132, 2009.

DA CUNHA, I. H.; SILVA, L. F. P.; LEITE, V. J. S.; KLUG, M. Analysis and synthesis conditions for T-S fuzzy continuous-time systems with partially matched premises. In: ELSEVIER. 21ST IFAC World Congress. [S.l.: s.n.], 2020. P. 1–6.

DAAFOUZ, J.; BERNUSSOU, J. Parameter dependent Lyapunov functions for discrete time systems with time varying parametric uncertainties. **Systems** & **Control Letters**, Elsevier, v. 43, n. 5, p. 355–359, 2001.

DE CAIGNY, J.; CAMINO, J. F.; OLIVEIRA, R. C. L. F.; PERES, P. L. D.; SWEVERS, J. Gain-scheduled $\mathcal{H}_2$ and $\mathcal{H}_\infty$ control of discrete-time polytopic time-varying systems. **IET Control Theory** & **Applications**, IET, v. 4, n. 3, p. 362–380, 2010.

DE CAIGNY, J.; CAMINO, J. F.; OLIVEIRA, R. C. L. F.; PERES, P. L. D.; SWEVERS, J. Gain-scheduled dynamic output feedback control for discrete-time LPV systems. **International Journal of Robust and Nonlinear Control**, Wiley Online Library, v. 22, n. 5, p. 535–558, 2012.

DE CAIGNY, J.; CAMINO, J. F.; OLIVEIRA, R.C.L.F.; PERES, P.L.D.; SWEVERS, J. Gain-scheduled $\mathcal{H}_\infty$ -control for discrete-time polytopic LPV systems using homogeneous polynomially parameter-dependent Lyapunov functions. **IFAC Proceedings Volumes**, Elsevier, v. 42, n. 6, p. 19–24, 2009.

DE SOUZA, C. **Robustez na estabilidade entrada-estado de sistemas discretos no tempo com atraso nos estados e saturação de atuadores**. 2017. MA thesis – Centro Federal de Educação Tecnológica de Minas Gerais (CEFET-MG), Divinópolis, MG.

DE SOUZA, C.; CASTELAN, E.B.; LEITE, V.J.S. Dynamic controllers for local input-to-state stabilization of discrete-time linear parameter-varying systems with delay and saturating actuators. **International Journal of Robust and Nonlinear Control**, Wiley Online Library, v. 31, n. 1, p. 131–147, 2021a.

DE SOUZA, C.; CASTELAN, E.B.; LEITE, V.J.S. Input-to-state stabilization of discrete-time LPV systems with bounded time-varying state delay and saturating actuators through a dynamic controller. In: IEEE. 58TH Conference on Decision and Control (CDC). Nice, France: [s.n.], 2019a. P. 3782–3787.

DE SOUZA, C.; LEITE, V. J. S.; CASTELAN, E. B.; SILVA, L. F. P. ISS Robust Stabilization of State-Delayed Discrete-time Systems with Bounded Delay Variation and Saturating Actuators. **IEEE Transactions on Automatic Control**, IEEE, 2019b.

DE SOUZA, C.; LEITE, V. J. S.; CASTELAN, E. B.; SILVA, L. F. P. ISS Stabilization of Discrete-time LPV Systems with Interval Time-varying State Delay and Saturating Actuators. **IFAC-PapersOnLine**, Elsevier, v. 51, n. 26, p. 143–148, 2018.

DE SOUZA, C.; LEITE, V. J. S.; TARBOURIECH, S.; CASTELAN, E. B. Emulation-based dynamic output-feedback control of saturating discrete-time LPV systems. **IEEE Control Systems Letters**, IEEE, v. 5, n. 5, p. 1549–1554, 2020a.

DE SOUZA, C.; LEITE, V.J.S.; CASTELAN, E.B. Avaliação de duas condições para a estabilização entrada-estado de sistemas LPV discretos no tempo com atraso e atuadores saturantes. 14° **Simpósio Brasileiro de Automação Inteligente - Ouro Preto, Minas Gerais, Brasil**, 2019c.

DE SOUZA, C.; LEITE, V.J.S.; TARBOURIECH, S.; CASTELAN, E.B. Event-triggered policy for DOF stabilization of discrete-time LPV systems under input constraints. **System** & **Control Letters**, Elsevier, v. 153, p. 104950, 2020b.

DE SOUZA, C.; LEITE, V.J.S.; TARBOURIECH, S.; CASTELAN, E.B.; SILVA, L. F. P. A direct parameter-error co-design approach of discrete-time saturating LPV systems. **IEEE Transactions on Automatic Control**, IEEE, 2021b. Submitted.

DE SOUZA, C.; TARBOURIECH, S.; CASTELAN, E.B.; LEITE, V.J.S. Event-triggered dynamic output-feedback controller for discrete-time LPV systems with constraints. In: 24TH International Symposium on Mathematical Theory of Networks and Systems. Cambridge, UK: [s.n.], 2020c. P. 1–6. Accepted.

DE SOUZA, C.; TARBOURIECH, S.; LEITE, V.J.S.; CASTELAN, E.B. Co-design of an event-triggered dynamic output feedback controller for discrete-time LPVsystems with constraints. **Journal of The Franklin Institute**, Elsevier, 2020d.

DING, S.; XIE, X.; LIU, Y. Event-triggered static/dynamic feedback control for discrete-time linear systems. **Information Sciences**, Elsevier, 2020.

DO, A. L.; DA SILVA, J. M. G.; SENAME, O.; DUGARD, L. Control design for LPV systems with input saturation and state constraints: an application to a semi-active suspension. In: IEEE. 50TH IEEE Conference on Decision and Control and 2011 European Control Conference (CDC-ECC). Orlando, FL, USA: [s.n.], 2011. P. 3416–3421.

DOU, X.; ZHANG, R.; ZHANG, Y. Stabilization control for LPV systems with time delay and actuator saturation. In: IEEE. 26TH Chinese Control and Decision Conference (CCDC). Changsha, China: [s.n.], 2014. P. 453–458.

DOYLE, J. C.; SMITH, R. S.; ENNS, D. F. Control of plants with input saturation nonlinearities. In: IEEE. 1987 American Control Conference (ACC). Minneapolis, MN, USA: [s.n.], 1987. P. 1034–1039.

EL HAOUSSI, F.; TISSIR, E. H. An LMI-based approach for robust stabilization of time delay systems containing saturating actuators. **IMA Journal of Mathematical Control and Information**, Oxford University Press, v. 24, n. 3, p. 347–356, 2006.

EMEDI, Z.; KARIMI, A. Fixed-structure LPV discrete-time controller design with induced $\mathcal{L}_2$-norm and $\mathcal{H}_2$ performance. **International Journal of Control**, Taylor & Francis, v. 89, n. 3, p. 494–505, 2016.

EQTAMI, A.; DIMAROGONAS, D. V.; KYRIAKOPOULOS, K. J. Event-triggered control for discrete-time systems. In: IEEE. 2010 American control conference (ACC). Baltimore, MD, USA: [s.n.], 2010. P. 4719–4724.

FRIDMAN, E. **Introduction to time-delay systems: analysis and control**. [S.l.]: Birkhäuser, 2014.

GILBERT, W.; HENRION, D.; BERNUSSOU, J.; BOYER, D. Polynomial LPV synthesis applied to turbofan engines. In: IFAC Symposium on Automatic Control in Aerospace. Toulouse, France: [s.n.], 2007.

GIRARD, A. Dynamic triggering mechanisms for event-triggered control. **IEEE Transactions on Automatic Control**, IEEE, v. 60, n. 7, p. 1992–1997, 2014.

GOLABI, A.; MESKIN, N.; TÓTH, R.; MOHAMMADPOUR, J.; DONKERS, T. Event-triggered control for discrete-time linear parameter-varying systems. In: IEEE. 2016 American Control Conference (ACC). [S.l.: s.n.], 2016. P. 3680–3685.

GOLABI, A.; MESKIN, N.; TÓTH, R.; MOHAMMADPOUR, J.; DONKERS, T.; DAVOODI, M. Event-triggered constant reference tracking control for discrete-time LPV systems with application to a laboratory tank system. **IET Control Theory & Applications**, IET, v. 11, n. 16, p. 2680–2687, 2017.

GROFF, L.B.; MOREIRA, L.G.; GOMES DA SILVA, J.M. Event-triggered control co-design for discrete-time systems subject to actuator saturation. In: 2016 IEEE Conference on Computer Aided Control System Design (CACSD). Buenos Aires, Argentina: [s.n.], 2016. P. 1452–1457.

GU, K.; CHEN, J.; KHARITONOV, V. L. **Stability of time-delay systems**. [S.l.]: Springer Science & Business Media, 2003.

HEEMELS, W. P. M. H.; DAAFOUZ, J.; MILLERIOUX, G. Observer-based control of discrete-time LPV systems with uncertain parameters. **IEEE Transactions on Automatic Control**, IEEE, v. 55, n. 9, p. 2130–2135, 2010.

HEEMELS, W. P. M. H.; JOHANSSON, K. H.; TABUADA, P. An introduction to event-triggered and self-triggered control. In: IEEE. 51ST IEEE Conference on Decision and Control (CDC). Maui, HI, USA: [s.n.], 2012. P. 3270–3285.

HETEL, L.; DAAFOUZ, J.; IUNG, C. Equivalence between the Lyapunov-Krasovskii functionals approach for discrete delay systems and that of the stability conditions for switched systems. **Nonlinear Analysis: Hybrid Systems**, Elsevier, v. 2, n. 3, p. 697–705, 2008.

HU, T.; LIN, Z. **Control systems with actuator saturation: analysis and design**. Virginia, USA: Springer Science & Business Media, 2001.

HUANG, J.; WEN, C.; WANG, W.; JIANG, Z.-P. Adaptive output feedback tracking control of a nonholonomic mobile robot. **Automatica**, Elsevier, v. 50, n. 3, p. 821–831, 2014.

HUANG, J. J.; PAN, X. Z.; HAO, X. Z. Event-triggered and self-triggered $\mathcal{H}_\infty$ output tracking control for discrete-time linear parameter-varying systems with network-induced delays. **International Journal of Systems Science**, Taylor & Francis, v. 51, n. 15, p. 3098–3117, 2020.

JING, Z.; BAOYONG, Z.; YIJUN, Z. Dynamic output-feedback gain-scheduled control for LPV systems with time-varying delays. In: IEEE. 34TH Chinese Control Conference (CCC). Hangzhou, China: [s.n.], 2015. P. 2961–2966.

JUNGERS, M.; CASTELAN, E. B. Gain-scheduled output control design for a class of discrete-time nonlinear systems with saturating actuators. **Systems** & **Control Letters**, Elsevier, v. 60, n. 3, p. 169–173, 2011.

JUNLING, W.; WEI, Y.; ZHEXING, S. Observer-based gain-scheduled $\mathcal{H}_\infty$ control for LPV discrete-time systems with a time-varying delay. In: IEEE. 27TH Chinese Control Conference (CCC). Kunming, China: [s.n.], 2008. P. 702–706.

KAPILA, V.; HADDAD, W. M. Memoryless $\mathcal{H}_\infty$ controllers for discrete-time systems with time delay. **Automatica**, Elsevier, v. 34, n. 9, p. 1141–1144, 1998.

KIENER, G. A.; LEHMANN, D.; JOHANSSON, K. H. Actuator saturation and anti-windup compensation in event-triggered control. **Discrete event dynamic systems**, Springer, v. 24, n. 2, p. 173–197, 2014.

LAURAIN, V.; GILSON, M.; TOTH, R.; GARNIER, H. Direct identification of continuous-time LPV models. In: IEEE. 2011 American Control Conference (ACC). San Francisco, CA, USA: [s.n.], 2011. P. 159–164.

LEITE, V. J. S.; CASTELAN, E. B.; MIRANDA, M. F.; VIANA, D. C. Dynamic output compensator design for time-varying discrete time systems with delayed states. In: IEEE. 2010 American Control Conference (ACC). Baltimore, MD, USA: [s.n.], 2010. P. 5775–5780.

LI, L.; ZOU, W.; FEI, S. Event-based dynamic output-feedback controller design for networked control systems with sensor and actuator saturations. **Journal of the Franklin Institute**, Elsevier, v. 354, n. 11, p. 4331–4352, 2017.

LI, P.; SUN, X. M.; JABBARI, F.; WANG, L. Gain-scheduled control of time-varying delay systems with input constraint. **International Journal of Control**, Taylor & Francis, p. 1–9, 2018.

LI, S.; JIANG, S.; PAN, F. Event-triggered fault detection for networked LPV systems. **Circuits, Systems, and Signal Processing**, Springer, v. 38, n. 7, p. 2992–3019, 2019.

LI, S.; SAUTER, D.; XU, B. Co-design of event-triggered $\mathcal{H}_\infty$ control for discrete-time linear parameter-varying systems with network-induced delays. **Journal of the Franklin Institute**, Elsevier, v. 352, n. 5, p. 1867–1892, 2015.

LI, S.; SAUTER, D.; XU, B. Uniformly ultimate boundedness event-triggered control for discrete-time uncertain linear parameter-varying systems. In: IEEE. 33RD Chinese Control Conference. [S.l.: s.n.], 2014. P. 5733–5738.

LIU, D.; YANG, G. H. Event-triggered control for linear systems with actuator saturation and disturbances. **IET Control Theory** & **Applications**, IET, v. 11, n. 9, p. 1351–1359, 2017.

LIU, D.; YANG, G.-H. Robust event-triggered control for networked control systems. **Information Sciences**, Elsevier, v. 459, p. 186–197, 2018.

LIU, P. L. Delay-dependent stabilization for linear time-delay uncertain systems with saturating actuators. **International Journal of General Systems**, Taylor & Francis, v. 40, n. 3, p. 301–312, 2011.

LOFBERG, J. YALMIP: A toolbox for modeling and optimization in MATLAB. In: IEEE. 2004 IEEE International Conference on Robotics and Automation. New Orleans, LA, USA: [s.n.], 2004. P. 284–289.

LUNZE, J.; LEHMANN, D. A state-feedback approach to event-based control. **Automatica**, Elsevier, v. 46, n. 1, p. 211–215, 2010.

MA, D.; HAN, J.; ZHANG, D.; LIU, Y. Co-design of event generator and dynamic output feedback controller for LTI systems. **Mathematical Problems in Engineering**, Hindawi, 2015.

MAHMOUD, M. S. Linear parameter-varying discrete time-delay systems: stability and l_2-gain controllers. **International Journal of Control**, Taylor & Francis, v. 73, n. 6, p. 481–494, 2000.

MAHMOUD, M. S.; HAMDAN, M. M. Fundamental issues in networked control systems. **IEEE/CAA Journal of Automatica Sinica**, IEEE, v. 5, n. 5, p. 902–922, 2018.

MENG, X.; CHEN, T. Event detection and control co-design of sampled-data systems. **International Journal of Control**, Taylor & Francis, v. 87, n. 4, p. 777–786, 2014.

MIRANDA, M. F.; LEITE, V.J.S. Robust stabilization of polytopic discrete-time systems with time-varying state delay: A convex approach. **Journal of the Franklin Institute**, Elsevier, v. 348, n. 4, p. 568–588, 2011.

MOHAMMADPOUR, J.; SCHERER, C. W. **Control of linear parameter varying systems with applications**. Boston, MA, USA: Springer, 2012.

MONTAGNER, V. F.; OLIVEIRA, R. C. L. F.; PERES, P.L.D.; TARBOURIECH, S.; QUEINNEC, I. Gain-scheduled controllers for linear parameter-varying systems with saturating actuators: LMI-based design. In: IEEE. 2007 American Control Conference (ACC). New York, NY, USA: [s.n.], 2007. P. 6067–6072.

MONTAGNER, V. F.; OLIVEIRA, R.C.L.F.; LEITE, V.J.S.; PERES, P.L.D. Gain scheduled state feedback control of discrete-time systems with time-varying uncertainties: an LMI approach. In: IEEE. 44TH IEEE Conference on Decision and Control (CDC) and 2005 European Control Conference (ECC). Seville, Spain: [s.n.], 2005. P. 4305–4310.

MOREIRA, L. G.; GROFF, L. B.; GOMES DA SILVA JR, J.M.; TARBOURIECH, S. PI event-triggered control under saturating actuators. **International Journal of Control**, Taylor & Francis, v. 92, n. 7, p. 1634–1644, 2019.

NEJEM, I.; BOUAZIZI, M. H.; BOUANI, F. $\mathcal{H}_\infty$ Based State Feedback Control of LPV Time-Delay Systems via Parameter-Dependent Lyapunov Krasovskii Functionals. In: SPRINGER, CHAM. INTERNATIONAL Conference on Electrical Engineering and Control Applications. Constantine, Algeria: [s.n.], 2017. P. 60–71.

NGUYEN, A.-T.; CHEVREL, P.; CLAVEAU, F. Gain-scheduled static output feedback control for saturated LPV systems with bounded parameter variations. **Automatica**, Elsevier, v. 89, p. 420–424, 2018.

NI, W.; ZHAO, P.; WANG, X.; WANG, J. Event-triggered control of linear systems with saturated inputs. **Asian Journal of Control**, Wiley Online Library, v. 17, n. 4, p. 1196–1208, 2015.

NICULESCU, S. I. **Delay effects on stability: a robust control approach**. [S.l.]: Springer, London, 2001. v. 269.

OLIVEIRA, R. C. L. F.; PERES, P.L.D. Robust stability analysis and control design for time-varying discrete-time polytopic systems with bounded parameter variation. In: IEEE. 2008 American Control Conference (ACC). Seattle, WA, USA: [s.n.], 2008. P. 3094–3099.

OLIVEIRA, R. C. L. F.; PERES, P.L.D. Time-varying discrete-time linear systems with bounded rates of variation: Stability analysis and control design. **Automatica**, Elsevier, v. 45, n. 11, p. 2620–2626, 2009.

PAL, V. C.; NEGI, R. Delay-dependent stability criterion for uncertain discrete time systems in presence of actuator saturation. **Transactions of the Institute of Measurement and Control**, SAGE Publications Sage UK: London, England, v. 40, n. 6, p. 1873–1891, 2018.

PANDEY, A. P.; DE OLIVEIRA, M. C. A new discrete-time stabilizability condition for linear parameter-varying systems. **Automatica**, Elsevier, v. 79, p. 214–217, 2017.

PEIXOTO, M. L. C.; LACERDA, M. J.; PALHARES, R. M. On discrete-time LPV control using delayed Lyapunov functions. **Asian Journal of Control**, Wiley Online Library, 2020.

PENG, C.; YANG, T. C. Event-triggered communication and $\mathcal{H}_\infty$ control co-design for networked control systems. **Automatica**, Elsevier, v. 49, n. 5, p. 1326–1332, 2013.

PING, X.; LI, Z.; AL-AHMARI, A. Dynamic output feedback robust MPC for LPV systems subject to input saturation and bounded disturbance. **International Journal of Control, Automation and Systems**, Springer, v. 15, n. 3, p. 976–985, 2017.

POUSSOT-VASSAL, C.; SENAME, O.; DUGARD, L.; GASPAR, P.; SZABO, Z.; BOKOR, J. A new semi-active suspension control strategy through LPV technique. **Control Engineering Practice**, Elsevier, v. 16, n. 12, p. 1519–1534, 2008.

RICHARD, J.-P. Time-delay systems: an overview of some recent advances and open problems. **Automatica**, Elsevier, v. 39, n. 10, p. 1667–1694, 2003.

RODRIGUES, L.A.; CAMINO, J.F.; PERES, P.L.D. Gain-Scheduled $\mathcal{H}_\infty$ Control for Discrete-Time Polynomial LPV Systems Using Homogeneous Polynomial Path-Dependent Lyapunov Functions. **IFAC-PapersOnLine**, Elsevier, v. 51, n. 26, p. 179–184, 2018.

ROSA, T. E.; FREZZATTO, L.; MORAIS, C. F.; OLIVEIRA, Ricardo C.L.F. $\mathcal{H}_\infty$ Static Output-Feedback Gain-Scheduled Control for Discrete LPV Time-Delay Systems. **IFAC-PapersOnLine**, Elsevier, v. 51, n. 26, p. 137–142, 2018.

RUGH, W. J.; SHAMMA, J. S. Research on gain scheduling. **Automatica**, Elsevier, v. 36, n. 10, p. 1401–1425, 2000.

RUIZ, A.; ROTONDO, D.; MORCEGO, B. Design of state-feedback controllers for linear parameter varying systems subject to time-varying input saturation. **Applied Sciences**, Multidisciplinary Digital Publishing Institute, v. 9, n. 17, p. 3606, 2019.

SAADABADI, H.; WERNER, H. Event-Triggered Dynamic Output Feedback Control For Discrete-Time Polytopic Linear Parameter-Varying Systems. In: IEEE. 59TH IEEE Conference on Decision and Control (CDC). [S.l.: s.n.], 2020. P. 98–103.

SCHERER, C.; GAHINET, P.; CHILALI, M. Multiobjective Output-Feedback Control via LMI Optimization. v. 42, n. 7, p. 896–911, July 1997.

SEURET, A.; GOMES DA SILVA JR, J. M. Taking into account period variations and actuator saturation in sampled-data systems. **Systems** & **Control Letters**, Elsevier, v. 61, n. 12, p. 1286–1293, 2012.

SEURET, A.; PRIEUR, C.; TARBOURIECH, S.; ZACCARIAN, L. LQ-based event-triggered controller co-design for saturated linear systems. **Automatica**, Elsevier, v. 74, p. 47–54, 2016.

SHAMMA, J. S. **Analysis and design of gain scheduled control systems**. 1988. PhD thesis – Massachusetts Institute of Technology.

SHANBIN, L.; BUGONG, X. Event-triggered control for discrete-time uncertain linear parameter-varying systems. In: IEEE. 32ND Chinese Control Conference. Xian, China: [s.n.], 2013. P. 273–278.

SILVA, L. F. P.; CASTELAN, E. B.; LEITE, V. J. S. Local ℓ_2-stabilization of nonlinear discrete-time systems with delayed states through T-S fuzzy models. In: IEEE. 2016 American Control Conference (ACC). Boston, MA, USA: [s.n.], 2016. P. 3934–3939.

SILVA, L. F. P.; LEITE, V. J. S.; CASTELAN, E. B.; KLUG, M. Local stabilization of time-delay nonlinear discrete-time systems using Takagi-Sugeno models and convex optimization. **Mathematical Problems in Engineering**, Hindawi, v. 2014, 2014.

SONG, G.; LAM, J.; XU, S. Robust quantized output feedback control for uncertain discrete time-delay systems with saturation nonlinearity. **International Journal of Robust and Nonlinear Control**, Wiley Online Library, v. 25, n. 18, p. 3515–3527, 2015.

SONG, G.; WANG, Z. A delay partitioning approach to output feedback control for uncertain discrete time-delay systems with actuator saturation. **Nonlinear Dynamics**, Springer Netherlands, v. 74, n. 1-2, p. 189–202, 2013.

SONG, S. H.; KIM, J. K.; YIM, C. H.; KIM, H. C. $\mathcal{H}_\infty$ control of discrete-time linear systems with time-varying delays in state. **Automatica**, Elsevier, v. 35, n. 9, p. 1587–1591, 1999.

TABUADA, P. Event-triggered real-time scheduling of stabilizing control tasks. **IEEE Transactions on Automatic Control**, IEEE, v. 52, n. 9, p. 1680–1685, 2007.

TAKAGI, T.; SUGENO, M. Fuzzy identification of systems and its applications to modeling and control. **IEEE Transactions on Systems, Man, and Cybernetics**, IEEE, n. 1, p. 116–132, 1985.

TARBOURIECH, S.; GARCIA, G.; GOMES DA SILVA JR., J. M.; QUEINNEC, I. **Stability and stabilization of linear systems with saturating actuators**. London, UK: Springer, 2011.

TIPSUWAN, Y.; CHOW, M. Y. Control methodologies in networked control systems. **Control Engineering Practice**, Elsevier, v. 11, n. 10, p. 1099–1111, 2003.

TÓTH, R. **Modeling and identification of linear parameter-varying systems**. [S.l.]: Springer, 2010. v. 403.

TÓTH, R.; FELICI, F.; HEUBERGER, P. S. C.; VAN DEN HOF, P. M. J. Crucial aspects of zero-order hold LPV state-space system discretization. **IFAC Proceedings Volumes**, Elsevier, v. 41, n. 2, p. 4952–4957, 2008.

VELASCO, M.; MARTÍ, P.; BINI, E. On Lyapunov sampling for event-driven controllers. In: IEEE. 48H IEEE Conference on Decision and Control (CDC) held jointly with 28th Chinese Control Conference. Shanghai, China: [s.n.], 2009. P. 6238–6243.

VERDULT, V. **Nonlinear system identification: State-space approach**. 2002. PhD thesis – Faculty of Applied Physics,University of Twente, Enschede, The Netherlands.

WANG, L.; LIU, X. Gain scheduled state feedback control for discrete-time-varying polytopic systems subject to input saturation. **Circuits, Systems, and Signal Processing**, SP Birkhäuser Verlag Boston, v. 30, n. 6, p. 1165–1182, 2011.

WANG, X.; LEMMON, M. D. Event design in event-triggered feedback control systems. In: IEEE. 47TH IEEE Conference on Decision and Control (CDC). [S.l.: s.n.], 2008. P. 2105–2110.

WEI, Y.; ZHENG, W. X.; XU, S. Robust output feedback control of uncertain time-delay systems with actuator saturation and disturbances. **Journal of the Franklin Institute**, Elsevier, v. 352, n. 5, p. 2229–2248, 2015.

WHITE, A. P.; ZHU, G.; CHOI, J. **Linear parameter-varying control for engineering applications**. London, UK: Springer, 2013.

WHITE, B. A.; BRUYERE, L.; TSOURDOS, A. Missile autopilot design using quasi-LPV polynomial eigenstructure assignment. **IEEE Transactions on Aerospace and Electronic Systems**, IEEE, v. 43, n. 4, 2007.

WU, F.; GRIGORIADIS, K. M. LPV systems with parameter-varying time delays: analysis and control. **Automatica**, Elsevier, v. 37, n. 2, p. 221–229, 2001.

WU, F.; PRAJNA, S. SOS-based solution approach to polynomial LPV system analysis and synthesis problems. **International Journal of Control**, Taylor & Francis, v. 78, n. 8, p. 600–611, 2005.

WU, W.; REIMANN, S.; LIU, S. Event-triggered control for linear systems subject to actuator saturation. **IFAC Proceedings Volumes**, Elsevier, v. 47, n. 3, p. 9492–9497, 2014.

XIE, X.; LI, S.; XU, B. Output-based event-triggered control for networked control systems: tradeoffs between resource utilisation and robustness. **IET Control Theory & Applications**, IET, v. 12, n. 15, p. 2138–2147, 2018.

XU, S.; FENG, G.; ZOU, Y.; HUANG, J. Robust Controller Design of Uncertain Discrete Time-Delay Systems With Input Saturation and Disturbances. **IEEE Transactions on Automatic Control**, IEEE, v. 57, n. 10, p. 2604–2609, 2012.

ZHANG, J.; FENG, G. Event-driven observer-based output feedback control for linear systems. **Automatica**, Elsevier, v. 50, n. 7, p. 1852–1859, 2014.

ZHANG, L.; WANG, J.; GE, Y. Constrained distributed MPC for LPV systems with actuator saturation and state delay. In: IEEE. 2014 American Control Conference. Portland, OR, USA: [s.n.], 2014. P. 4901–4906.

ZHANG, W.; BRANICKY, M. S.; PHILLIPS, S. M. Stability of networked control systems. **IEEE control systems magazine**, IEEE, v. 21, n. 1, p. 84–99, 2001.

ZHANG, X. M.; HAN, Q. L. Event-triggered dynamic output feedback control for networked control systems. **IET Control Theory & Applications**, IET, v. 8, n. 4, p. 226–234, 2014.

ZHANG, X. M.; HAN, Q. L.; SEURET, A.; GOUAISBAUT, F.; HE, Y. Overview of recent advances in stability of linear systems with time-varying delays. **IET Control Theory & Applications**, IET, v. 13, n. 1, p. 1–16, 2019.

ZHOU, S.; ZHENG, W. X. A parameter-dependent Lyapunov function based approach to $\mathcal{H}_\infty$-control of LPV discrete-time systems with delays. In: IEEE. 47TH IEEE Conference on Decision and Control (CDC). Cancun, Mexico: [s.n.], 2008. P. 4669–4674.

ZOPE, R.; MOHAMMADPOUR, J.; GRIGORIADIS, K.; FRANCHEK, M.
Delay-dependent output feedback control of time-delay LPV systems. In: CONTROL of Linear Parameter Varying Systems with Applications. Boston, MA, USA: Springer, 2012. P. 279–299.

ZUO, Z.; LI, Q.; LI, H.; WANG, Y. Co-design of event-triggered control for discrete-time systems with actuator saturation. In: IEEE. 12TH World Congress on Intelligent Control and Automation (WCICA). Guilin, China: [s.n.], 2016. P. 170–175.